

Biochemical Basis of Autoactivity of a Pair of Plant NLR Immune Receptors

Dissertation

der Mathematisch-Naturwissenschaftlichen Fakultät
der Eberhard Karls Universität Tübingen
zur Erlangung des Grades eines
Doktors der Naturwissenschaften
(Dr. rer. nat.)

vorgelegt von

Diep Thi Ngoc Tran

aus Hanoi, Vietnam

Tübingen

2016

Gedruckt mit Genehmigung der Mathematisch-Naturwissenschaftlichen Fakultät der
Eberhard Karls Universität Tübingen.

Tag der mündlichen Qualifikation:	25 Juli 2016
Dekan:	Prof. Dr. Wolfgang Rosenstiel
1. Berichterstatter:	Prof. Dr. Detlef Weigel
2. Berichterstatter:	Prof. Dr. Hans-Georg Rammensee

ACKNOWLEDGEMENTS

I deeply thank “thầy” Detlef Weigel for giving me the chance to work in Weigelworld and mentoring me during my PhD. His supervision and encouragement are invaluable, helping me to gain more confidence in myself.

My sincere thanks go to Prof. Hans-Georg Rammensee, my second supervisor, and Dr. Hernán Burbano and Dr. Michael Hothorn, both members of my PhD Advisory Committee, for their scientific advice and input.

I would like to thank Prof. Thorsten Nürnberger and Dr. Thomas Lahaye, for agreeing to be two other members of my PhD examiner committee.

I especially thank Eunyoung Chae, who continuously supports me and directly works with me in the project I present in this thesis. Collaboration with Eunyoung helps me to develop various skills in project design, experimental analysis, and scientific reading and writing.

I thank Rebecca Schwab not only for her awesome assistance and critical arguments during the project development and thesis writing, but also for lots of good cakes and gummy bears.

I thank my collaborators from the University of North Carolina (Chapel Hill, NC, USA), Prof. Jeffery Dangl and Dr. Eui-Hwan Chung, for their excellent collaboration and advice for my PhD project.

I thank Beth Rowan for working with me during the first two years of my PhD. Her great scientific guidance laid the foundation to build up my knowledge in plant immunity.

I thank Ignacio Rubio Somoza, Iuliia Boichenko, Julia Santiago, Gautam Shirsekar, and Chang Liu for their helpful discussions. I thank Monika Demar and Paula Vilchez for their assistance with my experiments.

I thank the International PhD Program by the Max Planck Institute for Developmental Biology (Tübingen, Germany) for awarding me the PhD scholarship. I thank Dagmar Sigurdardottir, the PhD Program coordinator, and Hülya Wicher, the secretary in my lab, for their administrative supports.

Many thanks to my “Lab Ladies+” gang (Patricia Lang, Maricris Zaidem, Subhashini Muralidharan, Giovanna Capovilla, Efthymia Symeonidi, Noemi Skorzinski, and

Moisés Expósito Alonso), my bench mates (Wanyan Xi and also Patricia Lang), other fellow lab mates (Ana-Cristina Barragan Lopez, Anna-Lena Van de Weyer, Anette Habring-Müller, Christa Lanz, Claude Becker, Claudia Friedemann, Danelle Seymour, Daniel Koenig, Derek Lundberg, Dino Jolic, Eshita Sharma, Emanuele Scacchi, Ezgi Dogan, François Vasseur, Frank Küttner, George Wang, Jane Devos, Jonas Müller, Jorge Quitana, Josip Perkovic, Jörg Hagmann, Kavita Venkataramani, Leily Rabbani, Lisa Smith, Manuela Neumann, Markus Schmid, Rafał Gutaker, Rui Wu, Sang-Tae Kim, Silvio Collani, Sonja Kersten, Talia Karasov, Verena Kottler, Vinicius Costa Galvão, Wangsheng Zhu, and Xi Wang), and my friends outside the lab, especially Elke Lamberti and Hân Witte. Without their wonderful friendship and company, my life in the lab and in Tübingen could never have been so meaningful and joyful.

I am especially grateful to my family, my in-laws, and my little angel, who give me spiritual support and motivation to pursue my career.

And Chi, thank you so much, my dearest husband, for endless strength and love, for never minding traveling hundreds of miles from Greifswald to Tübingen to help me when suddenly I needed a spare hand at work, and for always being on my side.

TABLE OF CONTENTS

ABSTRACT	1
ZUSAMMENFASSUNG	3
INTRODUCTION	5
1. Plant immunity.....	5
2. Trade-off between immunity and growth in plants.....	9
3. NLR-mediated effector recognition in plants.....	11
3.1. Recognition specificity of NLRs.....	11
3.2. NLR diversity.....	13
3.3. Effector-recognition mechanisms.....	15
4. NLR-mediated immune activation.....	20
4.1. NLR domain structure and associated function.....	20
4.2. An autoinhibitory conformation of NLR proteins.....	22
4.3. Oligomerization between NLRs activation.....	24
4.4. Downstream signaling upon NLR activation.....	26
4.5. NLR accumulation by HSP90-SGT1-RAR1 co-chaperone complex.....	29
5. Autoimmunity in plants.....	30
6. Aim of the PhD thesis.....	34
RESULTS	35
CHAPTER 1. Characterization of DM1/DM2d-dependent Autoimmunity	35
1. Genetic requirements for DM1/DM2d-triggered autoimmune signaling.....	35
2. DM1/DM2d signaling requires of both proteins in full length.....	39
3. DM1/DM2d cell-death signaling requires the P-loops of both proteins.....	42
CHAPTER 2. Physical Association of DM1 and DM2d	46
1. Structural modeling of the TIR domain of DM1 and DM2d.....	46
2. Physical associations of DM1 and DM2d in yeast.....	48
3. Physical associations of DM1 and DM2d in planta.....	50
4. Correlation of physical association of the TIR domains and DM1/DM2d signaling.....	53
5. P-loop mutations do not disrupt the physical association of DM1 and DM2d.....	57
CHAPTER 3. Unequal Contribution of DM1 and DM2d to signaling	59
1. Distinct contributions of DM1 and DM2d to signaling.....	59
2. Asymmetric contribution of the MHD motifs in DM1 and DM2d to the signaling ...	62

CHAPTER 4. Analysis of Natural Variants of DM2	68
1. Polymorphisms in DM2 variants.....	68
2. Physical interaction between DM1 and the DM2d paralog (DM2g).....	69
3. Polymorphisms in TIR and LRR domains determine DM2 activity.....	72
4. Polymorphisms in the center of LRR domain determine DM1 activity	75
DISCUSSION	77
1. DM1/DM2d NLRs signal through EDS1	77
2. RAR1 and SGT1b regulate DM1/DM2d protein accumulation	79
3. Signaling interdependency of DM1 and DM2d and physical associations	81
4. Functional significance of NLR conformation	83
5. Preformed DM1 complex and higher-order DM1/DM2d oligomerization.....	87
6. Functional diversification of DM2 variants.....	91
PERSPECTIVES	93
MATERIALS AND METHODS.....	95
General equipment and reagents.....	95
Growth media (for bacteria, yeast, and plants)	96
Bacterial media.....	96
Yeast media	96
Plant media	96
Oligonucleotides.....	96
Overlapping PCR to generate chimeric constructs	96
DNA plasmid cloning.....	97
DNA isolation and purification	98
Plant materials and growth conditions.....	98
RNA extraction	99
cDNA synthesis.....	99
Reverse transcription followed by quantitative real-time PCR (qRT-PCR).....	100
<i>Agrobacterium</i> -mediated transient expression assays in <i>N. benthamiana</i>	100
Conductivity assays	101
Yeast-two hybrid assays and yeast crude protein extraction	102
Plant protein extraction and co-immunoprecipitation assays	102
Other tools.....	103
SUPPLEMENTARY MATERIAL.....	104
Table S1. Bacterial and yeast strains.....	104
Table S2. Antibodies and beads	104

Table S3. Oligonucleotides for amplification of <i>TUB2</i> , <i>PR1</i> , <i>NPR1</i> and <i>WRKY46</i> ..	104
Table S4. Oligonucleotides for DM2d/DM2g chimeric amplification and site-directed mutagenesis	105
Table S5. Binary T-DNA constructs	106
SUPPLEMENTARY FIGURES	108
REFERENCES	122
PUBLICATIONS	139
LEBENS LAUF	140

ABSTRACT

An immune system enables organisms to defend themselves against a myriad of pathogens and diseases. Plants, which can rely only on innate immunity, have evolved different types of receptors to detect pathogens. Transmembrane receptors can recognize pathogenic conserved structures called pathogen-associated molecular patterns (PAMPs) such as flagellin, leading to PAMP-triggered immunity (PTI). Intracellular receptors recognize specific molecules delivered by pathogens into plant cells, known as effectors, and activate effector-triggered immunity (ETI) when PTI is overcome. Most of the ETI-mediating intracellular receptors belong to the NLR protein family characterized by a nucleotide-binding domain and leucine-rich repeats. NLRs perceive matching effectors, through either physical binding to the effector (direct recognition) or by sensing effector-induced biochemical modifications of a host target (indirect recognition). NLR-dependent signaling often leads to a hypersensitive response (HR), featured by localized cell death at the site of the infection, which stops pathogen spread and disease development. Mis-regulation of NLRs in the absence of pathogens can lead to inappropriate responses of the immune system, known as autoimmunity, causing spontaneous cell death, necrotic lesions and developmental defects.

Autoimmunity can occasionally be observed in hybrid plants. This type of hybrid weakness can result from deleterious epistatic interactions between NLR genes from the two parents. In this thesis, I investigated the biochemical mechanism of autoimmunity in hybrids of two natural *Arabidopsis thaliana* accessions from Umkirch (Southwestern Germany). The two causal genes involved, *DM1* (*DANGEROUS MIX 1*) from Uk-3 and *DM2* from Uk-1, both encode NLRs. The causal *DM2* variant is located in a multi-gene cluster with diverse NLR members, while *DM1* is a single-gene *NLR* locus. In this study, I showed that signaling mediated by *DM1* and *DM2* uses the same pathway that other plant NLRs deploy upon non-self recognition. Cell death signaling induced by *DM1* and *DM2* involves heteromeric association of both proteins through their N-terminal regions including TIR domains, with *DM1* forming inactive homo-oligomers in the absence of *DM2*. Mutations in the P-loop of either *DM1* or *DM2* suppressed HR, indicating the

contribution of both proteins to signaling. The contributions of the two NLRs to downstream signaling are, however, not symmetrical. Mutations in an NLR signature motif that are likely to affect conformation around the ATP binding pocket greatly change the activity of only DM2. Taken together, my results suggest that DM1 acts primarily as a signal transducer, and DM2 as a signal trigger. Autoimmunity triggered by joint action of this NLR pair thus suggests that the activity of the signaling complex depends on the sum of the complementary activities of the partner NLRs. Knowledge of the biochemical basis of autoactivity induced by plant NLR pairs will help us to understand how plant autoimmunity arises through NLR interaction, and how NLR activity is regulated to avoid inappropriate activation to minimize the plant fitness cost in the absence of pathogens.

ZUSAMMENFASSUNG

Ein Immunsystem ermöglicht es Organismen, sich gegen unzählige Pathogene und Krankheiten zu verteidigen. Pflanzen, die sich nur auf ihre angeborene Immunität verlassen können, haben verschiedene Arten von Rezeptoren entwickelt, um Pathogene wahrzunehmen. Transmembran-Rezeptoren können konservierte pathogene Strukturen, sogenannte Pathogen-assoziierte molekulare Muster (engl. *Pathogen-associated molecular patterns*, PAMPs) wie Flagellin erkennen, was zu PAMP-ausgelöster Immunität führt (*PAMP-triggered immunity*, PTI). Intrazelluläre Rezeptoren erkennen spezifische, von Pathogenen in Pflanzenzellen eingebrachte Moleküle, sogenannte Effektoren, und aktivieren die Effektor-ausgelöste Immunität (*Effector-triggered immunity*, ETI), wenn die PTI überwunden worden ist. Die meisten der ETI-vermittelnden intrazellulären Rezeptoren gehören der NLR Proteinfamilie an, die durch eine Nukleotid-bindende Domäne und *Leucine-rich repeat* Motive charakterisiert ist. NLR-Rezeptoren erkennen passende Effektoren entweder durch physisches Binden des Effektors (direkte Erkennung) oder dadurch, dass sie Effektor-erzeugte biochemische Veränderungen im Wirt wahrnehmen (indirekte Erkennung). NLR-abhängige Signalgebung führt oft zu einer hypersensiblen Reaktion (HR), die sich durch Zelltod an der Infektionsstelle auszeichnet, welcher die Ausbreitung des Pathogens und das Fortschreiten der Erkrankung eindämmt. Fehlregulierung von NLRs in Abwesenheit von Krankheitserregern kann zu unpassenden Immunreaktionen führen, bekannt als Autoimmunität, die spontanen Zelltod, nekrotische Läsionen und Entwicklungsstörungen mit sich führen.

Autoimmunität kann gelegentlich in Pflanzenhybriden beobachtet werden. Diese Art von Hybridschwäche kann aus schädlichen epistatischen Interaktionen zwischen NLR-Genen unterschiedlicher Elternteile resultieren. In der vorliegenden Doktorarbeit habe ich den biochemischen Mechanismus der Autoimmunität zweier natürlicher *Arabidopsis thaliana* Akzessionen aus Umkirch (Südwestdeutschland) untersucht. Die beiden beteiligten Gene, *DM1* (*DANGEROUS MIX 1*) von Uk-3 und *DM2* von Uk-1 kodieren für NLR-Rezeptoren. Die kausale *DM2* Variante liegt gemeinsam mit verschiedenen weiteren NLRs in einem Multigen-Cluster, während es sich bei *DM1* um einen einzelnen NLR-Locus handelt. Ich konnte zeigen, dass *DM1* und *DM2* über denselben Signalweg agieren, den andere pflanzliche NLRs für

Fremd-Erkennung nutzen. Die durch DM1 und DM2 induzierte Zelltod-Signalgebung nutzt eine heteromere Verbindung beider Proteine über deren N-terminale Regionen inklusive der TIR-Motive. Mutationen im P-loop von sowohl DM1 oder DM2 unterdrückt die HR, was eine Beteiligung beider Proteine an der Signalgebung andeutet. Die Beiträge der beiden NLR-Proteine zu den nachgeschalteten Signalwegen sind jedoch nicht symmetrisch. Mutationen in einem Kernmotiv der NLRs, die mit hoher Wahrscheinlichkeit die Konformation rund um die ATP-Bindungstasche beeinflussen, verändern nur die DM2-Aktivität stark. Zusammengefasst legen meine Ergebnisse nahe, dass DM1 primär als Signalüberträger agiert, und DM2 als Signalauslöser. Die gemeinsame Aktivität dieses NLR-Paares beim Auslösen von Autoimmunität deutet daher an, dass die Aktivität des Signalkomplexes die komplementären Eigenschaften beider Partner-NLRs benötigt. Kenntnis der biochemischen Grundlagen von durch pflanzliche NLR-Paare ausgelöster Autoaktivierung wird dazu beitragen zu verstehen, wie pflanzliche Autoimmunität durch NLR-Interaktion entsteht und wie NLR-Aktivität reguliert ist, um unpassende Aktivierung zu vermeiden und entstehende Fitness-Kosten für die Pflanze in Abwesenheit eines Krankheitserregers zu minimieren.

Credit: The German abstract of my thesis was translated by Patricia Lang and proofread by Rebecca Schwab

INTRODUCTION

1. Plant immunity

An effective immune system is essential for plants and animals to defend themselves from numerous pathogens, and successfully survive and reproduce. Unlike vertebrate animals with both innate and adaptive immune systems, plants rely on only an innate immune system as well as structural defenses to counter attacks by herbivores and pathogens in different geographic and climatic environments.

The plant epidermis makes up the first barrier to protect plants from damage caused by herbivores such as caterpillars, mites, or wasps. Specialized cell types of the epidermis such as trichomes to some extent can impede first physical damages. In addition, the cuticle, a waxy layer covering outside the epidermis, also contributes to prevent plant tissues from invasion by microorganisms. Many phytopathogens can overcome the physical barriers formed by the epidermis, and penetrate into plant tissues, often through stomata as an initial entry.

A second layer of plant defense occurs at the molecular level, by recognizing foreign molecules delivered by infecting pathogens (non-self), which need to be distinguished from host substances (self). This second layer, in turn, has two parts, whose interplay have been illustrated in the “zigzag” model (Jones and Dangl, 2006) (**Fig. 11**). The first part is shared with animals and comprises detection of pathogen (or microbe)-associated molecular patterns (PAMPs or MAMPs) by pattern recognition receptors (PRRs). PAMPs/MAMPs are molecules that often conserved across microbial species because of their essential roles in growth or physiology. Examples are flagellin, elongation factor EF-Tu, chitin, lipopolysaccharide (LPS), as well as peptidoglycan (Boller and Felix, 2009). The defense responses following PAMPs/MAMPs perception are generally called PAMP-triggered immunity (PTI) (Chinchilla et al., 2006; Sun et al., 2013; Zipfel et al., 2004). PTI subsequently triggers a series of downstream defense responses to mount host resistance in order to rapidly restrain pathogen dispersal (Tsuda and Katagiri, 2010). However, successful pathogens can escape or suppress PTI. Once inside the host tissue, pathogens use specialized structures not only to uptake nutrients from the host but also to deliver pathogenic molecules, known as effectors, into the host. The specialized structure for exchange between fungal or oomycete hyphae and plant

cells is called haustorium (Szabo and Bushnell, 2001). Many gram-negative bacteria, such as *Pseudomonas syringae*, use filamentous supramolecular structures known as the type III secretion system (T3SS) to deliver effectors that enhance their pathogenicity (Büttner and He, 2009) and induce effector-triggered susceptibility (ETS) (Jones and Dangl, 2006). To overcome ETS, plants deploy intracellular receptors, known as resistance (R) proteins that specifically recognize effectors or host molecules whose structures are modified by the effector. This results in effector-triggered immunity (ETI), which subsequently initiates a defense-signaling cascade and induces hypersensitive response (HR) and localized cell death (Jones and Dangl, 2006). The relationship between ETI and ETS is an outstanding example of the co-evolutionary dynamics between plants and pathogenic microbes.

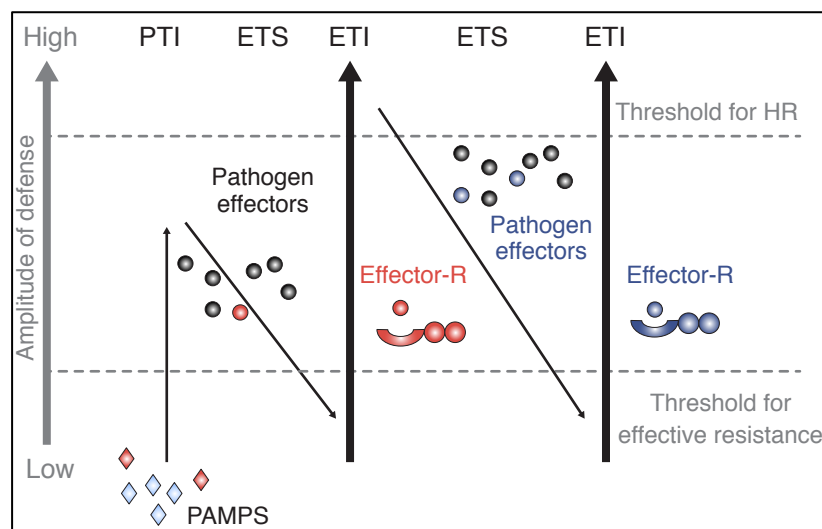


Figure 11. Zigzag model of the plant immune system (adapted and modified from Jones and Dangl, 2006). The presence of PAMPs triggers PTI, which in turn is suppressed by pathogen effector during ETS. Plants evolved R protein that can recognize the effector (in red), leading to ETI. Newly evolved effectors (in blue) can suppress ETI, resulting in ETS again, which in turn may be overcome by another set of plant R proteins (in blue), triggering ETI again. PAMP molecules are illustrated as diamonds, pathogen effectors as particles (Jones and Dangl, 2006).

PTI is the conserved layer of defense found in many immune systems (Ausubel, 2005; Nürnberger et al., 2004). Animals employ two types of PRRs to recognize PAMPs: transmembrane receptors and intracellular receptors (Ausubel, 2005). The transmembrane receptors, known as Toll-like receptors (TLRs), contain

two domains: an extracellular C-terminal leucine rich repeat (LRR) domain and an intracellular N-terminal Toll/interleukin 1 (IL-1) receptor domain. The intracellular receptors, known as CATERPILLER (CLR) or nucleotide-binding oligomerization domain (NOD) proteins, consist of three domains: a C-terminal LRR domain, a central NOD domain, and a variable N-terminal domain (Ausubel, 2005). Upon PAMP perception, TLRs and NOD proteins initiate a downstream signaling cascade, including up-regulating transcription factors and production of antimicrobial peptides and cytokines, as well as activation of caspase 1 and IL-1. The downstream signaling components thereby trigger immune-mediated apoptosis in the host to restrict pathogen colonization (Ausubel, 2005).

Plant PTI, however, utilizes only transmembrane PRRs to recognize PAMPs. Similar to the overall structure of animal TLRs, plant PRRs also consist of two domains: a C-terminal LRR domain and an N-terminal kinase domain. All known plant PRRs belongs to the family of receptor-like kinases (RLKs) (Ausubel, 2005). In *Arabidopsis thaliana*, the RLK-encoding gene family consists of more than 600 genes grouped into 44 subfamilies (Shiu and Bleecker, 2001). Examples of *A. thaliana* RLKs are FLS2 (FLAGELLIN SENSITIVE 2), EFR (EF-TU RECEPTOR), and CERK (CERAMIDE KINASE) that recognize flg22 (a conserved 22-amino-acid peptide of bacterial flagellin), EF-Tu, and chitin, respectively (Miya et al., 2007; Zipfel et al., 2006; Zipfel et al., 2004). Flg22-activated FLS2 rapidly associates with a second RLK, BAK1 (BRI1-ASSOCIATED KINASE 1), which dimerizes with another co-receptor, BIK1 (BOTRYTIS-INDUCED KINASE 1) in the absence of flg22 (Chinchilla et al., 2007; Lin et al., 2014; Lu et al., 2010; Schulze et al., 2010; Sun et al., 2013). Subsequent trans-phosphorylation of BAK1 and FLS2 is required for flg22-dependent response activation (Chinchilla et al., 2007; Roux et al., 2011; Schulze et al., 2010). Dimerization of receptor kinases and phosphorylation upon ligand recognition is now considered a common feature of PTI (Boller and Felix, 2009). PTI includes activation of microtubule-associated protein kinase (MAPK) signaling, up-regulation of pathogen-responsive genes, formation of reactive oxygen species (ROS), release of antimicrobial substances, and increase of callose accumulation that strengthens the host cell wall at infected sites (Bigéard et al., 2015). ROS burst, one of the early PTI responses, is produced by NADPH oxidases, which belong to the respiratory burst oxidase homolog (RBOH) family (Kadota et al., 2015). Two members of *RBOH* gene family, *RBOHD* and *RBOHF*, have been shown to be involved in ROS generation in *A. thaliana* upon challenging plants with different strains of *P. syringae* (Torres et al.,

2002). While *RBOHD* likely contributes more to ROS production in leaves, *RBOHF* has a stronger effect on cell death (Torres et al., 2002). *RBOHD* has been shown to be part of the FLS2/BAK1/BIK1 complex at the plasma membrane, in which *RBOHD* directly interacts with and is phosphorylated by BIK1 upon PAMP perception (Kadota et al., 2014; Li et al., 2014).

What is called ETI today was initially conceptualized as the gene-for-gene hypothesis based on the genetics of rust (*Melampsora lini*) disease resistance in flax (*Linum usitatissimum*) by H.H. Flor in the 1940s (Flor, 1942). Molecular studies over the last two decades have revealed that the biochemical basis consists of plant R proteins that recognize pathogen race-specific effectors (Dangl and Jones, 2001). Most R proteins are nucleotide-binding domain (NB) and leucine rich repeat (LRR) containing receptors (NLRs) (Ting et al., 2008). They are further classified into two sub-classes: TIR-NLRs (or TNLs) with a TOLL/interleukin 1 receptor domain at the N-terminus; CC-NLRs (or CNLs) with a coiled-coil (CC) domain (Dangl and Jones, 2001). The N-terminal TIR and CC domains is unique in plant NLRs (Jacob et al., 2013; Yue et al., 2012) while the central NB structure is also found in animal kinase and NOD receptors (Ausubel, 2005). Plants also encode atypical NLRs that carry only either NB-LRR or CC-NB, and these have been hypothesized as the ancestral members of the receptor family (Dangl and Jones, 2001; Yue et al., 2012). It is noted that the TIR domains of plant intracellular TNL receptors and of animal transmembrane TLR receptors, although identical in structural basis, belong to two different immune receptor classes that recognize distinct pathogenic molecules, effectors and PAMPs.

The downstream events following R protein activation appear to overlap with those of PTI, yet with enhanced robustness in signaling upon effector interference (Tsuda et al., 2009). The overlapping events, including transcriptional reprogramming, MAPK activation, and production of phytohormones, indicate a synergistic relationship between PTI and ETI (Tsuda et al., 2009). ROS burst can also be induced during ETI, but at a slower pace than during PTI (Kadota et al., 2015). Evidence of the relationship between ETI and ROS comes from EDS1 (ENHANCED DISEASE SUSCEPTIBILITY 1), one of the regulators of TNL receptors (Feys et al., 2001; Parker et al., 1996; Wirthmueller et al., 2007), being required for *RBOHD*-dependent oxidative responses (Straus et al., 2010).

2. Trade-off between immunity and growth in plants

Resistance is a costly trait that requires energy and nutrient consumption, often at the expense of growth and development (Karasov et al., 2014; Tian et al., 2003; Todesco et al., 2010). In line with this thought, high growth rate can potentially incur a risk of disease susceptibility (Tian et al., 2003). The negative impact of defense response on plant fitness has been demonstrated by measuring the fitness cost in plants carrying an extra *R* gene in the genome (Tian et al., 2003). Transgenic *A. thaliana* lines carrying *RPM1* (*RESISTANCE TO PSEUDOMONAS SYRINGAE PV. MACULICOLA 1*) have fewer siliques and seeds per silique, and less shoot biomass than the non-*RPM1* carriers. Tian and colleagues (2003) emphasized the large magnitude of the cost in the *RPM1*-carrier plants as the total seed production of these plants was on average 9% less than that produced by the non-*RPM1* carrier plants (Tian et al., 2003). Given that *A. thaliana*, and plants in general, have dozens, often hundreds of *R* genes, several questions regarding *R* gene-mediated cost have been raised: (1) Do all *R* genes incur fitness costs? (2) What are the mechanisms of the growth/resistance antagonism? And (3) How are fitness costs minimized? To answer these questions, one approach is to examine the molecular and genetic pathways interconnecting plant growth and immunity.

In addition, because phytohormones are participating in numerous plant growth and defense pathways, it has become evident that hormone crosstalk is important for fine-tuning the growth and defense balance. The key hormonal players of plant immunity are salicylic acid (SA), jasmonic acid (JA) and ethylene (ET), whilst those governing plant growth and development are mostly auxin, abscisic acid (ABA), cytokinins, gibberellins and brassinosteroids (Denancé et al., 2013; Huot et al., 2014). Auxin, involved in many growth-related aspects of development (Kieffer et al., 2010; Swarup and Peret, 2012), has negative impacts on defense responses. Cell walls of rice treated with auxin facilitate *Xanthomonas oryzae* infection (Ding et al., 2008). In addition, many pathogenic bacteria of the *Agrobacterium*, *Erwinia* and *Pseudomonas* genera are able to synthesize auxin and/or hijack auxin biosynthesis and signaling in plants, thereby promoting disease (Brandl and Lindow, 1998; Gaudin and Jouanin, 1995; Glickmann et al., 1998; Suzuki et al., 2003; Yang et al., 2007). Several PAMPs (e.g. flg22) and effectors (e.g. AvrRpt2) have auxin signaling or homeostasis as a potential target (Chen et al., 2007; Navarro et al., 2006). Suppression of auxin signaling components through miRNAs enhances *A. thaliana*

resistance upon flg22 challenge (Navarro et al., 2006). Auxin can specifically interfere with SA-mediated defense. Overexpression of the AFB1 F-box protein, a plant auxin receptor, suppresses SA biosynthesis induced by pathogen infection, rendering plants more susceptible to infection (Robert-Seilaniantz et al., 2011).

The effect of defense hormones, for example SA, on fitness can be validated in the presence vs. absence of pathogen infection. SA is important for plant resistance against biotrophic and hemi-biotrophic pathogens (Fu and Dong, 2013). Elevated SA accumulation or signaling can cause constitutive activation of defense, which in turn reduces growth. Reduced growth and seed set is seen in wheat treated with a SA synthetic analog, benzothiadiazole (BTH), in the absence of pathogens (Heil et al., 2000). However when challenging wheat plants with the powdery mildew *Erysiphe graminis*, BTH application not only reduced disease symptoms by 35%, but also increased wheat yield by 17% (Görlach et al., 1996). Because different hormone pathways are interconnected, SA can interfere growth and development by negatively hijacking the biosynthesis and signaling of other growth hormones such as auxins, gibberellins, and brassinosteroids (Huot et al., 2014). BTH treatment down-regulates a number of auxin-related genes including those involved in auxin reception, import, export and signaling (Wang et al., 2007), and up-regulates two genes encoding GH3 enzymes that lower the level of free endogenous auxin (Woodward and Bartel, 2005). Auxin signaling is inhibited due to the stabilization of Aux/IAA transcriptional repressor either via an enhanced interaction of Aux/IAA with TIR1 (TRANSPORT INHIBITOR RESPONSE1) F-box protein (Wang et al., 2007) or reduction in expression of a regulatory miRNA (Navarro et al., 2006). Modification of a particular hormonal signaling pathway can result in disturbance in hormone homeostasis of other pathways, which in turn can affect balance between growth and defense if these hormonal pathways are mis-regulated.

Constitutive expression of a defense hormone is always disadvantageous. To minimize cost caused by strong pathogen pressure, for example, plants develop a so-called “immunological memory”, whose molecular basis is different from immunological memory in animals (Sun et al., 2014). Plants that have been exposed to a biotic stress such as pathogen attack (or priming state) can systemically induce long-lasting responses in a more rapid and more robust manner to subsequent stress, known as systemic acquired resistance (SAR) (Vlot et al., 2008). SA, which is a crucial component of SAR, can exist as various biological derivatives. One of them,

methyl-SA (MeSA), generates the long-distance mobile signal for SAR by hydrolyzing MeSA into SA that subsequently triggers SAR in the systemic tissue, the tissue that does not receive the primary infection (Park et al., 2007). Therefore, SAR can help plants to be effectively resistant against secondary infection.

3. NLR-mediated effector recognition in plants

3.1. Recognition specificity of NLRs

The specificity of NLRs has been analyzed using NLR homologs that directly bind to different effectors (Botella et al., 1998; Xiao et al., 2001; Rose et al., 2004; Dodds et al., 2006; Krasileva et al., 2010, 2011; Bourras et al., 2015). Correlation between NLR-mediated resistance and effector recognition shows that different NLR variants have distinct spectra of specificity. For example, polymorphic *L* locus in flax *L* proteins shows recognition specificity for different strains (or races) of flax rust fungus *M. lini* (Ellis et al., 1999; Dodds et al., 2006). This phenomenon is called race-specific recognition. In another example, three members of *RPP1* (*RECOGNITION OF PERONOSPORA PARASITICA1*) locus in *A. thaliana* accession Wassilewskija-0 (*Ws-0*), *RPP1-WsA*, *RPP1-WsB* and *RPP1-WsC*, confer different levels of resistance to different isolates of the downy mildew *H. arabidopsidis ex parasitica* (or *Hpa*) such as Noco2, Emoy2, Maks9 and Cala2 (Botella et al., 1998). While *RPP1-WsA* can recognize and confer resistance to all four isolates, *RPP1-WsB* recognizes only Noco2, Emoy2 and Maks9, and *RPP1-WsC* only Noco2 (Botella et al., 1998). Follow-up studies on different *RPP1* genes and *Hpa* isolates confirmed that direct interaction of the *RPP1* variants with the matching effector variants of *ATR1* determines specificity (Krasileva et al., 2010, 2011; Steinbrenner et al., 2015). In a global analysis of *A. thaliana/Hpa* interactions, Krasileva and colleagues (2011) have provided evidence that divergent *A. thaliana* populations often adopt different recognition abilities to *Hpa* effector variants and that intermediate resistance levels are prevalent among *A. thaliana/Hpa* interactions, suggesting an arms-race co-evolution between the cognate *NLR* genes and effectors (Krasileva et al., 2011).

Systematic studies of interactions between a large number of immune-related *A. thaliana* proteins with effector proteins from the oomycete *Hpa* and the bacterium *P. syringae* have shown that effectors tend to converge on the same plant proteins (Mukhtar et al., 2011). As further discussed in the following sections, effector

recognition is not a simple one effector – one target relationship, and the number of NLR-effector systems that we know and have been studying so far constitute only the tip of the iceberg, generally the strongest interactions and resistances. It suggests that many more, weaker NLR – effector interactions exist as a reservoir for the evolution of full-fledged resistance.

Table 1. Plant NLR pairs in pathogen resistance

NLR pair	Type of NLR	Host plant	Pathogen	Reference
Pikm1-TS/ Pikm2-TS	(CC)/ unknown	<i>Oryza sativa</i>	Rice blast fungus (<i>Magnaporthe grisea</i>)	Ashikawa et al., 2008
RGA4/ RGA5	CC/CC _{RATX1}	<i>Oryza sativa</i>	Rice blast fungus (<i>Magnaporthe oryzae</i>)	Césari et al., 2013; Césari et al., 2014
RPP2A/ RPP2B	TIR/TIR	<i>A. thaliana</i>	<i>Hpa</i> isolate Cala2	Sinapidou et al., 2004
RPS4/ RRS1	TIR/TIR _{WRKY}	<i>A. thaliana</i>	<i>P. syringae</i> (AvrRPS4), <i>R. solanacearum</i> (PopP2), <i>Colletotrichum higginsianum</i>	Narusaka et al., 2009
Lr10/ RGA2	CC/CC	<i>Triticum</i> spp.	Wheat leaf rust (<i>Puccinia triticina</i>)	Loutre et al., 2009
TAO1/ RPM1	TIR/CC	<i>A. thaliana</i>	<i>P. syringae</i> (AvrB)	Eitas et al., 2008

Another way to increase the recognition specificity and confer new resistance may be cooperation between different NLR receptors, as reported in several plant species (Table 1). The first example of a functional NLR pair in *A. thaliana* identified by map-based cloning is *RPP2A/RPP2B*, which are encoded by adjacent genes in the genomes (Sinapodou et al., 2004). *RPP2A* and *RPP2B* together complement an incomplete resistance conferred by each single gene to the *Hpa* isolate Cala2 (Sinapodou et al., 2004). In wheat, the partners in the CNL pair *Lr10* and *RGA2* cooperatively function in resistance to leaf rust caused by *Puccinia triticina*, in which *RGA2* is postulated to act downstream of *Lr10* in signaling (Loutre et al., 2009). Cooperation of NLRs also can occur between NLRs belonging to different classes or not encoded at the same locus. For example, resistance to pathogenic *P. syringae* effector AvrB is conferred by a TNL-encoding gene, *TAO1* (*TARGET OF AVR B OPERATION 1*), together with an unlinked CNL gene, *RPM1*, in *A. thaliana* (Eitas et al., 2008). Cooperation has also been described between one canonical NLR and the other containing an addition domain, examples being *A. thaliana* RPS4 (RESISTANCE TO *PSEUDOMONAS SYRINGAE* 4)/RRS1 (RESISTANCE TO

RALSTONIA SOLANACEARUM 1) and rice *RGA4/RGA5* (*RESISTANCE GENE ANALOG 4/5*) (Williams et al., 2014; Césari et al., 2014). In both cases, the two partners have distinct roles in contributing to the overall resistance conferred by the pair. While RRS1 and RGA5 mainly serve as effector-recognition sensors, RPS4 and RGA4 are signaling triggers (Williams et al., 2014; Césari et al., 2014; Le Roux et al., 2015; Sarris et al., 2015). The separation of functions among the partners in an NLR pair can also help prevent inappropriate immune activation, which is costly and often comes at the expense of plant growth and development, as discussed above. The existence of NLR pairs in recognition of pathogens therefore suggests that a structural and functional co-evolution of these NLRs is keys to mount a successful immune defense.

3.2. NLR diversity

The number of the genes encoding NLRs varies greatly across angiosperm genomes, and there is no correlation with genome size (Jacob et al., 2013). Some species carry only a small number of *NLR* genes, such as papaya (*Carica papaya*) with only 34 genes and cucumber (*Cucumis sativus*) with 53 genes. Other species such as rice (*Oryza sativa*) or grape (*Vitis vinifera*) encode more than 400 *NLR* genes (Jacob et al., 2013) (**Fig. I2A**). Interestingly, TNL encoding genes are not found in monocots such as purple false brome (*Brachypodium distachyon*), rice (*O. sativa*), sorghum (*Sorghum bicolor*), and maize (*Zea mays*) (Jacob et al., 2013) (**Fig. I2B**).

Genome-wide analyses in different plant species have demonstrated that NLR encoding genes are found unevenly distributed in the genome, with many of them residing in close proximity, forming so-called *NLR* clusters that contain multiple closely related gene copies or paralogs (Dangl and Jones, 2001; Guo et al., 2011; Jupe et al., 2012; Meyers et al., 2003; Zhou et al., 2004b). NLR genes can also exist in single loci with one or multiple functional alleles (Dangl and Jones, 2001). In the reference genome from *A. thaliana* Col-0 accession, 46 *NLRs* are found as singletons (no related copy in close proximity), 25 loci comprise two *NLR* copies, seven loci contain three copies and individual loci with up to nine NLR encoding genes (Dangl and Jones, 2001). Similar genomic organizations of NLR genes have also been identified in other plant species. For example in flax, an individual yet polymorphic NLR gene encoded at the *L* locus contains 12 different alleles conferring resistance to different strains of the flax rust fungus *M. lini* (Ellis et al., 1999). Another flax rust resistance locus is the *M* cluster, consists of 15 related genes or paralogs

(Anderson et al., 1997). Similarly, in wheat, *Pm3* conferring race-specific resistance to powdery mildew fungus *Blumeria graminis* is a cluster containing 10 paralogs (Srichumpa et al., 2005).

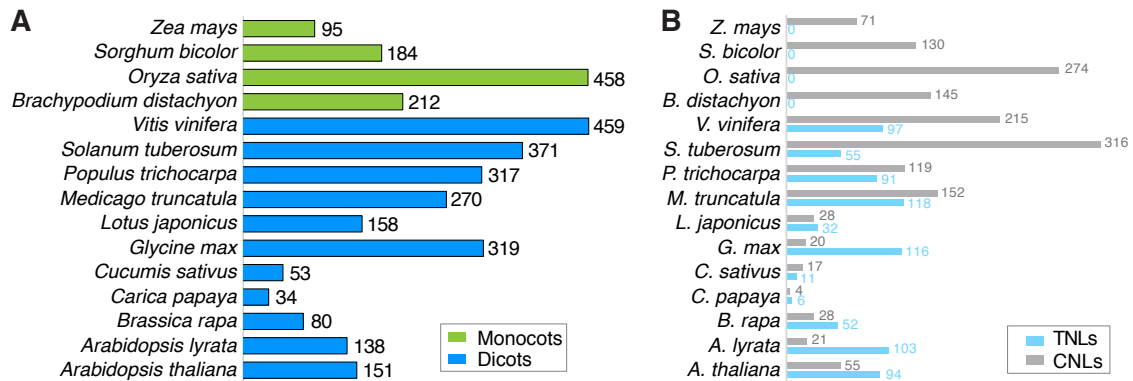


Figure 12. Plant NLR gene repertoires (summarized by Jacob et al., 2013)

Extreme polymorphisms are commonly found in NLR genes, suggesting a role for balancing selection in maintaining the diversity of these genes (Bergelson et al., 2001; Wang et al., 2011). Variations of *NLR* clusters can be observed between and within species levels. At both levels, *NLR* cluster homologs often differ in gene copy number. For example, the *RPP7* (*RECOGNITION OF PERONOSPORA PARASITICA 7*) cluster contains eight genes in the *A. thaliana* Col-0 accession, while it contains only three genes in *A. lyrata* (Guo et al., 2011). Similarly, the *DM2* (*DANGEROUS MIX 2*) gene cluster, which is located at the same locus with *RPP1*, from different *A. thaliana* accessions also varies in size: it contains two genes in Col-0, and eight genes in Bla-1 and Uk-1 accessions (Chae et al., 2014). Paralogs within the same cluster and in different accessions can be highly polymorphic in their sequences, particularly in the region encoding the LRR domain, which is responsible for effector recognition (Mondragón-Palomino et al., 2002; Bakker et al., 2006; Chen et al., 2010; Seeholzer et al., 2010; Chae et al., 2014). Polymorphisms at the *DM2* locus are distributed differently in each of the three typical NLR domains, with the highest polymorphism rate located at the LRR region and the lowest at the NB-ARC region (Chae et al., 2014). For NLRs that perceive pathogen effectors through direct interaction at the LRR domain (such as *DM2/RPP1* cluster), the high polymorphism level at this coding region could be explained by balancing selection produced by pathogen pressures. Evolutionarily conserved nature in the NB-ARC sequence

among NLR receptors implies an extremely conserved molecular function performed by the domain. As being further discussed below, NB-ARC domain is responsible for modulating the active or inactive states of an NLR, therefore the low polymorphism rate in this region may also prevent NLRs from untimely activation. The great diversity in LRR sequence compared to other domain sequence within NLRs implies a sign of diversifying selection imposed by the co-evolution between *NLR* receptor genes and their cognate effectors. Genetic variation of NLR genes and clusters therefore allows us to functionally study NLR activities.

3.3. Effector-recognition mechanisms

Direct recognition

The first notion implying direct effector recognition has come from the gene-for-gene hypothesis postulated by Flor, stating that rust resistance is determined by specific matching gene pairs – one from the flax host and the other from the rust fungus (Flor, 1942; 1947; 1955; 1971). A concrete example supporting the gene-for-gene hypothesis is the polymorphic *A. thaliana* TNL *RPP1* locus and the matching *Hpa ATR1* effector gene. Different *ATR1* alleles from various *Hpa* strains are only recognized when matched with distinct alleles at the *RPP1* locus, suggesting that the recognition is race-specific (Krasileva et al., 2010, Krasileva et al., 2011, Steinbrenner et al., 2015).

Direct recognition of Avr effectors by the corresponding NLR receptor is supported by evidence both from yeast-two hybrid (Y2H) system as well as from co-immunoprecipitation (coIP). Physical interaction has been observed, for example, for rice Pik/ *M. oryzae* AVR-Pik (Kanzaki et al., 2012), *A. thaliana* RRS1-R/ *Ralstonia solanacearum* PopP2 (Deslandes et al., 2003), *A. thaliana* RPP1/ *Hpa ATR1* (Krasileva et al., 2010, Steinbrenner et al., 2015), and flax L/ *M. lini* AvrL variants (Dodds et al., 2006; Ravensdale et al., 2012; Bernoux et al., 2016). Particularly, the LRR domain, but not TIR and NB domains, of RPP1 has been shown to associate with ATR1 effectors (Krasileva et al., 2010). These findings together with the high level of polymorphisms in the LRR domain of NLR receptors support a direct recognition model.

Indirect recognition

Considering that a large number of pathogen molecules can potentially be delivered into plant cells, direct recognition of effectors by a limited number of plant

NLR immune receptors is not sufficient to fully explain how plants can effectively fight multiple pathogens. Based on experimental data, different models involving indirect recognition have been proposed, including the “guard model” and the “decoy model” (Dangl and Jones, 2001; van der Hoorn and Kamoun, 2008) (**Fig. I3**). In these models, effectors do not directly bind to the NLR receptor, but to other host proteins, known as operative targets, leading to structural or biochemical modification of the target.

In the guard model, the operative target acts at the same time as a guardee, and effector-mediated modifications of the guardee can be sensed by an NLR receptor (a guard protein) (Dangl and Jones, 2001) (**Fig. I3A**). The guardee itself is required for virulence of the effector protein when not sensed by an NLR receptor. The guard model posits that guard NLR receptors can sense effector-mediated modifications of the effector target (or guardee) proteins and subsequently mount immune responses (Dangl and Jones, 2001). The classical guard model often implies a one-on-one matching relationship of effector, guardee, and guard protein (Dangl and Jones, 2001; **Fig. I3A**), but one guardee can be targeted by multiple pathogen effectors with different origins or different biochemical properties, while modifications of a guardee can be recognized by multiple host NLRs. An example supporting this model comes from studies of two *A. thaliana* plasma membrane CNL receptors, RPM1 and RPS2 (RESISTANCE TO *PSEUDOMONAS SYRINGAE* 2), in perceiving unrelated T3SS effectors AvrRpm1, AvrB, and AvrRpt2 secreted by different *P. syringae* strains (Mackey et al., 2002, 2003; Axtell and Staskawicz, 2003). RPM1 can recognize and confer resistance to AvrRpm1 and AvrB, while RPS2 to AvrRpt2. RIN4 (RPM1-INTERACTING PROTEIN 4), a host target of the three effectors as well as a guardee of both RPM1 and RPS2, has been shown to directly associate with both the effectors and the CNL receptors (Mackey et al., 2002, 2003; Axtell and Staskawicz, 2003, Desveaux et al., 2007). In the absence of RPM1 and RPS2, AvrRpm1 and AvrRpt2 are able to enhance the growth of *P. syringae* bacteria and suppress PTI responses in *A. thaliana* (Kim et al., 2005) through post-translational modifications of their host target, RIN4 (Mackey et al., 2002, 2003; Axtell and Staskawicz, 2003). AvrRpm1 and AvrB induce RIN4 phosphorylation (Mackey et al., 2002; Desveaux et al., 2007), while AvrRpt2 induces RIN4 degradation (Mackey et al., 2003; Axtell and Staskawicz, 2003). RPM1 and RPS2 effectively suppress the growth of *P. syringae* strains expressing AvrRpm1, AvrB, and AvrRpt2 effectors, and induce robust HR (Mackey et al., 2002, 2003; Axtell and Staskawicz, 2003; Desveaux et al., 2007).

However, the RPM1-mediated resistance to AvrRpm1 and AvrB is reduced in the loss-of-function *rin4* mutant (Mackey et al., 2002). This finding and the physical association of RIN4 with both AvrRpm1 and AvrB as well as with RPM1 suggest that RPM1 can sense effector-mediated modifications on RIN4 to trigger defense responses. In fact, AvrRpm1- and AvrB-induced phosphorylation of RIN4 activates RPM1-mediated cell death response in the heterologous system in *Nicotiana benthamiana* and also in *A. thaliana* (Mackey et al., 2002; Desveaux et al., 2007; Chung et al., 2011). In the case of AvrRpt2, a cysteine protease, it leads to RIN4 degradation followed by proteolytic cleavage of the substrate (Mackey et al., 2003; Axtell and Staskawicz, 2003; Chisholm et al., 2004, Kim et al., 2005), which in turn serves as modified signal to activate RPS2-mediated resistance (Coaker et al., 2005). Therefore, RIN4 could act as a common guardee, targeted by different effectors and at the same time guarded or sensed by different NLR receptors through different molecular modifications.

One question remains is that how the same RIN4 protein can function as a hub? *RIN4* encodes a 211-amino-acid protein consisting of plant-specific nitrate-induced domain (NOI) on both N- and C-terminal regions, which are responsible for interaction with the effectors, and the C-terminal palmitoylation/prenylation sequence containing triple cysteines, which anchors RIN4 to the plasma membrane and requires for the activation of RPM1 (Kim et al., 2005; Desveaux et al., 2007; Afzal et al., 2011). A recent study has suggested that RIN4 may have a flexible structure with unfixed three-dimensional regions interspersed along the molecule (Sun et al., 2014). This type of protein, known as intrinsically disordered proteins, plays roles in numerous signaling pathways and protein interactions in animals (Collins et al., 2008; Iakoucheva et al., 2002; Sandhu, 2009). Having the flexible structure, RIN4 might easily adopt a so-called “induced fit” (Arai et al., 2015) of conformations due to specific effector-induced modifications. The plasticity in modified RIN4 conformation might therefore explain why it could interact with different NLR receptors (Sun et al., 2014).

However, the guard model alone does not explain all the indirect recognition patterns performed by plant immune system. Several studies have discovered cases of an effector manipulating multiple host targets to maximize pathogenicity (Xiang et al., 2008; Shan et al., 2008; Wang et al., 2015) (**Fig. I3B**). For example, the *P.*

syringae AvrPto effector can target different PRRs such as FLS2 and EFR in tomato, and thereby inhibits PTI mediated by both PRRs (Xiang et al., 2008).

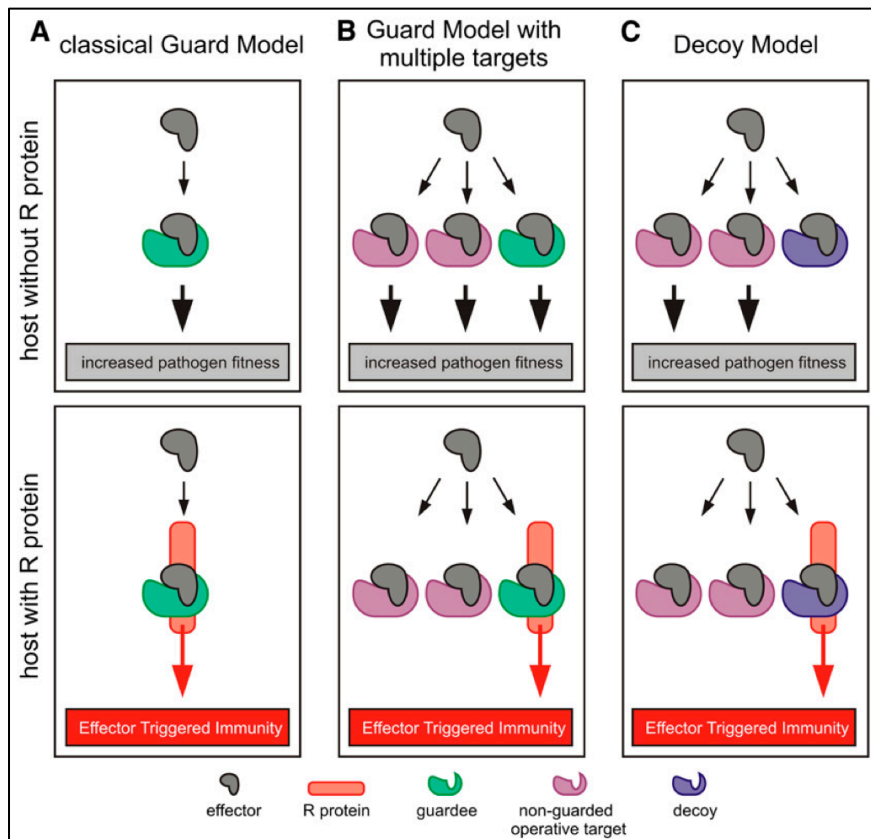


Figure 13. Guard and decoy models (adapted from van der Hoorn and Kamoun, 2008).

Another mode of indirect effector recognition has been summarized in the decoy model. Plants mitigated the effect of guardee modification by generating “fake” effector targets, which are termed decoys (van der Hoorn and Kamoun, 2008) (**Fig. 13C**). Unlike guardees, the absence of decoys does not affect pathogenicity of an effector (van der Hoorn and Kamoun, 2008). Modifications of decoys by effectors, however, are perceived by matching NLRs, leading to ETI (van der Hoorn and Kamoun, 2008; Zipfel and Rathjen, 2008). An example comes from studies of the activity of tomato Prf (*PSEUDOMONAS* RESISTANCE AND FENTHION SENSITIVITY), a CNL receptor, in conferring resistance to *P. syringae* AvrPto (Mucyn et al., 2006; Ntoukakis et al., 2012). AvrPto targets several tomato PRRs including FLS2 and EFR for its pathogenicity (Xiang et al., 2008). Subsequent phosphorylation of AvrPto by FLS2 is essential for AvrPto pathogenicity and the

absence of FLS2 suppresses AvrPto virulence, indicating that FLS2 is the operative target (Xiang et al., 2008). At the same time, AvrPto also targets Pto kinase (Tang et al., 1996), which in turn activates Prf-mediated defense responses, involving Pto-Prf oligomerization (Mucyn et al., 2006; Ntoukakis et al., 2012). However, the absence of Pto does not inhibit AvrPto virulence, therefore did not impede the growth of the *P. syringae* strain expressing *avrPto* in tomato (Chang et al., 2000). These findings suggested that Pto is a decoy target of AvrPto.

The dynamics of plant NLR receptors in indirectly perceiving diverse pathogen effectors are also demonstrated in an example of *A. thaliana* ZAR1 (HopZ-ACTIVATED RESISTANCE 1) that can recognize effectors from distinct origins and with different enzymatic activities, e.g. HopZ1a from *P. syringae* and AvrAC from *Xanthomonas campestris*, by forming different pre-activation complexes with other host protein partners (Lewis et al., 2013; Wang et al., 2015). Genetic screens for suppressors of HopZ1a or AvrAC-induced HR in *A. thaliana* identified two mutants, namely *zed1* (*hopZ-ETI deficient1*) and *rks1* (*resistance related kinase 1*), which have impaired resistance to HopZ1a and AvrAC, respectively (Lewis et al., 2013; Wang et al., 2015). Both ZED1 and RKS1 are members of the receptor-like cytoplasmic kinase (RLCK) family of pseudokinases, and independently associate with ZAR1 in different preformed complexes, i.e. without effectors (Lewis et al., 2013 and Wang et al., 2015). HopZ1a can bind to ZED1 and subsequently acetylates it. HopZ1a virulence is still retained in the *zed1* mutant plants, suggesting that ZED1 acts as a decoy target of HopZ1a, although the real target remains to be identified (Lewis et al., 2013). AvrAC is indirectly recognized by ZAR1 through a different mechanism, requiring not only RKS1, but also an additional protein, PBL2 (AvrPphB SUSCEPTIBLE 1 (PBS1)-LIKE2), a paralog of the kinase receptor BIK1. AvrAC uridylylates PBL2 and subsequently leads to the recruitment of PBL2 to the ZAR1/RKS1 complex, which in turn can sense the AvrAC-induced modification on PBL2 and trigger defense responses (Guy et al., 2013; Wang et al., 2015). These findings demonstrate that the formation of pre-activation complexes between an NLR and different host targets (decoys) can expand the NLR recognition specificity. This also suggests that one can engineer a decoy protein to trap different effectors, thereby broadening NLR recognition specificity. To test this idea, Kim and colleagues (2015) have used the system of a CNL RPS5 (RESISTANCE TO *PSEUDOMONAS SYRINGAE*5) and PBS1 (AvrPphB SUSCEPTIBLE 1) – the latter being a decoy target of *P. syringae* AvrPphB. The authors modified the recognition site in PBS1,

which is normally targeted by AvrPphB, to other sites that would be recognized by different bacterial effectors (*P. syringae* AvrRpt2) or viral elicitors (Nla protease from tobacco etch virus). The newly acquired target sites in modified PBS1 strikingly allowed RPS5 to recognize AvrRpt2 and Nla as robustly as the authentic PBS1 allowed RPS5 to recognize AvrPphB (Kim et al., 2016). This finding thus brings us a new chance to apply the “decoy engineering” approach to numerous plant species, especially crops, for broad resistance spectrum.

4. NLR-mediated immune activation

4.1. NLR domain structure and associated function

As discussed, a typical plant NLR receptor consists of three domains: N terminal domain (TIR or CC), central NB-ARC domain, and LRR domain. The N-terminal domain is usually responsible for transducing the downstream immune signaling upon effector perception (Lukasik and Takken, 2009; Takken et al., 2006). The molecular mechanism of downstream signaling initiation will be further discussed in following sections. The C-terminal LRR domain comprises tandem LRR motifs with conserved pattern LxxLxLxxN/CxL. Crystallized LRR domains from mammalian and plant proteins suggest that the domain structure is relatively conserved and forms a horseshoe shape, providing a platform for ligand binding (Kobe and Deisenhofer, 1993; Kobe and Kajava, 2001; She et al., 2011; Sun et al., 2013). The central NB-ARC sequence is also highly conserved among animal and plant proteins (Takken et al., 2006; van der Biezen and Jones, 1998). Based on structure homology prediction, the plant NB-ARC domain is postulated to contain three subdomains: NB, containing the so-called P-loop nucleoside-triphosphatase (NTPase) fold, followed by a four-helix fold bundle (called ARC1) and a wing-helix fold (called ARC2) (Albrecht and Takken 2006, Takken et al., 2006, Lukasik et al., 2009). Together, NB, ARC1 and ARC2 form a pocket for nucleotide binding and most of the conserved residues of the NB-ARC domain reside at this binding pocket (Albrecht and Takken 2006, Takken et al., 2009).

The most conserved motif in the NB subdomain is termed WalkerA/P-loop with the consensus sequence GxxxxGKS/T. The P-loop plays a crucial role in regulating NLR activity by binding to either ADP or ATP. ADP is preferentially bound in an inactive (or “OFF”) state of the receptor when it does not bind to any effector,

while ATP in an active (or “ON”) state upon the receptor mediated recognition of an effector (Takken et al., 2006, Lukasik et al., 2009). Another conserved motif located at the ARC2 subdomain consists of a consensus sequence of Methionine-Histidine-Aspartate, known as MHD motif. The motif has been hypothesized to participate in ADP binding and nucleotide-dependent conformation change, and therefore maintaining the inactive state of the NLR (vanOoijen et al., 2008; Takken et al., 2006). Different activity states of plant NLR receptors are proposed to associate with protein conformation changes involving domain reorganization (Moffet et al., 2002; Lukasik et al., 2009; Sloomweg et al., 2013, Steinbrenner et al., 2015; Bernoux et al., 2016).

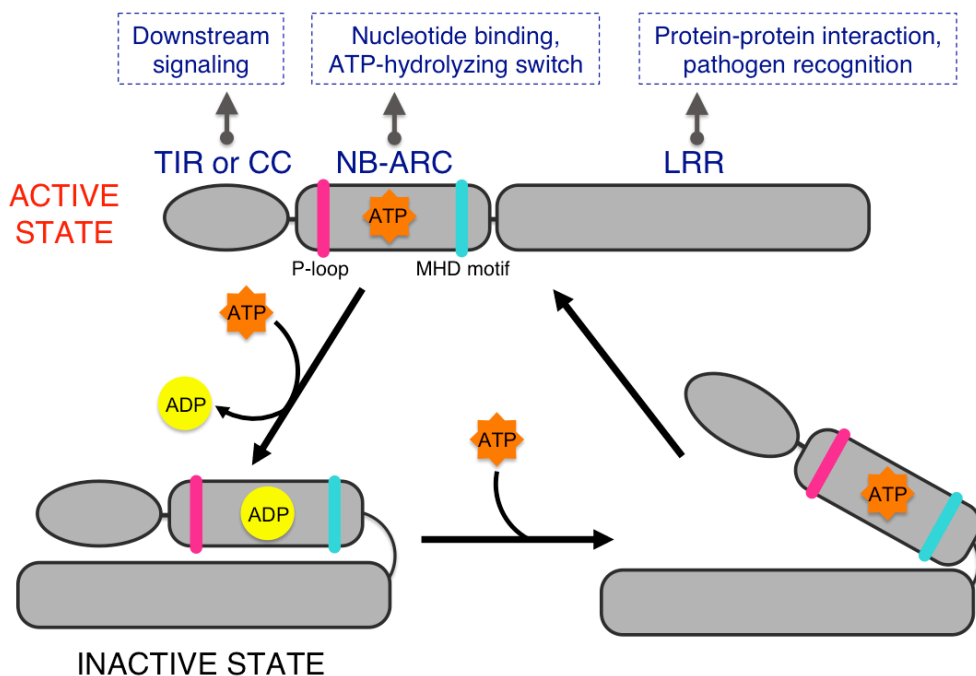


Figure 14. Illustration of a plant NLR activation model (Adapted from Takken et al., 2006; Lukasik et al., 2009). Functions of each domain are shown on the top. The NLR activation involves three reversible states. In the inactive state, the NLR receptor has a tightly folded conformation and binds to ADP. Effector recognition induces conformational reorganization of NLR domains and facilitates ATP binding. In the active state, the NLR has an open conformation. Hydrolysis of ATP into ADP resumes to the NLR inactive state.

Several modeling studies have proposed that the mode of NLR activation involves three reversible states (**Fig. 14**) (Takken et al., 2006; Lukasik et al., 2009). In the ADP-associated inactive state, the C-terminal LRR domain embraces the NB-ARC domain and the N-terminal domain, resulting in a tightly folded or closed

conformation. Effector recognition by the LRR domain presumably alters interaction contacts at the N-terminal part of the LRR domain and ARC2 subdomain, leading to a more relaxed protein conformation. In the active state, which is characterized by the exchange of ADP by ATP, the NLR receptor is speculated to have a completely unfolded or open conformation. This open conformation could therefore facilitate downstream signaling components to access the signal transducing N-terminal domain. The hydrolysis of ATP into ADP can subsequently reverse the receptor into the inactive state by accompanying conformation refolding (Takken et al., 2006; Lukasik et al., 2009).

4.2. An autoinhibitory conformation of NLR proteins

The inactive state of NLR receptors is supposedly maintained by interactions among different domains within a NLR molecule (Lukasik and Takken, 2009; Sukarta et al., 2016; Takken et al., 2006). A tight or closed conformation of NLR receptors in their inactive state has been shown in both animals and plants (Sukarta et al., 2016; von Moltke et al., 2013). Similar to plant NLRs, animal NLRs also are modular molecules consisting of one of a variety of possible N-terminal domains; a central NOD domain containing NBD, HD1, WHD and HD2 subdomains; and a C-terminal repetitive domain (Zhong et al., 2013). As in plants, the nature of the N-terminal domain is used to classify NOD receptors into different subgroups (Zhong et al., 2013). The topological structure of several animal NOD receptors, as partial proteins, has been dissolved. Examples are human APAF-1 (APOPTOTIC PEPTIDASE ACTIVATING FACTOR 1), nematode CED-4 (CELL DEATH PROTEIN 4), fruit fly DARK (DEATH-ASSOCIATED APAF-1-RELATED KILLER), and mouse NLRC4 (NLR FAMILY CARD DOMAIN-CONTAINING PROTEIN 4) (Hu et al., 2013; Qi et al., 2010; Riedl et al., 2005; Yu et al., 2006). Strongly physical association between the N-terminal CARD and the central subdomains of APAF-1, as shown for the C-terminus-deleted APAF-1 molecule, forms a compact conformation in the inactive state, i.e. without a cell death stimulus such as cytochrome c (Riedl et al., 2005). The inactive APAF-1 molecule exists as monomer as demonstrated by gel filtration experiments, pointing to intramolecular rather than intermolecular contacts in APAF-1 to maintain its compact conformation in the absence of a trigger. Similar to APAF-1, the inactive NLRC4 also exists as monomer and forms a tightly folded conformation through the intradomain contacts between NBD-HD2/NBD-LRR, as shown in a crystalized NLRC4 structure lacking the N-terminal CARD domain (Hu et al., 2013).

In plants, since a crystal structure is only available for the N-terminal domains of few NLR receptors, the autoinhibitory conformation and its role in NLR activation in the absence of effectors is inferred from interaction assays and domain swaps between related proteins with different activity status (Ade et al., 2007; Bernoux et al., 2016; Bernoux et al., 2011; Moffett et al., 2002; Rairdan and Moffett, 2006; Ravensdale et al., 2012; Sloatweg et al., 2013; Steinbrenner et al., 2015; Wang et al., 2015). Physical interaction between different domains in the absence of the matching effector has been detected in several NLRs, such as potato Rx (Moffett et al., 2002; Rairdan and Moffett, 2006) and *A. thaliana* RPS5 (Ade et al., 2007). Further characterization of the intramolecular interaction interface in Rx has revealed that the physical interaction between ARC2 and LRR domains presumably leads to the folded conformation of the receptor (Rairdan and Moffett, 2006; Sloatweg et al., 2013). Mutations that disrupt ARC2-LRR interaction at the same time cause Rx to trigger constitutive cell death (Sloatweg et al., 2013), indicating that a closed structural conformation formed by intramolecular interactions likely prevents inappropriate NLR autoactivation in the absence of the effector. Domain swaps between closely related but polymorphic NLR receptors with different recognition specificities have identified residues and domains contributing to the OFF state of the inactive NLR receptor. For example, domain swap experiments between potato virus X (PVX) resistance protein Rx and its homologous nematode resistance protein Gpa2 have shown that cooperation of the ARC2 subdomain and the N-terminal region of the LRR domain determines the distinct recognition specificities of each NLR (Sloatweg et al., 2013). Substitution of the ARC2 subdomain and LRR N-terminal region of Rx by those of Gpa2 results in autoactivation of Rx, suggesting that the two regions form a regulatory unit within the Rx molecule in the inactive state (Sloatweg et al., 2013). In another report, polymorphisms in the TIR domain (amino acid position 83, 85, and 86) and the NB-ARC domain (position 288) between flax L6 and L7, which differ in recognition specificity for rust fungus AvrL567 effector, have been shown to determine the activity discrepancy between the two proteins (Bernoux et al., 2016). Substitutions of the polymorphic amino acids in L7 into those in L6 convert L7 activity from inactive into active, implying that the TIR and NB domains of L7 might be held in a tight conformation formed by interactions between polymorphic sites of these two regions that inhibit effector-triggered activation of L7 (Bernoux et al., 2016). Structural prediction based on the previously crystalized L6 TIR domain (Bernoux et al., 2011) also suggests a proximal contact of the two regions in the inactive state of L proteins

(Bernoux et al., 2016). Even only small mutations in residues located around the ATP/ADP binding pocket in NB-ARC domain of potato Rx, which functions as an ON/OFF “switch” of the NLR, can significantly change its activity and recognition specificity, implying the involvement of the domain in maintaining the autoinhibitory conformation in the native condition (Harris et al., 2013). These findings suggest that plant NLRs, similar to animal NOD receptors, may also exist in a closed conformation in their inactive form. Effector recognition might induce NLR conformational changes, thereby triggering signaling.

4.3. Oligomerization between NLRs activation

Oligomerization of NLR proteins upon effector recognition has been observed in both plant and mammalian NLRs. In human cells, APAF-1 is activated in the presence of cell death stimuli, such as free cytochrome c (Hu et al., 1998). Cytochrome c can bind to the C-terminal domain and release the inhibitory state of APAF-1 through initiation of conformational changes, resulting in the formation of a homo-oligomerization structure known as apoptosome, a wheel-like heptameric structure consisting of seven APAF-1 monomers, which in turn triggers caspase activation (Riedl et al., 2005; Yuan et al., 2013). Intermolecular contacts within the apoptosome involve interfaces located at the N-terminal CARD domain and the central NOD domain (Hu et al., 1998; Riedl et al., 2005). Disruption of the APAF-1 oligomer, either by deletion of the central NOD domain or mutations in the P-loop, abolishes APAF-1-mediated signaling (Hu et al., 1998), indicating the necessity of the oligomerization for APAF-1 activation. The presence of ADP promotes the monomeric form of APAF-1, while ATP associates with the oligomeric form of APAF-1 (Reubold et al., 2011; Riedl et al., 2005), suggesting that APAF-1 inactive/active states relate to their ADP/ATP binding status. Furthermore, the ADP binding pocket forms at the junction of four domains (CARD, NB, HD1, and WHD). ADP could serve to induce spatial proximity of these domains, thereby forming the tightly packed APAF-1 molecule (Riedl et al., 2005).

In addition to homo-oligomers, several animal NLRs, such as NAIPs (NLR APOPTOSIS INHIBITORY PROTEINS) and NLRC4 in mouse, form hetero-oligomers (Hu et al., 2015; Zhang et al., 2015). Recognition of *Salmonella typhimurium* T3SS PrgJ effector induces the formation of a multi-subunit wheel-like structure consisting of one NAIP2 and 10 NLRC4 molecules known as inflammasome (Hu et al., 2015; Zhang et al., 2015). In the APAF-1 apoptosome, each subunit undergoes

conformational activation induced by its ligand prior to assembly (Riedl et al., 2015). In contrast, a single PrgJ-activated NAIP2 molecule is sufficient to trigger conformational changes in an inactive NLRC4 molecule to form a hetero-dimer NAIP2/NLRC4, which in turn activates and recruits successive NLRC4 molecules to the complex in a domino-like reaction (Hu et al., 2015; Zhang et al., 2015). In summary, information about animal NLR oligomerization and activation are helpful for understanding the activation of their plant homologs.

Plant NLRs, as deduced from *in vitro* and *in planta* interaction assays, may also form dimers or higher-order complexes. CoIP assays have demonstrated that several TNLs and CNLs can self-associate either dependent or independent of the presence of an effector (Ade et al., 2007; Gutierrez et al., 2010; Mestre and Baulcombe, 2006). Tobacco N protein, for example, self-associates upon perception of the tobacco mosaic virus (TMV) P50 effector (Mestre and Baulcombe, 2006). *Arabidopsis thaliana* RPS5 self-associates in the absence of *P. syringae* AvrPphB effector (Ade et al., 2007). Particularly, the N-terminal domains of N protein (TIR) and RPS5 (CC) can interact to form homodimers independent of the respective effectors (Mestre and Baulcombe, 2006; Ade et al., 2007). Structural data obtained from the N-terminal domains of two plant NLR proteins, flax L6 and barley MLA10, have revealed the topologies of L6 TIR/TIR and MLA10 CC/CC homodimers that can trigger constitutive cell death signaling (Bernoux et al., 2011, Maekawa et al., 2011). Mutations that disrupt L6 TIR and MLA10 CC homodimerization also impaired the autoactivation, suggesting that association at the N-terminus of these NLRs is critical for signaling activity (Bernoux et al., 2011, Maekawa et al., 2011).

Hetero-association between different plant NLRs has been shown for several NLR pairs, including *A. thaliana* RPS4/RRS1 (Williams et al., 2014) and rice RGA4/RGA5 (Césari et al., 2014). Different types of oligomerization (homodimerization and hetero-dimerization) between the partners exist in both pairs even without effector triggers (Césari et al., 2014; Williams et al., 2014), suggesting that associations of NLR receptors are not that unusual in plants either. Crystallization of the TIR domains of RPS4 and RRS1 has revealed that they form a hetero-dimer via an interface located at the N-terminal ends of the TIR domains. These interfaces are also involved in homodimerization of both RPS4 TIRs and RRS1 TIRs (Williams et al., 2014). It is noted that the L6 TIR as well as the RPS4 and RRS1 TIR domains, despite their similarity in structural topology, are very different in amino acid

sequences. Therefore the TIR/TIR interface in L6 TIR homodimers and in RPS4/RRS1 homo- and heterodimers involves different amino acid residues (Bernoux et al., 2011; Williams et al., 2014). In addition, similar to L6 TIR and MLA10 CC domain, expression of RPS4 TIR alone in tobacco can cause effector-independent cell death (Williams et al., 2014). Mutations at the RPS4 TIR/TIR interface that disrupt the homodimerization also abolish RPS4 TIR-induced HR, suggesting that homodimerization of RPS4 TIR domain is important for signaling (Williams et al., 2014). Co-expression of RRS1 TIR inhibits RPS4 TIR-mediated cell death, while mutated versions of RRS1 TIR in which heterodimerization with RPS4 is disrupted do not, indicating that association with RRS1 through the TIR domain may fine-regulate the activity of RPS4 dependent on environmental cues (Williams et al., 2014). Consistently, co-expression of full-length RPS4 and RRS1 leads to HR only in the presence of effectors (AvrRps4 and PopP2) (Williams et al., 2014). The authors have also shown that effector-triggered HR is impaired when the RPS4/RRS1 TIR heterodimerization is abolished, indicating the importance of TIR/TIR association in mediating ETI (Williams et al., 2014). Collectively, the study suggests that different types of associations, at least at the N-terminal TIR domains, exist in the RPS4/RRS1 hetero-complex. Through TIR/TIR association in the complex, RRS1 and RPS4 may contribute distinctly to complex activity. Given that RRS1 directly binds to AvrRps4 and PopP2 using the integrated WRKY domain at its C-terminus (Le Roux et al., 2015; Sarris et al., 2015), a recognition event is likely altering the suppressive action of RRS1 on RPS4, which executes signaling (Williams et al., 2014; Le Roux et al., 2015; Sarris et al., 2015). These data support that plant NLR oligomerization induced by effector recognition leads to trigger signaling.

4.4. Downstream signaling upon NLR activation

Upon activation by effector recognition, NLR receptors initiate a series of signaling events to fully mount robust immune responses. These events include transcriptional activation of defense-related genes such as *PATHOGENESIS-RELATED (PR)* genes, increased accumulation of the phytohormones and related responses (Cui et al., 2015). ROS burst from the host cells is also produced during ETI, but at a slower speed compared to PTI (Kadota et al., 2015).

Shared components downstream of NLRs in ETI signaling include two non-NLR regulators in *A. thaliana*: NON-RACE-SPECIFIC DISEASE RESISTANCE 1 (NDR1) and ENHANCED DISEASE SUSCEPTIBILITY 1 (EDS1) (Cui et al., 2015).

Both NDR1 and EDS1 mediate basal immunity against virulent pathogens, and are recruited by different types of NLR receptors during ETI. While NDR1 functions downstream of several CNL receptors (Cai et al., 2006; Day et al., 2006), EDS1 is required for most TNL-mediated effector resistance (Bhattacharjee et al., 2011; Heidrich et al., 2011; Hu et al., 2005; Liu et al., 2002; Peart et al., 2002; Stuttmann et al., 2016; Wirthmueller et al., 2007). In basal resistance, EDS1 and its interacting partner, PHYTOALEXIN DEFICIENT 4 (PAD4) (Feys et al., 2001), cooperate in conferring resistance to biotrophic and hemi-biotrophic pathogens (Bhattacharjee et al., 2011; Heidrich et al., 2011; Parker et al., 1996) (**Fig. I5**). Mutations in *EDS1* enhance *A. thaliana* susceptibility to different races of the oomycete *Hpa* and modify resistance to a larger spectrum of other oomycete isolates such as *Peronospora hyoscyami f.sp. tabacina* (blue mold), *Bremia lactucae* (downy mildew), *Albugo candida* (white blister), and *A. tragopogonis* (white blister) (Parker et al., 1996). The non-specific role of EDS1 in pathogen resistance suggests that EDS1 functions as a hub for transducing signals from different NLR receptors. Furthermore, in TNL-triggered immune signaling, EDS1 has been proposed as a molecular bridge that engages the effector with its cognate receptor. A recent study has highlighted EDS1 physical interaction with several TNL receptors such as SNC1 (SUPPRESSOR OF NPR1-1, CONSTITUTIVE 1), RPS4 and RPS6 as well as with the sequence-unrelated effectors AvrRps4 and HopA1 (Bhattacharjee et al., 2011; Heidrich et al., 2011), although the interaction between EDS1 and AvrRps4 is sometime inconsistent when tested in different expression systems (Sohn et al., 2012). Particularly, EDS1, as an appropriate modifier of TNL receptors, has been alternatively reported to associate with microsomes and to locate inside the nuclei of host plant cells (Bhattacharjee et al., 2011; Heidrich et al., 2011; Stuttmann et al., 2016; Wirthmueller et al., 2007). Given that effector recognition by NLR receptors including TNLs often occurs in the cytoplasm, TNL translocation into the nuclei might facilitate their contact with DNA binding proteins responsible for transcriptional immune responses (Wiermer et al., 2007). The association of both TNLs and effectors with EDS1 in both cytoplasm and nucleus points to a potential role of EDS1 as a nucleo-cytoplasmic shuttle for TNL/effector complexes (Bhattacharjee et al., 2011; Heidrich et al., 2011).

In addition, EDS1 and PAD4 are required for salicylic acid (SA) accumulation induced by both PTI and TNL-mediated ETI (Clarke et al., 2001; Feys et al., 2001). SA has major roles not only in immunity against biotrophs and hemibiotrophs, but also in response to abiotic stresses (**Fig. I5**). In *A. thaliana*, SA is produced in

chloroplasts via two biosynthetic pathways involving either phenylalanine or isochorismate, in which the latter chiefly accounts for the accumulation of SA upon pathogen infection (Denancé et al., 2013; Fu and Dong, 2013). In response to pathogen attack or PTI, SALICYLIC ACID INDUCTION DEFICIENT 2/ISOCHORISMATE SYNTHASE 1 (SID2/ICS1) accumulates and increases the conversion of chorismate into isochorismate. Isochomarismate pyruvate lyase (IPL) then catalyzes isochorismate into SA (Mercado-Blanco et al., 2001; Serino et al., 1995).

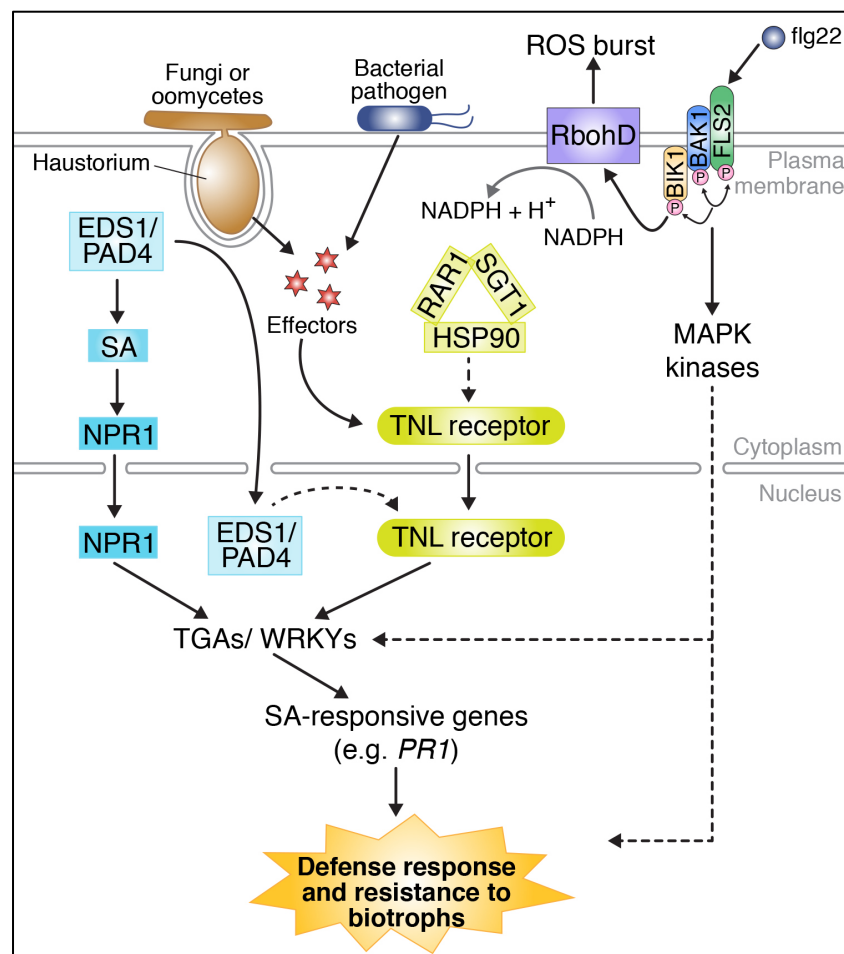


Figure 15. Downstream signaling cascades upon ETI activation of TNL receptors. (adapted and modified from Kadota et al., 2014; Panstruga et al., 2009; Pieterse et al., 2009).

A key role in orchestrating downstream responses to SA is played by NONEXPRESSOR OF PATHOGENESIS RELATED PROTEINS 1 (NPR1) and its homologs (Cao et al., 1994; Delaney et al., 1995; Wang et al., 2006). SA induces

degradation of cytoplasmic NPR1 oligomers, promoting monomeric NPR1 to translocate to the nucleus where it acts as a transcriptional co-activator for a range of defense related genes including *PR* genes and DNA binding factors (Kinkema et al., 2000; Spoel et al., 2009). WRKY transcription factors (TFs) act both upstream and downstream of NPR1 (van Verk et al., 2011). SA specifically up-regulates *WRKY46*, which in turn contributes to basal resistance against bacterial pathogens (Dong et al., 2003; Hu et al., 2012; Kalde et al., 2003). Another WRKY, *WRKY70* not only plays a role as a checkpoint orchestrating the balance between SA- and JA-dependent defense signaling (Li et al., 2006), but also is required for the activity of an NLR receptor (Knoth et al., 2007). The EDS1/PAD4 complex also regulates the antagonistic crosstalk between SA- and jasmonic acid/ethylene (JA/ET)-dependent responses (Brodersen et al., 2002). In fact, regulation of EDS1 and SA exists in a positive feedback loop, because the accumulation of both EDS1 and SA appears to be increased during PTI or ETI, leading to enhance the defense responses (Chandra-Shekara et al., 2004; Shirano et al., 2002; Xiao et al., 2003). Functional relation between EDS1 and SA is therefore important for immune signaling.

4.5. NLR accumulation by HSP90-SGT1-RAR1 co-chaperone complex

Many NLR receptors require a chaperone complex that consists of HSP90 (HEAT SHOCK PROTEIN 90), SGT1 (SUPPRESSOR OF G-2 ALLELE OF SKP1) and RAR1 (REQUIRED FOR MLA12 RESISTANCE 1) for their function (Kadota et al., 2010) (**Fig. 15**). While HSP90 is highly conserved in both prokaryotes and eukaryotes, SGT1 and RAR1 are eukaryote specific (Kadota et al., 2010). HSP90 is well known for its role in activation, stabilization and assembly of a wide range of client proteins (Pearl and Prodromou, 2006). SGT1 is involved in wide range of processes, including kinetochore assembly, ubiquitination, cyclic AMP activation, and kinase stabilization (Kadota and Shirasu, 2012). In *A. thaliana*, the *SGT1* locus has two genes (*SGT1a* and *SGT1b*) with highly similar sequence (Muskett and Parker, 2003). RAR1, a member of the cysteine and histidine-rich domain (CHORD) protein family, interacts with both HSP90 and SGT1, forming a scaffolding surface of the chaperon complex (Zhang et al., 2010). The HSP90-SGT1-RAR1 interaction network has been shown to stabilize both plant and mammalian NLR receptors (Shirasu, 2009).

Silencing or inactivation of one of the components of the co-chaperone complex reduces protein abundance of many NLR receptors, thereby enhancing plant susceptibility to different pathogens (Austin et al., 2002; Azevedo et al., 2006; Bieri et al., 2004; Holt et al., 2005; Hubert et al., 2003; Takahashi et al., 2003). However, not all NLRs are regulated the same way by the co-chaperone components. For example, the *A. thaliana* ADR1-L2, a helper NLR, can accumulate to a normal level even in the absence of functional RAR1 (Roberts et al., 2013). SGT1 and RAR1 also do not always act cooperatively, having antagonistic roles in regulating RPS5 accumulation (Holt et al., 2005).

5. Autoimmunity in plants

Autoimmunity refers to activation of processes that are harmful to the body, such as inflammation, in the absence of an appropriate trigger. In humans, defects in innate immune receptors such as TLRs and NOD-like receptors or self-recognition by lymphocytes and antibodies in the adaptive immune system can lead to autoimmune diseases (Baecher-Allan and Hafler, 2006; Dornmair et al., 2003; Marshak-Rothstein, 2006; Yanaba et al., 2008; Zhong et al., 2013). In plants, autoimmunity can also occur. Plants with autoimmune syndromes often have constitutive immune responses in the absence of pathogens and display spontaneous HR-like cell death on the leaves, morphological defects in vegetative and reproductive organs, and slow growth rate (Lorrain et al., 2003). A number of forward genetic screens have identified many autoimmune mutants, also known as lesion-mimic mutants (LMMs), in maize, rice, barley, and *A. thaliana* (Hoisington et al., 1982; Lorrain et al., 2003; Moeder and Yoshioka, 2008; Takahashi et al., 1999; Wolter et al., 1993). The causal mutations are general loss-of-function or gain-of-function variants of NLRs themselves, key regulators of immunity, and components of defense hormone synthesis and signaling (Bruggeman et al., 2015). Below, I will further focus on NLR-mediated autoimmunity in *A. thaliana*.

Table 2: Examples of *Arabidopsis thaliana* autoimmune mutants

Mutant	Gene ID	Gene Product	Type of mutation	Lesion Phenotype	Reference
Lesion-mimic mutants					
<i>chs2</i>	<i>At4g16860</i>	TNL (RPP4)	Gain-of-function	Chlorosis and wilting at low temperature	Huang et al., 2010
<i>slh1</i>	<i>At5g45260</i>	TNL-WRKY (RRS1-R)	Loss-of-function	Dwarfism and necrosis, sensitive to low humidity	Noutoshi et al., 2005
<i>snc1</i>	<i>At4g16890</i>	TNL	Gain-of-function	Necrosis and stunted growth	Zhang et al., 2003
<i>ssi4</i>		TNL	Gain-of-function	Chlorosis suppressed by high humidity	Shirano et al., 2002; Zhou et al., 2004a
Autoimmune suppressors					
<i>adr1</i>	<i>At1g33560</i>	CNL	Loss-of-function	Suppressed <i>Isd1</i> induced runaway cell death	Bonardi et al., 2011; Roberts et al., 2013
<i>adr1-11</i>	<i>At4g33300</i>	CNL	Loss-of-function	Suppressed <i>Isd1</i> induced runaway cell death	Bonardi et al., 2011; Roberts et al., 2013
<i>adr1-12</i>	<i>At5g04720</i>	CNL	Loss-of-function	Suppressed <i>Isd1</i> induced runaway cell death	Bonardi et al., 2011; Roberts et al., 2013
<i>DM2h (L. erecta)</i>		TNL		Suppress nuclear-enriched EDS1-mediated autoimmune phenotype	Stuttman et al., 2016
<i>laz5</i>	<i>At5g44870</i>	TNL	Loss-of-function	Suppress cell death in <i>acd11</i> autoimmune mutant	Palma et al., 2010
<i>mos3</i>	<i>At1g80680</i>	Homolog of nucleoporin (NUP96)	Loss-of-function	Suppress cell death in <i>snc1</i> autoimmune mutant	Zhang and Li, 2005
<i>mos6</i>	<i>At4g02150</i>	Importin α	Loss-of-function	Suppress cell death in <i>snc1</i> autoimmune mutant	Palma et al., 2005
<i>mos7</i>	<i>At5g05680</i>	Homolog of NUP88	Loss-of-function	Suppress cell death in <i>snc1</i> autoimmune mutant	Cheng et al., 2009
<i>mos11</i>	<i>At5g02770</i>	RNA binding protein	Loss-of-function	Suppress cell death in <i>snc1</i> autoimmune mutant	Germain et al., 2010
<i>summ2</i>	<i>At1g12280</i>	CNL	Loss-of-function	Suppress necrosis in the absence of MAK kinase	Zhang et al., 2012
Autoimmune enhancers					
<i>bon1</i>	<i>At5g61900</i>	Phospho-lipid binding protein	Loss-of-function	Leaf necrosis at low humidity and/or low temperature due to up-regulation of <i>SNC1</i>	Jambunathan et al., 2001; Yang and Hua, 2004
<i>exo70B1</i>	<i>At5g58430</i>	Exocyst subunits	Loss-of-function	Leaf necrosis and enhanced disease resistance due to activation of TIR-NBS2	Zhao et al., 2015

As discussed above, NLRs play a fundamental role in plant immunity. Therefore, mis-regulation or mutations in these receptors can lead to detrimental consequences for plants, including lesion-mimic phenotypes (LMM) (**Table 2**). Examples of such NLR mutants include *ssi4* (*suppressor of salicylic acid insensitivity of npr4*) (Shirano et al., 2002), *snc1* (*suppressor of npr1, constitutive 1*) (Zhang et al., 2003), *chs2* (*chilling-sensitive2*) (Huang et al., 2010), and *slh1* (*sensitive to low humidity 1*) (Noutoshi et al., 2005). These autoimmune mutants often constitutively up-regulate defense components such as *PR* genes, *WRKY* transcription factors, and SA accumulation and signaling, very similar to what is seen in NLR-dependent ETI (Huang et al., 2010; Noutoshi et al., 2005; Shirano et al., 2002; Zhang et al., 2003). The *ssi4* mutant produces much more SA than the corresponding wild-type parent (Shirano et al., 2002), while *snc1* and *slh1* up-regulate the expression of several defense markers including *PR1* and several *WRKY* transcription factor genes (Noutoshi et al., 2005; Zhang et al., 2003). The autoimmune syndromes of these mutants are sensitive to the environment and can change in the expressivity depending on ambient temperature and humidity (Huang et al., 2010; Noutoshi et al., 2005; Shirano et al., 2002; Zhang et al., 2003) (**Table 2**).

Other autoimmune mutants are defective in regulation of NLR activity. The involvement of NLRs in these cases was often deduced from NLR mutations suppressing or enhancing the autoimmune phenotypes. Examples in *A. thaliana* are found in *laz5* (*lazarus5*) (Palma et al., 2010), *adr1* (*activated disease resistance 1*) (Bonardi et al., 2011; Roberts et al., 2013), *mos* (*modifier of snc1*) mutants (Cheng et al., 2009; Germain et al., 2010; Palma et al., 2005; Zhang and Li, 2005), and *summ2* (*suppressor of mkk1 mkk2, 2-1*) (Zhang et al., 2012) (**Table 2**). The *acd11* (*accelerated cell death 11*) mutant, which shows constitutive activation of cell death and defense responses without pathogen trigger, has a deletion of a gene encoding a putative sphingosine transfer protein with unknown cellular function (Brodersen et al., 2002; Petersen et al., 2008). One of the *acd11* suppressor mutations changes the P-loop of a TNL, LAZ5, suggesting a connection of ACD11 to innate immunity (Palma et al., 2010). Similarly, *ADR1-L2*, a CNL encoding gene, has been found to be a positive regulator of *A. thaliana* *Isd1* (*lesion simulating disease resistance 1*) mediated cell death, which is only seen when the P-loop of ADR1-L2 is intact (Roberts et al., 2013). In addition, up-regulation of NLR genes, such as of *SNC1* in the *bon1-1* mutant, results in an enhanced necrosis compared to the wild-type plant (Yang and Hua, 2004). The engagement of NLRs and diverse immune activation

functions associated in autoimmune mutants and modifiers highlight the essential role of NLRs in immune-dependent cell death signaling.

Large-scale studies on hybrids between natural accessions of *A. thaliana* have shown that approximately 2% of the intraspecific hybrids suffer from autoimmunity, with spontaneous cell death, tissue collapse, leaf lesions, chlorosis, growth retardation, and dwarfism, in extreme cases leading to sterility and even death (Bomblies et al., 2007; Chae et al., 2014). These incompatible hybrids are examples of an autoimmune syndrome called hybrid necrosis (Bomblies et al., 2007). Similar to the autoimmune syndromes of LMM mutants, expression of hybrid necrosis depends on environmental conditions, particularly temperature. Most incompatible hybrids develop necrotic spots only at temperatures below 20°C or lower (Bomblies et al., 2007; Chae et al., 2014; Muralidharan et al., 2014). The genetic architecture of hybrid necrosis is generally simple and often involves an epistatic interaction between two loci that comply with the Bateson-Dobzhansky-Muller (BDM) model, which was developed to explain reproductive isolation (Bomblies and Weigel, 2007; Orr, 1996). It originally postulated that hybrid sterility is caused by a pair of interacting factors from two closely related varieties, where each factor has acquired distinct properties that are tolerated or even beneficial in the individual variety, yet detrimental when combined once plants are crossed (Orr, 1996).

Identifying the causal genes in necrotic hybrids has pointed to NLR receptors as a major contributor (Alcázar et al., 2010; Alcázar et al., 2009; Bomblies et al., 2007; Chae et al., 2014). Efforts to pinpoint the underlying causal genes for one incompatible cross, Uk-1 x Uk-3, started in 2007 with quantitative trait locus (QTL) mapping, which identified two genomic regions with NLR genes. The first gene, contributed by Uk-3, is *DM1* (*DANGEROUS MIX 1*) on chromosome 5, and the second from Uk-1 is *DM2* on chromosome 3. *DM1* is an example of a single-gene *NLR* locus (Bomblies et al., 2007), while *DM2* is located in a complex cluster, with only a single gene, *DM2d*, being necessary and sufficient for hybrid necrosis in combination with *DM1* (Chae et al., 2014).

Several NLR genes that contribute to hybrid necrosis have been shown to be subject to rapid sequence evolution under pathogen pressure and to have a high copy number variability (Chae et al., 2014). One example is the *DM2/RPP1* locus. As mentioned earlier, different variants of RPP1 receptors have been shown to directly and specifically recognize different isolates of *Hpa* expressing distinct ATR1 effectors

(Botella et al., 1998; Krasileva et al., 2010). In *A. thaliana*, the *DM2/RPP1* locus is a super cluster with many different paralogs. The size of the cluster as well as the number of *DM2/RPP1* paralogs within the cluster varies among *A. thaliana* accessions. Sequence analysis of the LRR encoding region, which is responsible for pathogen recognition, of different *DM2* alleles revealed a high number of polymorphisms across accessions, higher than in the TIR and NB-ARC regions, suggesting that the region is under diversifying selection. The high rate of divergence within the *DM2/RPP1* cluster therefore can explain why the cluster is major material of multiple incompatibilities (Chae et al., 2014).

6. Aim of the PhD thesis

In my PhD thesis, I aimed to elucidate the molecular basis of autoimmunity observed in the *A. thaliana* necrotic hybrid Uk-3 x Uk-1. The autoimmune syndrome of the hybrid is caused by the epistatic interaction of the TNL-encoding gene pairs, *DM1* and *DM2d*. Each of the genes has been independently evolved in two natural accessions Uk-3 and Uk-1 (Bomblies et al., 2007; Chae et al., 2014). Several questions of interest that I will address in this thesis include:

- What are the genetic requirements of DM1/DM2d dependent autoimmune signaling?
- Is there physical interaction of the two TNL receptors during the signaling? If so, how does the protein interaction contribute to the signaling?
- What is the functional role of each partner in the DM1/DM2d signaling?
- How do structure- and sequence-related features determine specialized functionality of DM1 and DM2d in comparison to their evolutionary homologs and paralogs?

By answering these questions, I hope to gain more insights in understanding how plant autoimmunity arises through NLR interaction. Evidence of unequal contributions to the signaling of each member in the pair will tell us about evolutionarily functional divergence in NLR activations. Despite the benefit of NLR activation in the presence of pathogens, their inappropriate activation, i.e. without pathogen pressure, can lead to a fitness cost to plants. My project will also provide a molecular explanation of how evolution avoids inappropriate activation of NLRs to minimize the fitness cost.

RESULTS

CHAPTER 1.

Characterization of DM1/DM2d-dependent Autoimmunity

1. Genetic requirements for DM1/DM2d-triggered autoimmune signaling

Plant immune responses mediated by NLR receptors often share common downstream signaling pathways to induce cell death during ETI (Cui et al., 2015; Qi and Innes, 2013). One of the most common pathways deployed by NLRs is through SA, in which EDS1 acts as a critical signaling regulator of both basal resistance and ETI mediated by TNL receptors (Bartsch et al., 2006; Feys et al., 2001; Venugopal et al., 2009; Wildermuth et al., 2001). Loss-of-function mutations in *EDS1* result in enhanced plant susceptibility to various pathogens accompanied by reduced immune gene induction upon pathogen attack (Aarts et al., 1998; Parker et al., 1996). EDS1 physically interacts with several TNLs, such as SNC1, RPS4 and RPS6, and nucleocytoplasmic shuttling of an EDS1-TNL complex appears to regulate TNL signaling upon effector recognition (Bhattacharjee et al., 2011; Heidrich et al., 2011; Wirthmueller et al., 2007).

ROS burst is one of the earliest signaling outputs in basal immunity and ETI (Kadota et al., 2015). Accumulation of ROS immediately follows PAMP perception through the PRR-associated kinase BIK1 directly regulating the NADP oxidase RBOHD for hydrogen peroxide production (Kadota et al., 2014; Li et al., 2014). Although extracellular ROS, primarily produced by RBOHD, positively correlates with disease resistance in general, RBOHD also functions to limit the spread of SA-associated cell death (Torres et al., 2005), as was shown in the CNL ADR1-L2 mediated cell death in *lesion simulating disease 1 (lsd1)* mutants (Roberts et al., 2013). Importantly, protein abundance of NLR receptors including TNLs is often under tight regulation by a chaperone complex consisting of RAR1, SGT1b, and HSP90 (Belkhadir et al., 2004b; Panstruga et al., 2009; Shirasu, 2009). Therefore, I asked whether autoimmunity triggered by the hybrid necrosis NLRs DM1 and DM2d, which I have discussed already in the Introduction of my thesis, is dependent on

EDS1, *RBOHD*, *RAR1* and *SGT1b*, which would indicate that it resembles other TNL signaling pathways to initiate the cell death.

Introduction of both a genomic *DM1* fragment including its endogenous promoter amplified from the Uk-3 accession (*pDM1::gDM1^{Uk-3}*) and a genomic *DM2d* fragment amplified from the Uk-1 accession (*pDM2d::gDM2d^{Uk-1}*) into the *A. thaliana* Col-0 accession are sufficient to trigger hybrid necrosis symptoms in the absence of pathogen effectors (Chae et al., 2014). I therefore first generated transgenic lines homozygous for either a 2xHA tagged fusion of *pDM1::gDM1^{Uk-3}* or a 4xMyc tagged fusion of *pDM2d::gDM2d^{Uk-1}* (hereafter *gDM1-HA* and *gDM2d-Myc*) in Col-0. Independent F₁ lines were generated by crossing at least 3 homozygous lines for each transgene (hereafter F₁[*gDM1-HAxgDM2d-Myc*]). At least 3 independent hybrid lines were grown at 16°C – the temperatures at which the original Uk-3 (carrying *DM1^{Uk-3}*) x Uk-1 (carrying *DM2d^{Uk-1}*) F₁ hybrid plants expressed autoimmune symptoms (Bomblies et al., 2007).

I observed that the F₁[*gDM1-HAxgDM2d-Myc*] hybrids in Col-0 resembled the F₁ hybrids of Uk-3 and Uk-1 with stunted growth and spontaneous cell death on leaves (**Fig. R1A**). I concluded the C-terminal epitope tags did not interfere with the activities of DM1 and DM2d, and that the reconstructed hybrid in Col-0 can be used for testing genetic requirements of the DM1/DM2d signaling.

To examine the roles of *EDS1*, *RAR1*, *SGT1b* and *RBOHD* in DM1/DM2d mediated signaling, I generated the F₁[*gDM1-HAxgDM2d-Myc*] hybrids in *eds1-1* (Parker et al., 1996), *rar1-21* (Tornerio et al., 2002), *sgt1b* (Tör et al., 2002) and *rbohD* (SALK_074825) mutants (see Table 3 for nature of mutations). The F₁[*gDM1-HAxgDM2d-Myc*] hybrids in *eds1-1*, *rar1-21* and *sgt1b* backgrounds grew healthily comparable to their parents (**Fig. R1A**). They also set seeds at 55 days after sowing (das) (**Fig. S2**). Genotyping using PCR with specific oligonucleotides confirmed the presence of the transgenes in parents and hybrids (**Table S4, Fig. R1B**). In addition, to confirm the integrity of *gDM1-HA* and *gDM2d-Myc* in the suppressed lines, I crossed the hybrids in *eds1-1*, *rar1-21* and *sgt1b* backgrounds to wild-type Col-0 and grew their progeny at 16°C. Because *eds1-1*, *rar1-21* and *sgt1b* mutations are recessive, I expected to observe plants with DM1/DM2d mediated autoimmune symptoms in 25% of progeny, those that inherited both transgenes. I observed that 13/307 (4.2%) of progeny from the outcross of *eds1-1*, 75/349 (21.4%) of *rar1-21*, and 8/268 (3%) of *sgt1b* recapitulated the necrotic phenotype of the F₁[*gDM1-HAxgDM2d-Myc*] hybrid in Col-0 (**Fig. S1**). The marked deviation from the expected 25% in the *eds1-1* and *sgt1b* cases could be explained as the transgenes might have

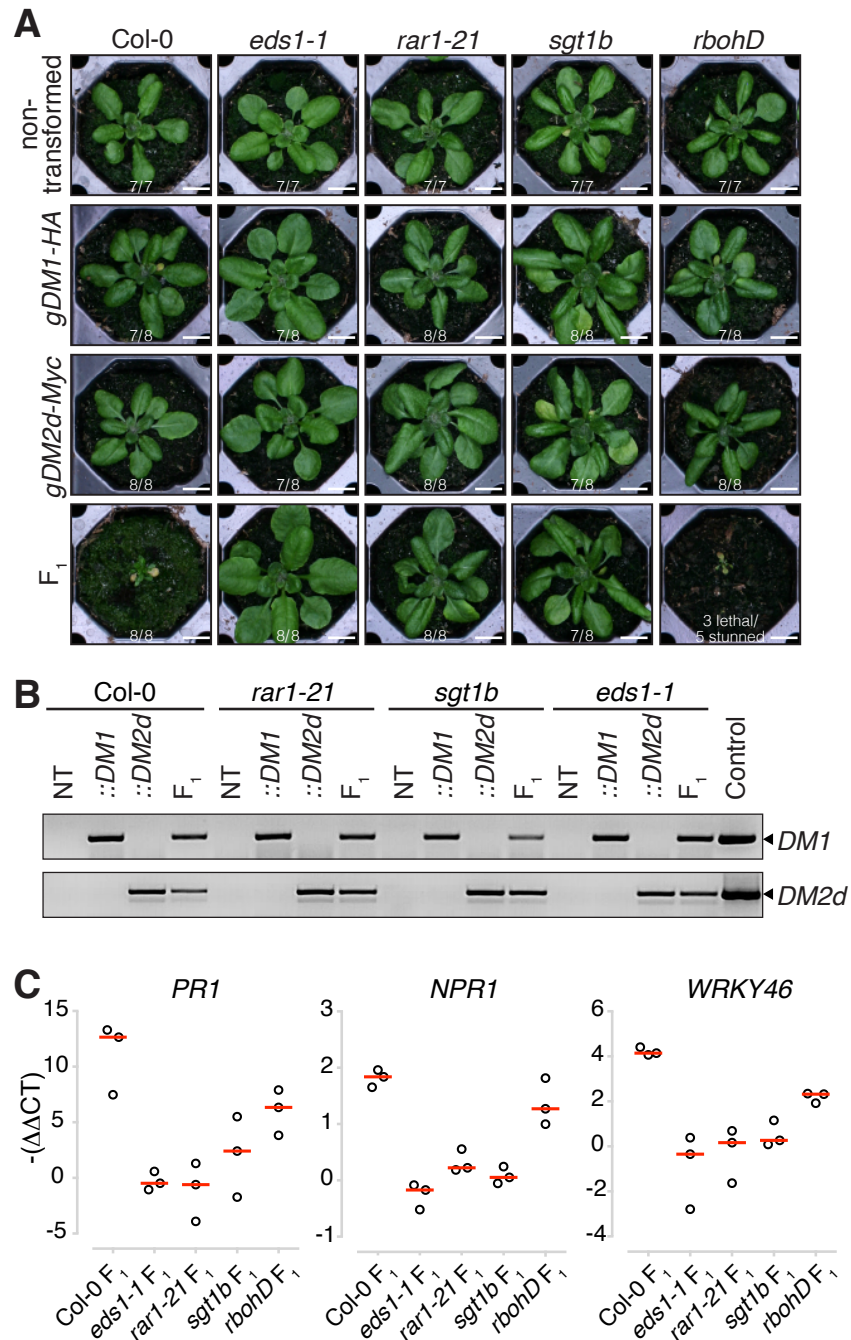


Figure R1. Genetic requirement for DM1/DM2d-dependent autoimmunity

(A) Rosettes at 30 das of *gDM1-HA* or *gDM2d-Myc* T_3 lines and of their F_1 progeny with both transgenes in *Col-0* or indicated mutant backgrounds. The numbers below each plant indicate the proportion of the presented phenotype in three rounds of sowing. Scale bars equal 1 cm.

(B) Genotyping of *gDM1-HA* and *gDM2d-Myc* in the indicated plants shown in (A). NT: no-transgene, ::DM1: transgenic individual carrying *gDM1-HA*; ::DM2d: transgenic individual carrying *gDM2d-Myc*; F_1 : hybrid of *gDM1-HA* x *gDM2d-Myc*.

(C) Expression analysis of immunity marker genes, *PR1*, *NPR1* and *WRKY46*. Leaf samples were collected at 20 das for RNA extraction. Relative expression of each marker gene in F_1 hybrids is indicated as $-(\Delta\Delta CT)$ values in three biological replicates with red bars for the median.

incomplete penetration, or some of severe phenotypes might die before assayed, or subtle warming in the growing condition might alleviate the necrotic symptom. Nevertheless, the recapitulation of the necrotic phenotype in at least some of the outcrossed individuals confirmed that the transgenes are in principle active.

PATHOGENESIS RELATED1 (PR1), *NONEXPRESSER OF PR GENES 1 (NPR1)* and several *WRKY* transcription factor genes are good marker for immune activation (Dong et al., 2003; van Loon et al., 2006; Wu et al., 2012). To test whether they were also activated in *DM1/DM2d* autoimmune signaling, I quantified transcript levels of *PR1*, *NPR1*, and *WRKY46* in 20-day-old $F_1[gDM1-HA \times gDM2d-Myc]$ seedlings in Col-0 as well as in *eds1-1*, *rar1-21* and *sgt1b* mutant backgrounds using qPCR. Relative expression of each target transcript was calculated by normalizing the obtained CT values to those of *TUB2* (ΔCT). To quantify the relative expression in the $F_1[gDM1-HA \times gDM2d-Myc]$ hybrid in wild-type Col-0 background, and immunity-defective mutants, ΔCt value of the F_1 was calibrated to that of one of the parents, the *gDM1-HA* parent ($\Delta\Delta Ct$) (See Methods).

PR1, *NPR1*, and *WRKY46* were up-regulated in the $F_1[gDM1-HA \times gDM2d-Myc]$ in Col-0, but much less in the hybrids in *eds1-1*, *rar1-21* and *sgt1b* mutant backgrounds (**Fig. R1C**). Relative to Col-0 background, transcripts were only about one tenth for *PR1*, half for *NPR1*, and a quarter for *WRKY46* (**Fig. R1C**). These results indicate that in the wild-type background, *DM1/DM2d* dependent autoimmune signaling leads to enhanced expression of immunity genes. A similar profile of marker gene expression was found in regular incompatible hybrids (Alcázar et al., 2009; Bomblies et al., 2007). The enhanced expression of immunity markers is largely correlated with the degree of visual cell-death symptoms on the plants (**Fig. R1A and C**). Impairing one of the downstream signaling components prevents up-regulation of immunity genes and other autoimmune syndromes. This indicates that *DM1* and *DM2d* signal through the same canonical pathway components deployed by other TNL receptors upon effector recognition (Cui et al., 2015).

Extracellular ROS production depends on the NADPH oxidase *RbohD* (Torres et al., 2002) (**Fig. I5**). Unlike in the other mutants I investigated, the cell-death phenotype of the $F_1[gDM1-HA \times gDM2d-Myc]$ hybrid was not reduced in the absence of *RBOHD*, but instead enhanced (**Fig. R1A**). Plants grew much more slowly compared to the control (in Col-0 background) and had a severely stunted adult

appearance. Some even died at 30 das (**Fig. S2**). At 55 das, the hybrids in Col-0 background, despite necrosis symptom at early development stages (**Fig. R1A**) could still flower and produce a few seeds, while the hybrid in the *rbohD* background did not flower (**Fig. S2**). Consistent with the morphological phenotype, expression level of immunity markers was much less changed than in *eds1-1*, *rar1-21* and *sgt1b* (**Fig. R1C**). However, despite the enhanced phenotype they were not as high as in Col-0 (**Fig. R1C**). The presumed discrepancy could be due to the early sampling time (20 das) of material used for qRT-PCR as the onset of enhanced necrosis in *rbohD* was more severe at later stages of development. Additional time points of sampling will be needed to clarify whether the expression level of the immune markers is enhanced when the F₁ hybrids in *rbohD* get older. The enhanced necrosis in the hybrids in *rbohD* background suggests that RBOHD functions to restrict cell death triggered by DM1/DM2 transgenes, consistent with previous finding for the run-away cell death phenotype in *Isd1* mutants mediated by the CNL protein ADR1-L2 (Roberts et al., 2013; Torres et al., 2005).

Taken together, the genetic analyses show that *DM1/DM2d* likely trigger autoimmune responses via a pathway typical of canonical ETI signaling and that these responses are negatively regulated by RBOHD, a known factor restricting SA-mediated cell death.

2. DM1/DM2d signaling requires of both proteins in full length

The autoimmune symptoms including a hypersensitive response (HR) caused by co-expression of *DM1^{Uk-3}* and *DM2d^{Uk-1}* in *A. thaliana* can be recapitulated by transient co-expression of both proteins in *Nicotiana benthamiana* (Chae et al., 2014), providing a tool for further investigation of DM1/DM2d signaling.

The extended N-terminal domain (CC or TIR plus some amino acids from the beginning of NB domain) of NLRs is often sufficient to trigger pathogen-independent cell death autoactivation (Bernoux et al., 2011; Frost et al., 2004; Swiderski et al., 2009). Examples are flax L10 (TIR + 39 amino acids) (Frost et al., 2004) and L6 (TIR + 20 amino acids) (Bernoux et al., 2011); and *A. thaliana* RPS4 (TIR + 80 amino acids) (Swiderski et al., 2009). Because the combination of full-length DM1/DM2d triggers cell death without the presence of pathogens, I asked whether N-terminal truncations of DM1 and/or DM2d could confer cell death activation by themselves, i.e. independent of their partner.

I generated truncations of different lengths (**Fig. R2A**) and fused them to 2xHA in the case of DM1 (amino acids 1-218, 1-308, 1-528, 529-1067 of DM1) and 4xMyc in the case of DM2d (amino acids 1-254, 1-358, 1-581, 687-1216 of DM2). Similar to the full-length DM1 and DM2d versions described above, the epitope tags were attached to the C-termini. The fragments comprised different functional domains: the conserved TIR, TIR and partial NB (additional 90 amino acid residues after TIR in DM1 and 104 residues in DM2d), TIR-NB and extended ARC, and LRR domain (hereafter TIR, TIR-pNB, TIR-NB-ARC, or LRR, respectively) (**Table 3, Fig. R2A**). The truncated proteins were expressed in *N. benthamiana* leaves, and when single proteins were assayed, β -glucuronidase (GUS) was co-expressed as control.

Table 3: List of truncations of DM1 and DM2d

Domains	DM1		DM2d	
	Amino acid position	Plasmid ID	Amino acid position	Plasmid ID
TIR	1-218	pDT157	1-254	pDT158
TIR-pNB	1-308	pMD444	1-358	pEC300
TIR-NB-ARC	1-528	pDT192	1-581	pDT105
LRR	529-1067	pMD341	687-1216	pMD344
Full length	1-1067	pEC209	1-1216	MD325

At 4 days post-infiltration (dpi), co-expression of full-length DM1 and DM2d conferred visible cell death symptoms (**Fig. R2B**), while neither full-length proteins nor truncated versions (TIR-containing fragments or the LRR domain) of DM1 and DM2d was sufficient to trigger HR on its own (when co-expressed GUS). Similarly, none of the truncations triggered HR when co-expressed with the corresponding truncation from the pairing partner (**Fig. R2B**). I confirmed that truncated proteins were expressed to a level comparable to the full-length proteins, indicating that the absence of HR was not due to a compromised protein expression (**Fig. R2C-D**). Taken together, these results demonstrated that all three domains (TIR, NB-ARC and LRR) of both DM1 and DM2d were necessary to initiate HR signaling. Unlike many NLRs whose N-terminal domain is not only necessary, but also sufficient to trigger cell death autonomously (Bernoux et al., 2011; Maekawa et al., 2011; Swiderski et al., 2009), DM1 and DM2d need to present as full-length proteins for combined autoactivation. My findings, therefore, differentiate DM1 and DM2d from other NLRs whose HR-triggering activities mainly locate to their N-terminal domains. This may imply that the functional cooperation among different domains within DM1 and DM2d is important for regulation of the DM1/DM2d signaling output.

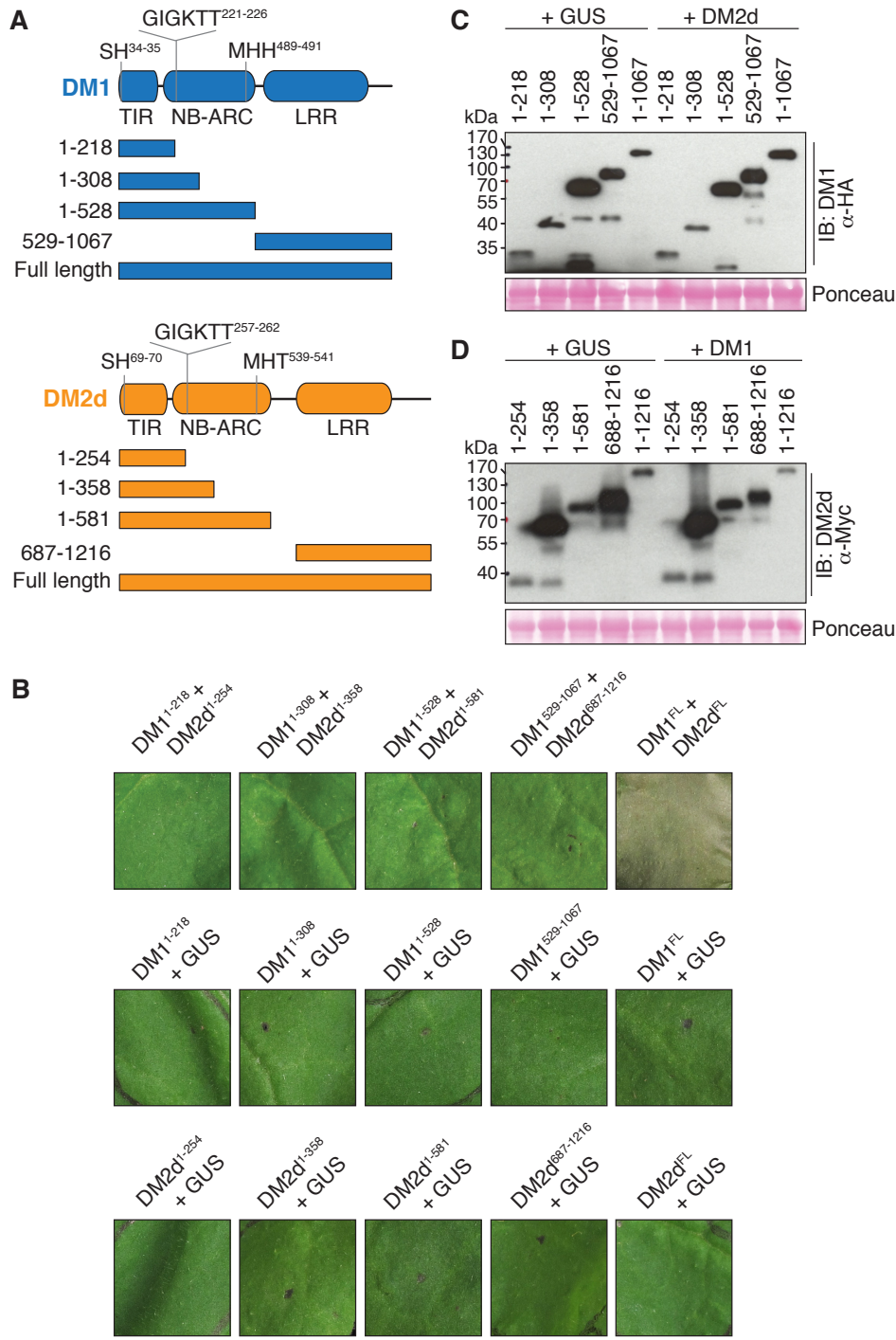


Figure R2. Requirement of full-length DM1 and DM2d for cell death signaling
 (A) Schematic diagram of DM1 (in blue) and DM2d (in orange) domain structures and derived fragments. Numbers indicate the position of amino acids. Residues mutated in this study are indicated above the diagram.
 (B) Representative HR results from co-expression of truncated DM1 and DM2d in *N. benthamiana* at 4 dpi. Scale bar equals 1 cm. Numbers correspond to fragments illustrated in (A), FL= full length, GUS was used as a negative control.
 (C-D) Protein blot of 2xHA tagged DM1 truncations (E) and of 4xMyc tagged DM2d truncations (F) that were transiently co-expressed in *N. benthamiana* either with GUS or with the corresponding fragments. Leaf samples for protein extraction were collected at 2 dpi. Ponceau-S staining shown to indicate loading.

To ensure that the cell death phenotype observed with the DM1 and DM2d full-length proteins was independent of the C-terminal epitope tags, I also repeated the transient expression assay using the full-length DM1 and DM2d fused with different tags at the C-terminus (2xFLAG, mCherry and eGFP). HR phenotypes were observed when DM1 and DM2d were combined regardless of the fused tags (**Fig. S3**), similar to the HR phenotypes caused by non-tagged DM1 and DM2d (Chae et al., 2014). This indicates that different C-terminal tags do not interfere with the activity of DM1 and DM2d proteins.

3. DM1/DM2d cell-death signaling requires the P-loops of both proteins

The conserved Walker A/P-loop, which is located in the N-terminal part of the NB-ARC domain, is responsible for ATP/ADP binding and ATP hydrolysis by NLR proteins (Lukasik and Takken, 2009; Takken et al., 2006). Several studies of plant NLR receptors have hypothesized that conformational changes occur between the ADP-binding inactive state and the ATP-binding active state, which in turn correlate with their downstream effects (Lukasik and Takken, 2009; Takken et al., 2006). Examples supporting this hypothesis come from the M protein in flax (Williams et al., 2011), I-2 in tomato (Tameling et al., 2002; Tameling et al., 2006), N in tobacco (Ueda et al., 2006), MLA27 in barley (Maekawa et al., 2011), as well as L6 and L7 proteins in flax (Bernoux et al., 2011). Mutations in the P-loop render NLR proteins unable to bind either ATP or ADP, and consequently inactivate them (Tameling et al., 2002; Ueda et al., 2006; Williams et al., 2011). Furthermore, effector recognition has been proposed to modulate ATP/ADP binding capacities of NLR receptors (Lukasik and Takken, 2009). Alternatively, effectors bind preferentially to NLRs in the active state, stabilizing the NLR and shifting the equilibrium towards “ON” status (Bernoux et al., 2016). Interaction studies with isolated NLR domains have suggested that NLR receptors likely have a more constrained conformation in the absence of effectors (Moffett et al., 2002; Rairdan and Moffett, 2006). A P-loop mutation, which results in a loss of Rx-mediated HR (Bendahmane et al., 2002), also abrogates the interaction between the corresponding CC-NB and LRR domains (Moffett et al., 2002). Homology modeling of plant NLR receptors after animal NLRs also supports the idea that ATP/ADP binding is accompanied by conformational change (Lukasik and Takken, 2009; Takken et al., 2006; Takken and Goverse, 2012).

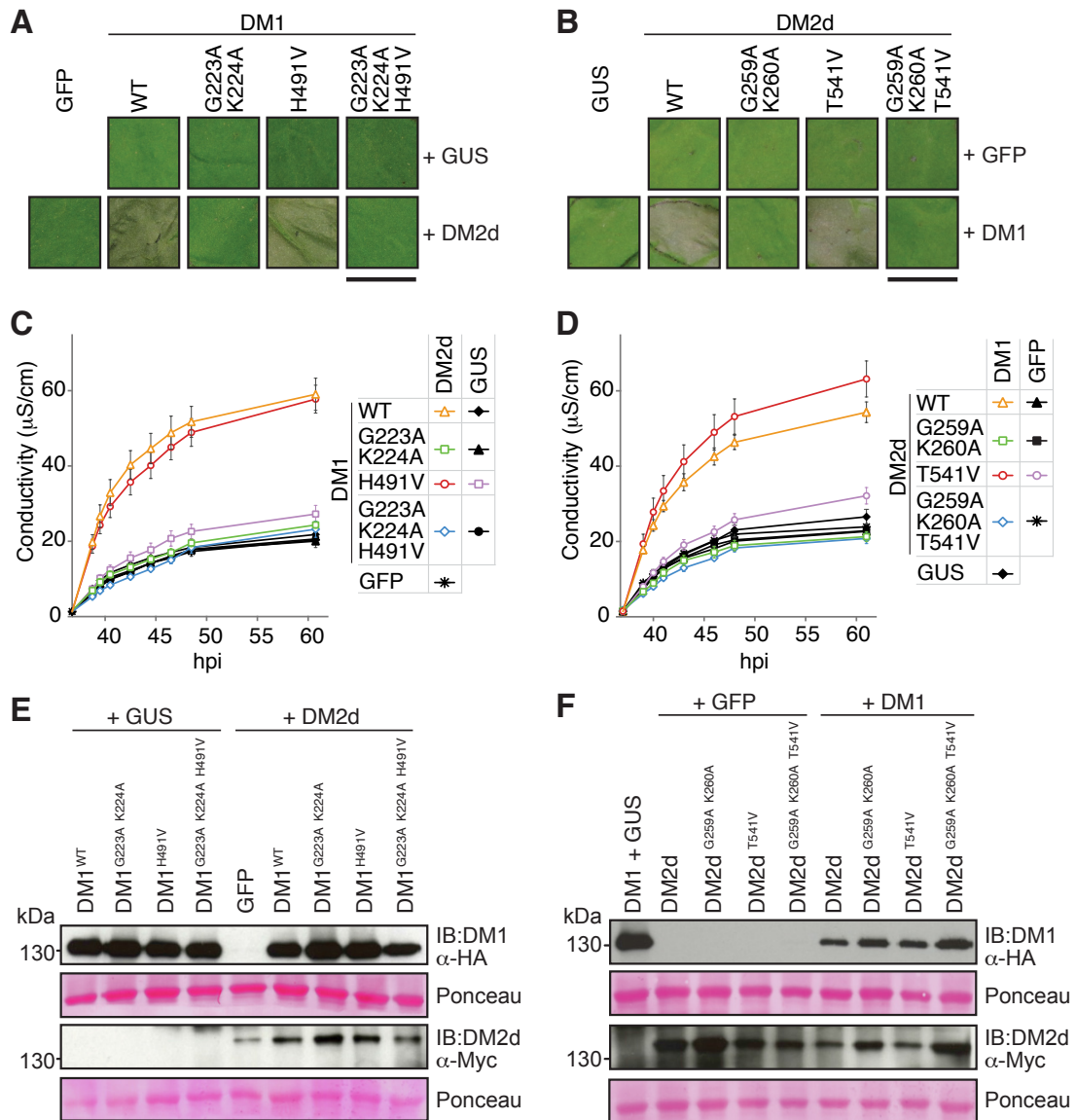


Figure R3. Contribution of the P-loops to DM1/DM2d signaling

(A-B) Representative HR results in *N. benthamiana* transiently coexpressing ethanol induced DM1 variants with DM2d (A); same as A but with ethanol induced DM1 combined with DM2d variants (B). The expression of DM1 constructs was induced by 1% ethanol at 18 hpi. The HR phenotype was recorded at 4 dpi. Scale bar equals 1 cm. hpi: hours post-infiltration; dpi: days post-infiltration.

(C-D) Conductivity measurements of DM1/DM2d-triggered HR. Values are means of 8 replicates ± SEM. hpi: hours post-infiltration.

(E-F) Protein blot analysis for experiments above. Samples were taken at 2 dpi. Ponceau-S staining shown to indicate loading.

The P-loop is conserved among plant NLR receptors (Ade et al., 2007; Tameling et al., 2002; Ueda et al., 2006; Williams et al., 2011). Both DM1 and DM2d contain the characteristic GIGKTT sequence in their P-loop, which is located between amino acids 221 to 226 in DM1 and 258 to 263 in DM2d (Fig. R2A). To

investigate whether DM1/DM2d signaling depends on intact P-loops, I constructed mutants, in which the consecutive glycine and lysine residues of the P-loop were both changed into alanine (GIGKTT to GIAATT), generating DM1^{G223A K224A} and DM2d^{G259A K260A}. To monitor and quantify the resulting cell death in *N. benthamiana* transient assays, I first established and optimized an ethanol inducible expression system for *DM1* (Zhao et al., 2010). To optimize inducible *DM1* (ind*DM1*) expression, I co-expressed different amounts of ind*DM1*-HA (OD₆₀₀ of 0.01, 0.03, and 0.1) with *DM2d*-Myc (OD₆₀₀ of 0.3) in *N. benthamiana* leaves and observed cell death in both conditions with and without ethanol induction (**Fig. S4**). The amount of ind*DM1*-HA chosen for further experiments (OD₆₀₀ of 0.1) satisfied two conditions: not cause cell death in the absence of the ethanol treatment and but trigger robust cell death when the treatment was applied (**Fig. S4**). After ethanol treatment, cell death was quantified as ion leakage index as measured by conductivity assays (Roberts et al., 2013). I observed HR at 3 days post-infiltration (dpi) when the wild-type ind*DM1*-HA was co-expressed with wild-type *DM2d* under its native promoter (**Fig. R3A-B**). In conductivity kinetics plots (**Fig. R3C-D**), the x-axis represents the time points of measurement after ethanol induction of *DM1* and the y-axis represents the ion leakage index (μS/cm). A higher ion leakage index corresponds to increased cell death.

In plants co-expressing wild-type *DM1* and *DM2d*, ion leakage started to rise at approximately 38-39 hours post-infiltration (hpi), then dramatically increased up to 45 dpi and reached a plateau after 50 hpi (**Fig. R3C-D**). Co-expression of either wild-type or mutant *DM1* or *DM2d* with the inert GUS or GFP partners only caused a slight increase in the ion leakage (**Fig. R3C-D**), likely due to physical damage of the cells while sampling. I considered this as “background”. Similarly, when the P-loop mutants were co-expressed with their wild-type partner, ion leakage was reduced to background levels (**Fig. R3C-D**). Protein blots confirmed that *DM1* and *DM2d* P-loop variants were expressed at levels comparable to that of wild-type proteins (**Fig. R3E-F**), indicating that the differences in the ion leakage kinetics were not due to different protein accumulation levels, but likely due to the mutations in the P-loops. Together, these results demonstrate that the P-loop integrity of both *DM* partners is required for cell death signaling.

The conserved MHD motif, which resides in the ARC2 subdomain at the C-terminal part of the NB-ARC domain, is located near the ATP/ADP binding pocket in three-dimensional space according to homology-based modeling (DeYoung and

Innes, 2006; Lukasik and Takken, 2009; Takken et al., 2006). Particularly, amino acid substitutions at the third position of the MHD motif result in alter NLR activity (Bai et al., 2012; Bendahmane et al., 2002; Gao et al., 2011; Howles et al., 2005; Tameling et al., 2006; Williams et al., 2011). For example, in L6 TNL receptor, mutations that changed the aspartate (D) of its MHD motif into valine (V), arginine (R), serine (S) or leucine (L) render the protein strongly autoactive (Howles et al., 2005). NLR variants with such an autoactive MHD motif preferentially bind to ATP (Tameling et al., 2006; Williams et al., 2011). I therefore tested the effect of substitutions in the MHD motifs of DM1 and DM2d using the inducible expression system in *N. benthamiana*. DM1 has variant MHH and DM2d a MHT motif instead of MHD (**Fig. R2A**). Substitutions of the third, polar residues in this motif into hydrophobic valine did not lead to autoactivation of DM1 or DM2d when they were co-expressed with GUS or GFP (**Fig. R3A-D**). When co-expressed with their corresponding partners, DM1^{H491V} and DM2d^{T542V} variants behaved similar to the wild-type proteins (**Fig. R3A-D**). DM1 and DM2d with inactivated P-loops and MHV mutant motifs were also inactive (**Fig. R3A-D**), indicating that the function of the MHD motif in both proteins likely depends on the P-loop (**Fig. R3A-D**). Comparable expression levels of wild-type and mutant variants were confirmed by protein blot (**Fig. R3E and F**). Together, these results confirm that DM1 and DM2d function similar to other NLRs, with ATP binding and hydrolysis and ensuing structural rearrangements being important for their activities.

CHAPTER 2.

Physical Association of DM1 and DM2d

1. Structural modeling of the TIR domain of DM1 and DM2d

Initiation of NLR-mediated signaling events is often coupled to physical association of NLR proteins or exchange of interacting partners (Césari et al., 2014a; Cui et al., 2015). Interactions are either homotypic, i.e. between two molecules of the same protein (e.g. L6 and MLA10) (Bernoux et al., 2011; Maekawa et al., 2011), or heterotypic, i.e. between different proteins (e.g. RPS4/RRS1 and RGA4/RGA5) (Césari et al., 2014b; Williams et al., 2014). The N-terminal domain of NLR receptors is mediating such intermolecular engagement, and similar N-terminal NLR domains can transduce effector-triggered signals to downstream components (Bernoux et al., 2011; Césari et al., 2014b; Hu et al., 2015; Maekawa et al., 2011; Williams et al., 2014; Zhang et al., 2015). The TIR domains of TNL receptors are relatively polymorphic although the available structural information for the TIR domains of L6, RPS4 and RRS1 indicate that the sequence differences do not greatly change their 3D structure (Bernoux et al., 2011; Williams et al., 2014). I therefore asked whether DM1 and DM2d TIR domains are likely to have similar structure to the crystalized TIR domains of other plant NLRs, and whether DM1 and DM2d TIR domains also mediate physical association of the two proteins.

I searched for structural homology of the TIR domains (TIR-pNB as indicated in **Table 2**) of DM1 and DM2d using the PHYRE2 homology prediction server (<http://www.sbg.bio.ic.ac.uk/phyre2/>). Both predicted structures were highly similar to those of characterized TIR domains from plant NLRs, including L6, RPS4 and RRS1 (Bernoux et al., 2011; Williams et al., 2014) (**Fig. R4A-D**). Homology prediction also suggested that the TIR domains of DM1 and DM2d could form structural conformations similar to those of flax L6, and of *A. thaliana* RPS4 and RRS1 (confidence of 100%). The modeled 3D structures of the TIR domains of DM1 and DM2d based on that of the *A. thaliana* RPS4 and RRS1 are presented in **Fig. R4A-D**.

The predicted TIR interaction interfaces of DM1 and DM2d predictably consisted of the more conserved α A and α E helical motifs (**Fig. R4E**). The serine and histidine residues that are critical for association of RPS4 and RRS1 (Williams et al., 2014) were also modeled as structurally conserved in DM1 and DM2d (**Fig. R4E**).

Taken together, the predicted structural homology suggests that DM1 and DM2d carry topologically canonical TIR domains (Bernoux et al., 2011; Williams et al., 2014).

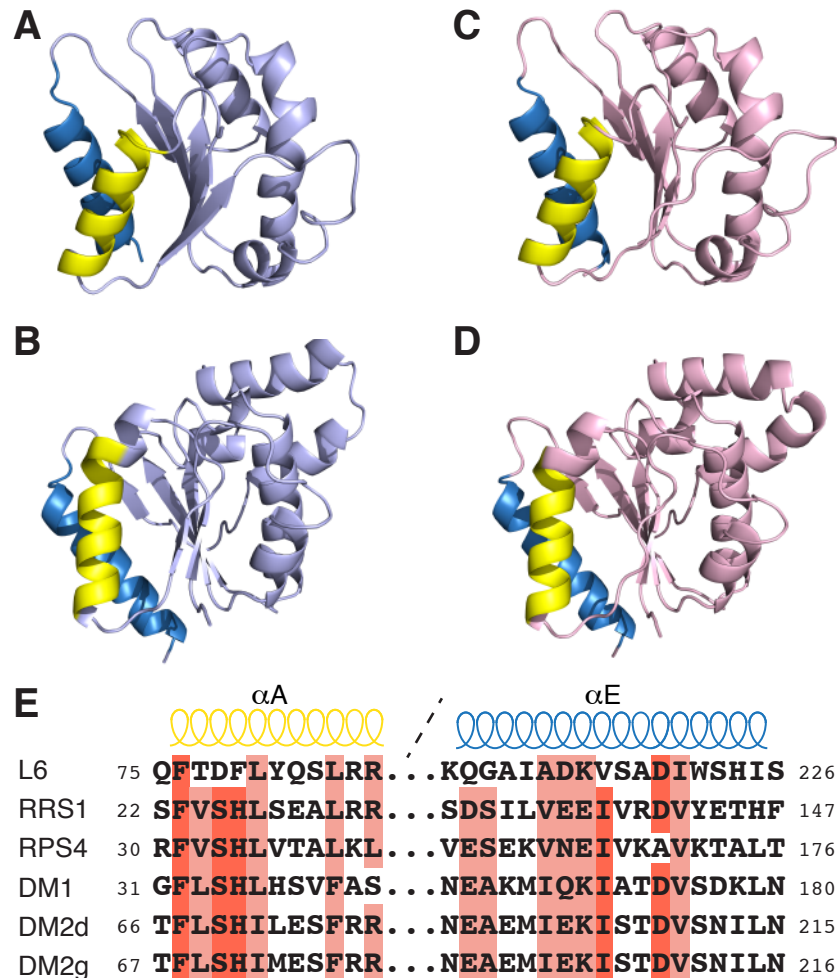


Figure R4. Homology-based structure prediction of DM1 and DM2d TIR domains

(A-B) Homology modeling of TIR domain of DM1 based on that of RRS1 (A) and RPS4 (B).

(C-D) Homology modeling of TIR domain of DM2d based on that of RRS1 (C) and RPS4 (D). Modeling was performed using PHYRE2 (Kelley et al., 2015). The αA and αE helical motifs, which form the interface of the RRS1/RPS4 TIR domains (Williams et al., 2014), are highlighted in yellow and blue, respectively.

(E) Amino acid sequence alignment of the putative αA and αE helical motifs in L6, RRS1, RPS4, DM1, DM2d and DM2g. Conserved and similar amino acid residues are highlighted in red and salmon. The numbers indicate amino acid position in each protein.

2. Physical associations of DM1 and DM2d in yeast

The structural modeling of the DM1 and DM2d TIR domains has revealed residues that might be involved in physical associations of DM1 and DM2d (**Fig. S4**). Therefore, I wanted to directly test their physical interaction in yeast two-hybrid (Y2H) assays. I generated truncated cDNA fragments of *DM1* and *DM2d* encoding TIR, TIR-pNB, TIR-NB-ARC, LRR domain and full-length protein (**Fig. R2A**). I cloned these fragments into the GAL4-activation domain (AD)-containing vector (for *DM1* fragments) and in DNA-binding domain (BD)-carrying vector (for *DM2d* fragments). An epitope tag (HA or Myc) was fused to the N-terminus of both proteins for detection of proteins in yeast cells (see Methods).

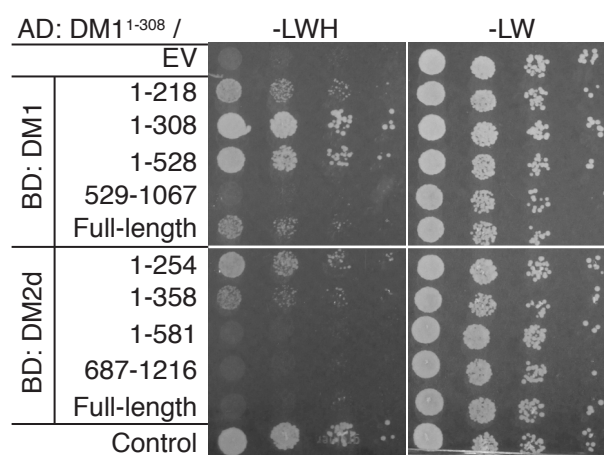


Figure R5. Homo- and heterotypic physical interactions of DM1 and DM2d in yeast

Y2H analysis defining the interface of DM1-DM1 and DM1-DM2d interactions. A serial dilution starting with OD_{600} of 0.5 (with dilution factor of ten) was used to visualize the strength of interactions on -LWH yeast SD plates. Yeast cells carrying AD: RGL3 and BD: AP1 (Yu et al., 2012) were used as positive control. AD: GAL4 activation domain, BD: DNA-binding domain of GAL4, EV: empty vectors. Numbers correspond to amino acid positions in the proteins. AD:RGL3 and BD:AP1 fusions (Yu et al., 2012) were used as positive control. (The yeast panel was prepared by Monika Demar).

The analysis revealed that the DM1^{TIR-pNB} fragment could interact with all TIR-containing fragments of DM1 (DM1^{TIR}, DM1^{TIR-pNB}, DM1^{TIR-NB-ARC} and full-length DM1), but not with the DM1^{LRR} fragment (**Fig. R5**), suggesting that DM1 TIR can self-associate in yeast and pointing to an interaction interface in the N-terminal region of DM1. This homotypic interaction was strongest when co-expressing AD:DM1^{TIR-pNB} with BD:DM1^{TIR-pNB} and weaker when co-expressing AD:DM1^{TIR-pNB} with either

BD:DM1^{TIR}, BD:DM1^{TIR-NB} or BD:DM1^{FL} (**Fig. R5**). This suggests that, at least in yeast, the TIR and NB domains may promote DM1-DM1 homotypic association, while the LRR domain might partially interfere with TIR-TIR interaction. I also found that DM1^{TIR-pNB} interacted with DM2d^{TIR} and DM2d^{TIR-pNB}, although these heterotypic associations were not as strong as the corresponding homotypic DM1-DM1 associations (**Fig. R5**). DM1^{TIR-pNB} failed to interact with the DM2d TIR-NB-ARC or LRR fragments and with full-length DM2d (**Fig. R5**), indicating that the heterotypic association is mediated by the TIR and the N-terminal region of the NB domain, and that this association is weakened by other domains in DM2d.

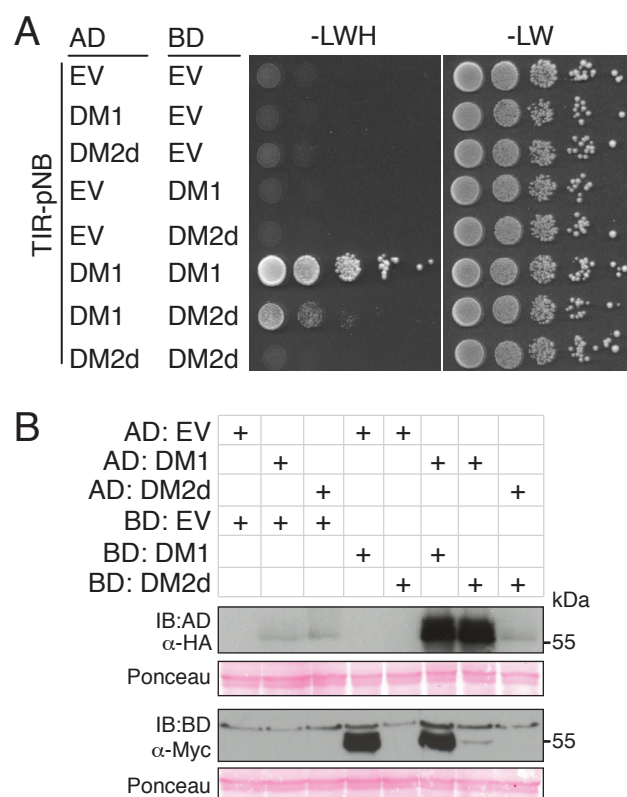


Figure R6. Physical interaction of DM1 and DM2d N-terminal fragments in yeast
 (A) Y2H analysis of TIR-pNB fragments of DM1 and DM2d revealed homotypic DM1-DM1 interaction, heterotypic DM1-DM2d interaction but not homotypic DM2d-DM2d interaction.

(B) Protein blot of TIR-pNB fragments of DM1 and DM2d used in (A). Ponceau-S staining shown to indicate loading.

I also tested whether DM2d can self-associate in yeast, Against my expectations, the TIR-pNB fragments did not give a positive result (**Fig. R6A**). Protein blot analysis showed that this was most likely because of insufficient accumulation of DM2d^{TIR-pNB} (**Fig. R6B**). In particular, the BD:DM2d^{TIR-pNB} fusion was

below the detection limit when co-expressed either with the AD domain alone or with the AD:DM2d^{TIR-pNB} (**Fig. R6B**, lanes 5 and 8). Co-expression of DM1^{TIR-pNB}, on the other hand, increased the levels of DM2d^{TIR-pNB} to a detectable level (**Fig. R6B**, lane 7), suggesting that DM1 might stabilize DM2d, e.g. through formation of a heterotypic association. Furthermore, the accumulation of AD:DM1^{TIR-pNB} was also relatively weak when co-expressed with the BD domain alone (**Fig. R6B**, lane 2) but strongly increased when co-expressed with the BD:DM1^{TIR-pNB} fragment (**Fig. R6B**, lane 6).

Although these experiments were carried out in a heterologous system, these findings suggest that DM1 might be less stable as a monomer. Taken together, my yeast data provide evidence that the N-terminal parts of DM1 and DM2d contain an interface that allows both DM1-DM1 and DM1-DM2d associations. The homotypic DM1-DM1 interaction was observed with longer fragments compared to the heterotypic interaction does, suggesting that DM1-DM1 homotypic association is less likely to be negatively regulated by other domains than DM1-DM2d heterotypic association. Both DM1 and DM2d accumulated to higher levels when co-expressed with the DM1 interacting partner, which complicates statements about protein-protein interactions, but might hint at an additional level of protein regulation.

3. Physical associations of DM1 and DM2d *in planta*

I made use of the transient expression system in *N. benthamiana* leaves (Chae et al., 2014) to confirm the interaction properties of DM1 and DM2d first observed in yeast. I transiently co-expressed full-length DM1-Myc/DM1-HA, DM1-Myc/DM2d-HA and DM2d-Myc/DM2d-HA from their native promoters. As expected, visible HR was only observed when combining DM1-Myc and DM2d-HA (**Fig. R7A**). Immunoprecipitation of DM1-Myc allowed detection of both DM1-HA and DM2d-HA (**Fig. R7B**, lanes 5 and 6), thus recapitulating DM1-DM1 homotypic and DM1-DM2d heterotypic associations *in planta*. Notably, I observed that the amount of co-immunoprecipitated DM1-HA (in the DM1-Myc/DM1-HA) was always higher than the amount of DM2d-HA (in the DM1-Myc/DM2d-HA) when compared to their input protein levels (**Fig. R7B**, 10% input), suggesting that DM1 might associate more strongly with itself than with DM2d.

I could also co-immunoprecipitate DM2d-Myc with DM2d-HA (**Fig. R7B**, lane 7), which was not predictable from the Y2H assays due to low protein expression of DM2d fragments in yeast cells (**Fig. R6**). In contrast to yeast, DM2d accumulated to

appreciable level in *N. benthamiana* leaves, which might explain the discrepancy of apparent interactions in the two systems. Collectively, the data indicates that full-length DM1 and DM2d associate not only with their partner to form heterodimeric DM1/DM2d complexes but also with themselves to form DM1/DM1 and DM2d/DM2d homodimers (**Fig. R7B**).

To validate the DM1/DM2d association in an endogenous context, i.e. in stable *A. thaliana* lines, I generated independent homozygous transgenic lines (Col-0 background) carrying ethanol inducible *DM1-HA* (*indDM1-HA*) and genomic *DM2d-Myc*, hereafter Col-0^{*indDM1-HA*} and Col-0^{*DM2d-Myc*}.

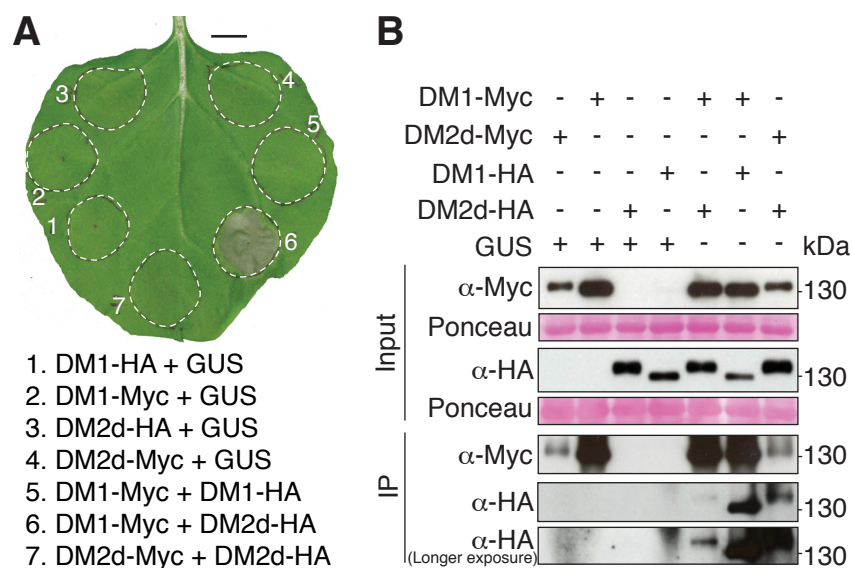


Figure R7. Homo- and heterotypic association of DM1 and DM2d in *N. benthamiana*

(A) HR from co-expression of DM1 and DM2d constructs at 4 dpi. Similar material was used for co-immunoprecipitation (coIP) in (B). Scale bar equals 1 cm.

(B) CoIP analysis of DM1 and DM2d from *N. benthamiana* samples. Total protein extracts were used with leaf samples collected at 2 dpi. 10% of total protein extract of each sample was loaded as input. Ponceau-S staining shown to indicate loading.

I grew F₁[*indDM1-HAxDM2d-Myc*] hybrid plants at 23°C in long-day conditions because the DM1/DM2d mediated cell death, which is often inactive at this temperature, can be manually monitored by inducing the expression of DM1. 15-day-old seedlings were irrigated with 1% EtOH and kept under a transparent dome for 3 days to induce the expression of DM1-HA. A control set of plants was not treated and grown in a separate, ethanol-free growth room.

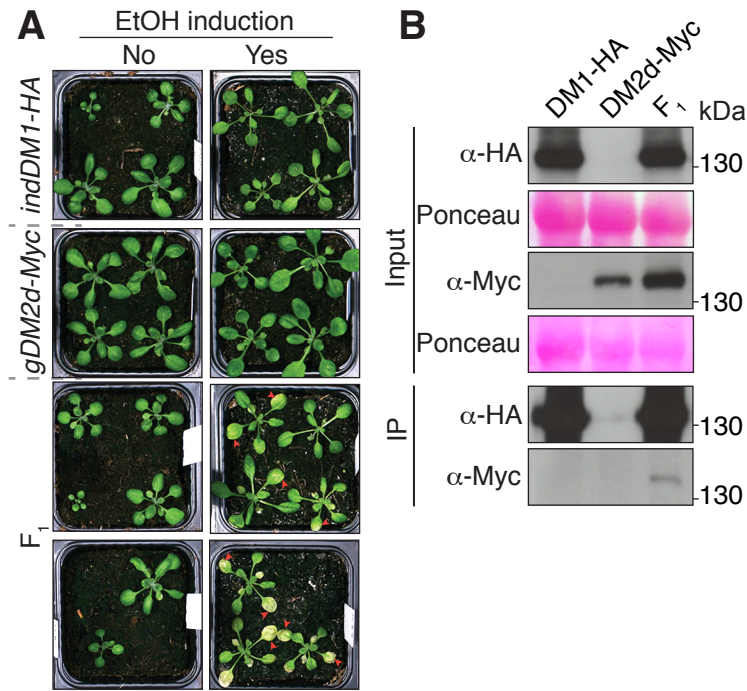


Figure R8. Co-immunoprecipitation of DM1 and DM2d in *A. thaliana*

(A) Recapitulated DM1/DM2d dependent necrosis in F₁[indDM1-HA/DM2d-Myc]. Ethanol induction was performed with 15-day-old seedlings by irrigating with 1% EtOH and covering the flat for 3 days with a transparent dome. Red arrows indicate onset of cell death at 3 days after induction (dai).

(B) CoIP analysis of DM1 and DM2d from *A. thaliana* samples shown in (D). Total protein extracts from the pooled leaf tissues collected at 18 dai were used for CoIP. Input indicates 10% of total protein extract. Ponceau-S staining shown to indicate loading.

In the non-inducing conditions, neither parents nor F₁ plants showed autoimmune symptoms on their leaves (**Fig. R8A**). However, six out of ten F₁ individuals from independent crosses did showed such symptoms after watering with ethanol. Of six F₁ lines having induced autoimmune symptoms, two showed severe and four mild HR (**Fig. R8A** and **Fig. S5**). I collected leaf samples in bulk at 18 days after ethanol treatment and performed coIP experiments. Pull-down of DM1-HA allowed detection of DM2d-Myc, indicating that heterotypic engagement between DM1 and DM2d also occurs in *A. thaliana* (**Fig. R8B**). The coIP assay was repeated twice with similar results. In addition, I obtained a consistent result when performing the coIP assay with more stringent detergent conditions (0.5% NP-40) (**Fig. S6**). Taken together, my experiments demonstrated that physical association of DM1 and DM2d can be observed upon co-expression, and goes hand in hand with the onset of cell death both in *N. benthamiana* as well as in *A. thaliana* leaves. DM1-DM1 pairing

is observed under similar experimental conditions in *N. benthamiana*, but does not involve cell death.

I demonstrated that DM1 and DM2d could associate in a heterodimeric form, but each receptor themselves could also self-associate as homodimer. The presence of DM1 seems to increase the accumulation of DM2d both in yeast and *in planta* (**Fig. R6B** and **R7B**), which might indicates that the association with DM1 stabilizes DM2 protein. In the other studied NLR pairs, RPS4/RRS1 and RGA4/5, heterotypic NLR association prevented auto-activity of the RPS4 TIR and of full-length RGA4 protein homodimers (Césari et al., 2014b; Williams et al., 2014). In the case of DM1/DM2d, however, I observed the reverse scenario: DM1/DM1 co-expression, although it led to homo-association, did not trigger cell death, while DM1/DM2d co-expression led to hetero-association as well as HR.

4. Correlation of physical association of the TIR domains and DM1/DM2d signaling

TIR domains provide an interface for TNL receptor pairing (Bernoux et al., 2011; Williams et al., 2014; and this study). The modeled structural similarity of DM1 and DM2d with RPS4 and RRS1 TIR domains (see above) prompted me to ask whether similar residues were responsible for the pairing in DM1 and DM2d and how physical associations would correlate with DM1/DM2d cell death signaling.

The SH motifs at the N-terminus of the RRS1 and RPS4 TIR domains contribute to TIR heterodimer and TIR homodimer formation (Williams et al., 2014). Mutations in the SH motif that abrogated heterotypic interaction of RPS4/RRS1 TIR domains also disabled the NLR complex so that it could no longer recognize its cognate AvrRps4 and PopP2 effectors (Williams et al., 2014). The SH motif resides at positions 34-35 in DM1, and at positions 69-70 in DM2d (**Fig. R2**).

To test whether DM1-DM2d association also involves the SH motif, I mutated both residues to alanine, resulting in DM1^{S34A H35A} and DM2d^{S69A H70A}. In Y2H assay with TIR-pNB fragments, substitutions in the SH motifs in either one or both partners compromised DM1-DM1 as well as DM1-DM2d interaction (**Fig. R9A**). This provides further evidence for the structural and functional similarity of the DM1, DM2d, RRS1 and RPS4 TIR domains.

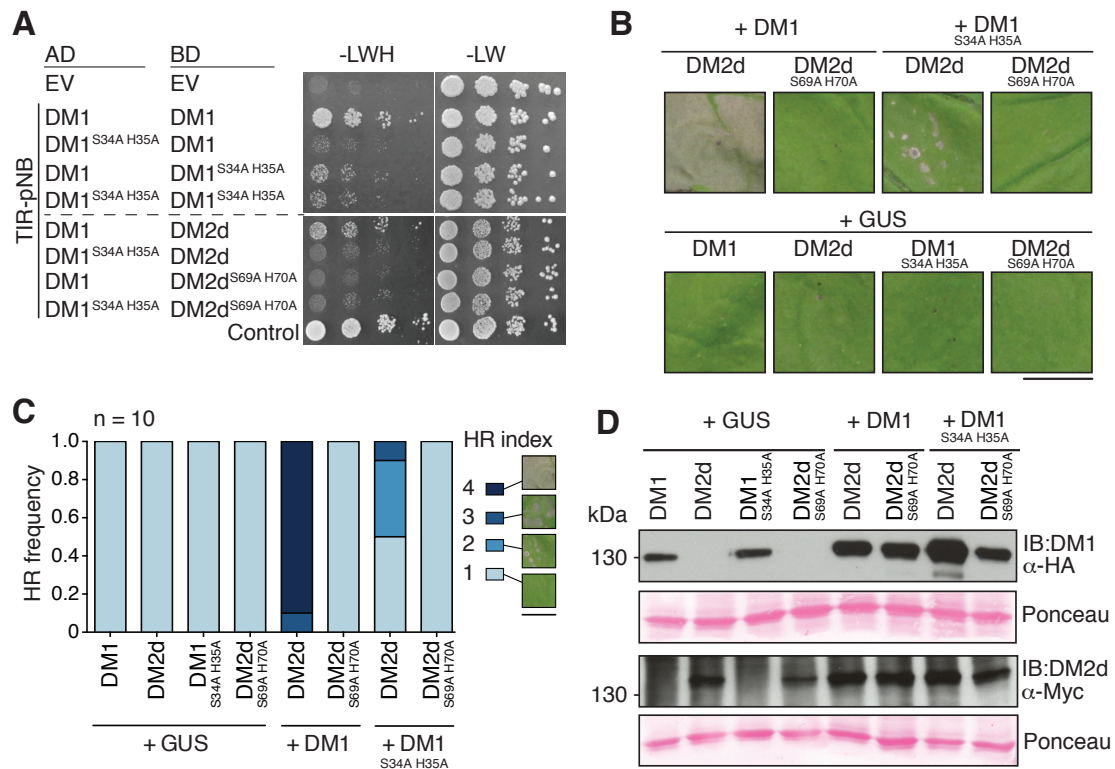


Figure R9. Role of the SH motif in DM1/DM2d cell death signaling

(A) Y2H analysis of TIR-pNB fragments of DM1 (DM1¹⁻³⁰⁸) and DM2d (DM2¹⁻³⁵⁸) carrying substitutions in the SH motif.

(B) The effect of the SH substitutions in DM1 and DM2d on their HR triggering ability in *N. benthamiana*. HR was scored at 4 dpi. Co-expressed constructs are indicated above each image. Scale bar equals 1 cm.

(C) Summary of semi-quantitative HR scoring. The HR index was determined by the relative area showing HR per total infiltrated leaf area and ranged from 1 (no HR), 2 (less than 20% HR), 3 (20 to 60% HR) to 4 (more than 60% HR). Representative HR symptoms (at 4 dpi) are shown in the black-lined squares on right. The scale bar equals 1 cm. n represents number of replicates.

(D) Protein accumulation of DM1^{S34A H35A} and DM2d^{S69A H70A} plus controls. All proteins were transiently expressed in *N. benthamiana*. Leaf samples for protein extraction were collected at 2 dpi. Ponceau-S staining shown to indicate loading.

To examine whether the physical association of DM1 and DM2d correlates with cell death signaling, I transiently co-expressed full-length DM2d^{S69A H70A} with either wild-type DM1 or DM1^{S34A H35A} in *N. benthamiana*. Mutations in the SH domain of DM2d eliminated HR symptoms (Fig. R9B). DM1^{S34A H35A}, however, seemed to retain some residual activity when co-expressed with wild-type DM2d (Fig. R9B). I also performed a semi-quantitative analysis of HR severity (Fig. R9C), scoring 10 independently co-infiltrated leaves for each DM1/DM2d combination. It confirmed that DM1^{S34A H35A} and wild-type DM2d could trigger low level of HR in *N. benthamiana*.

The expression of wild-type and mutated proteins was confirmed on western blots (Fig. R9D), demonstrating that reduced HR levels were not due to reduced protein abundance.

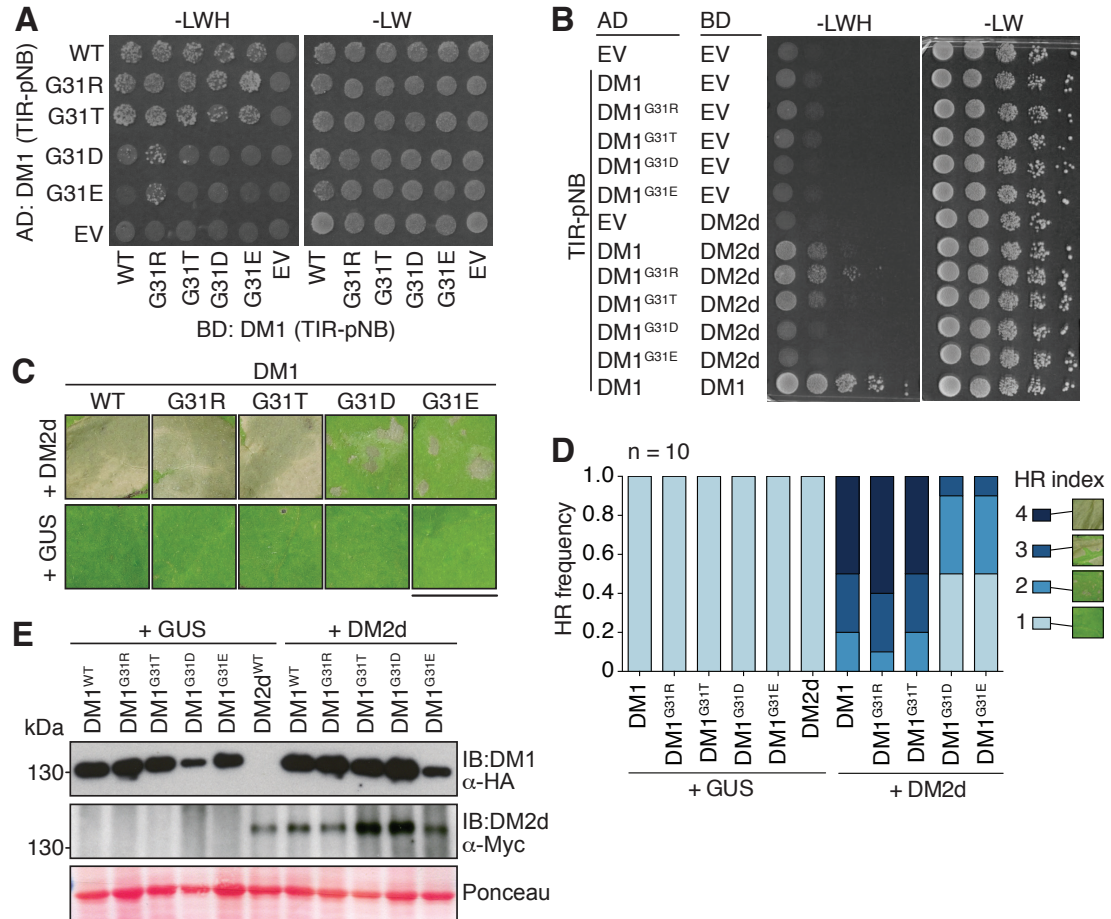


Figure R10. The contribution of the DM1 G31 residue to DM1/DM2d cell death signaling

Y2H assays with DM1 TIR-pNB fragments carrying G31 substitutions testing (A) DM1 homodimerization, and (B) interactions with the TIR-pNB fragment of DM2d^{WT}

(A) Y2H assays of TIR-pNB DM1 truncations carrying G31 substitutions.

(B) Y2H assays with TIR-pNB fragments of DM2d and G31 variants with that of DM2d^{WT}.

(C) HR symptoms upon co-expression of DM1 G31 variants with DM2d in *N. benthamiana*. HR was scored at 4 dpi. Scale bar equals 1 cm.

(D) Summary of semi-quantitative HR scoring. The HR index was determined by the relative area showing HR per total infiltrated leaf area and ranged from 1 (no HR), 2 (less than 20% HR), 3 (20 to 60% HR) to 4 (more than 60% HR). Representative HR symptoms (at 4 dpi) are shown in the black-lined squares on right. The scale bar equals 1 cm. n represents number of replicates.

(E) Protein blot for DM1 G31 from *N. benthamiana* samples as in (C). Leaves were collected at 2 dpi for protein extraction. Ponceau-S staining shown to indicate loading.

Collectively, these results showed that HR was observed after co-expression of proteins containing TIR domains that were able to interact in a heterologous system. It suggests a scenario in which NLR interaction (through TIR domains) precedes and initiates cell death signaling.

Because both DM1-DM1 and DM1-DM2d interactions were not abolished completely in yeast by SH mutations, I want to test whether other residues close to the SH motif contribute to TIR-TIR interaction. An arginine proximal to the SH motif (R30) affects homodimerization of RPS4 (Williams et al., 2014). R30A substitution enhanced RPS4 TIR dimerization as well as RPS4 TIR-mediated autoactivation (Williams et al., 2014). G31 in DM1 and T66 in DM2d correspond to RPS4 R30 (**Fig. R4E**). I introduced a series of substitutions on both sides to investigate how they would affect DM1 and DM2d association. Substitutions of G31 in DM1 either with arginine (R) or threonine (T) did not modify TIR-TIR homodimerization in yeast (**Fig. R10A**). Similarly, DM1^{G31R} and DM1^{G31T} mutations also did not disrupt the TIR-TIR heterotypic interaction with wild-type DM2d in yeast (**Fig. R10B**).

Consistent with the maintenance of their TIR interaction properties, full-length DM1^{G31R} and DM1^{G31T} triggered HR similar to the wild-type DM1 when co-expressed with wild-type DM2d in *N. benthamiana* (**Fig. R10C-D**). When G31 was substituted with negatively charged aspartate or glutamate (DM1^{G31D} and DM1^{G31E}), both DM1-DM1 and DM1-DM2d TIR interactions in yeast were abrogated (**Fig. R10A-B**). I observed only low levels of HR when co-expressing the respective full-length proteins with wild-type DM2d in *N. benthamiana* (**Fig. R10C-D**). The coincidence of TIR-TIR interaction/severe HR and TIR-TIR loss-of-interaction/reduced HR caused by DM1 G31 substitutions suggests that G31 may (directly or indirectly) contribute to DM1-DM2d dimerization that correlates with cell death symptoms on leaves upon co-expression.

Similar substitutions were introduced in DM2d at the T66 residue. TIR-pNB fragments containing DM2d^{T66A} or DM2d^{T66G} substitutions partially retained the ability to interact with TIR-pNB of wild-type DM1 in yeast (**Fig. R11A**). As expected, DM2d^{T66A} compromised, but did not abolish HR symptoms upon co-expression with wild-type DM1 in *N. benthamiana*. No cell death was however observed when DM2d^{T66G} was co-expressed with wild-type DM1 (**Fig. R11B-C**). I confirmed expression of all assayed proteins (**Fig. R10E and R11D**), indicating that the modified cell death symptoms were not due to differences in protein accumulation.

Therefore destabilizing of DM1-DM2d TIR-hetero-association may coincide with decreased cell death signaling upon heterologous co-expression.

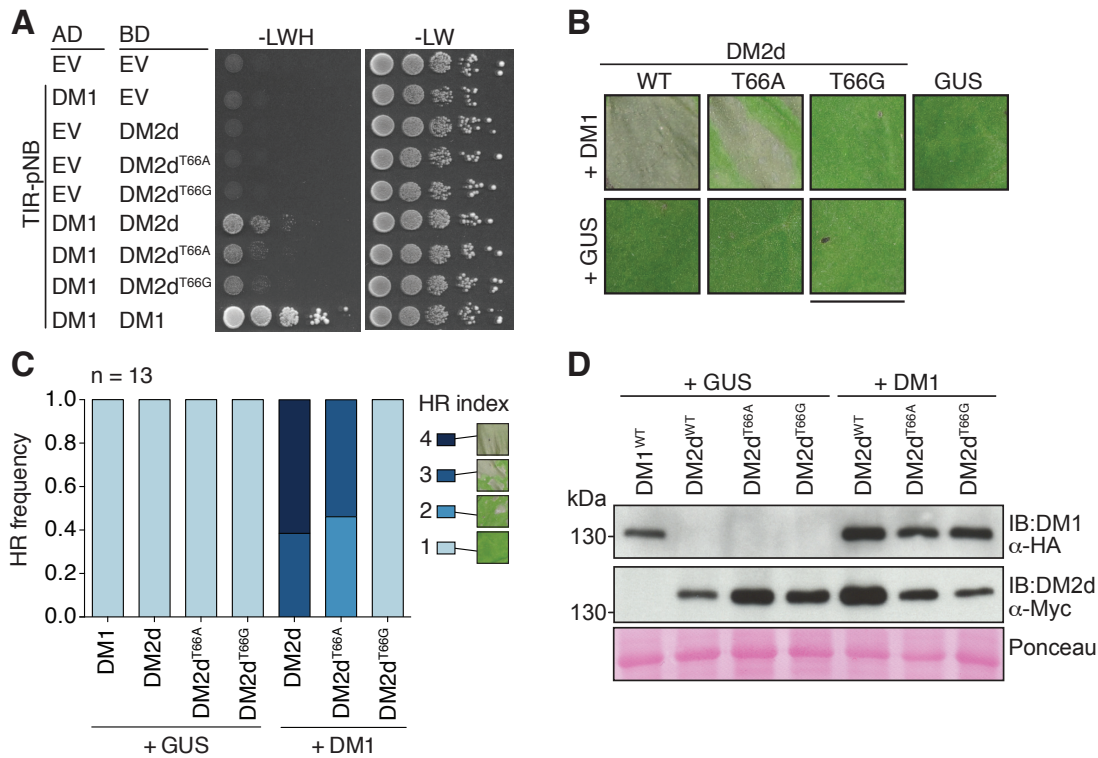


Figure R11. Contribution of the DM2d T66 residue to DM1/DM2d signaling
 (A) Y2H analysis of TIR-pNB truncations of DM2d^{T66} mutants with that of DM1^{WT}.
 (B) Testing HR triggering ability of the DM2d^{T66} mutants in *N. benthamiana*. The HR phenotype was scored at 4 dpi. Scale bar equals 1 cm.
 (C) HR symptoms upon co-expression of DM1 G31 variants with DM2d in *N. benthamiana*. HR was scored at 4 dpi. Scale bar equals 1 cm.
 (D) Summary of semi-quantitative HR scoring. The HR index was determined by the relative area showing HR per total infiltrated leaf area and ranged from 1 (no HR), 2 (less than 20% HR), 3 (20 to 60% HR) to 4 (more than 60% HR). Representative HR symptoms (at 4 dpi) are shown in the black-lined squares on right. The scale bar equals 1 cm. n represents number of replicates.
 (D) Protein blot of DM2d^{T66} mutants in transiently expressed *N. benthamiana*. The mutated variants of DM1 were co-expressed either with GUS or with DM1^{WT}. Leaf samples for protein extraction were collected at 2 dpi. Ponceau-S staining shown to indicate loading.

5. P-loop mutations do not disrupt the physical association of DM1 and DM2d

P-loop mutations can affect the oligomerization ability of several NLRs, for instance of the tobacco N protein in the presence of its cognate effector (Mestre and Baulcombe, 2006). To test whether the loss of signaling in P-loop mutants is due to

the loss of physical interaction between DM1 and DM2d, I performed Y2H assays using P-loop mutants of both DM1 (DM1^{G223A K224A}) and DM2d (DM2d^{G259A K260A}) TIR-pNB fragments (with the help of Monika Demar).

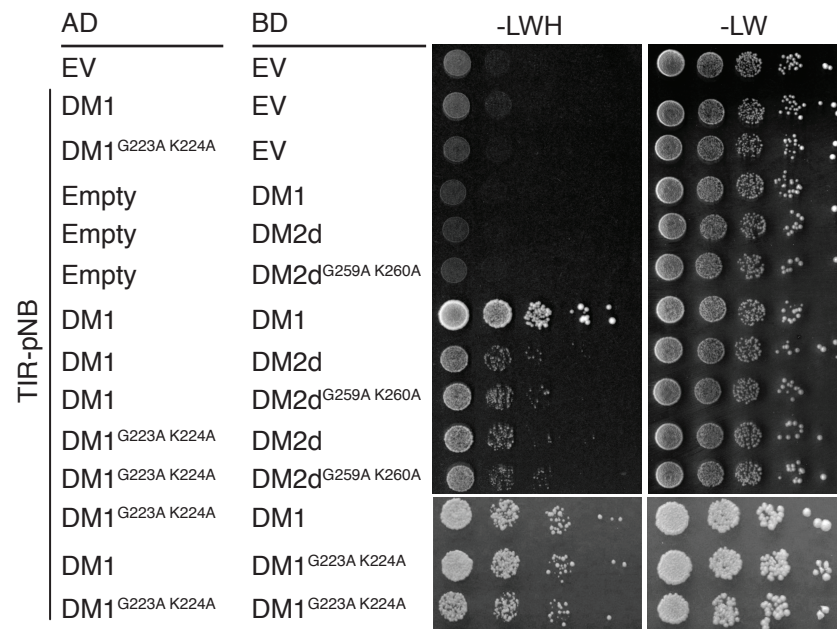


Figure R12. Physical interaction of DM1 and DM2d P-loop mutants in yeast
 Y2H analysis of physical interaction property of the P-loop mutants of DM1 and DM2d. The P-loop mutants in DM1 and DM2d neither alter the DM1-DM1 homotypic interaction nor DM1-DM2d heterotypic interaction. (The lower DM1-DM1 panel was prepared by Monika Demar).

Different from has been described for the N protein, P-loop mutated DM1 and DM2d maintained their interaction properties in Y2H assays, both for DM1-DM1 and DM1-DM2d associations (**Fig. R12**). This result suggests that in DM1/DM2d dependent signaling, the functional importance of the P-loop is independent from the protein interaction properties. The inability of P-loop mutants in induce HR *in planta* is therefore likely due to loss of ATP/ADP binding or conformational changes. The data also lead me to propose that physical associations of DM1 and DM2d are necessary, but not sufficient, for cell death signaling.

CHAPTER 3.

Unequal Contribution of DM1 and DM2d to signaling

Activation of NLR receptor complexes can involve unequal contributions of both partners in NLR pairs (Césari et al., 2014b; Hu et al., 2015; Le Roux et al., 2015; Maqbool et al., 2015; Sarris et al., 2015; Williams et al., 2014). An emerging theme from such plant NLR pairs is that one partner carries an extra domain that directly binds to effectors while the other partner signals through its P-loop (Césari et al., 2014a). DM1 and DM2 do not have an “integrated decoy”, suggesting DM1/DM2 signaling might be different from other plant NLR pairs. The structural similarities of TIR-TIR interface between DM1/DM2d and RPS4/RPS1 as well as my finding that DM1/DM1 homotypic and DM1/DM2d heterotypic association play different roles in signaling prompted me to ask whether DM1 and DM2d have distinct roles in signaling.

1. Distinct contributions of DM1 and DM2d to signaling

To investigate the importance of DM1 and DM2d for cell death signaling in the absence of effectors, I performed competition assays by providing increasing quantities of functionally compromised DM1 or DM2d versions to a constant combination of wild-type partners. Three different levels of the competitor (OD_{600} of 0.525, 1.05 and 2.1) were co-infiltrated with a mixture of wild-type DM1 and DM2d (both at OD_{600} of 0.525) in *N. benthamiana* leaves. I scored the degree of HR in a semi-quantitative manner (**Fig. R13A**). As control, I used DM1^{WT} as a competitor to ensure that an exact stoichiometric ratio of DM1 and DM2d was of minor importance for signaling and that excessive inoculum did not alter HR. Addition of DM1^{WT} at the highest OD ($OD_{600} = 2.1$) altered HR symptoms only mildly (**Fig. R13B**), suggesting that reduced HR in the presence of compromised competitors would report true protein competition.

I first used two functionally impaired DM1 variants as competitors: the P-loop mutant (G223A K224A) and a chimeric protein in which the LRR domain was replaced by that of the Col-0 homolog At5g41750 (DM1^{Col-0(495-988)}). Both DM1 competitors attenuated HR symptoms, with DM1^{G223A K224A} doing so to a greater

extent (**Fig. R14**). This points to a critical role of DM1 in cell death signaling where both homotypic DM1-DM1 and heterotypic DM1-DM2d contribute to.

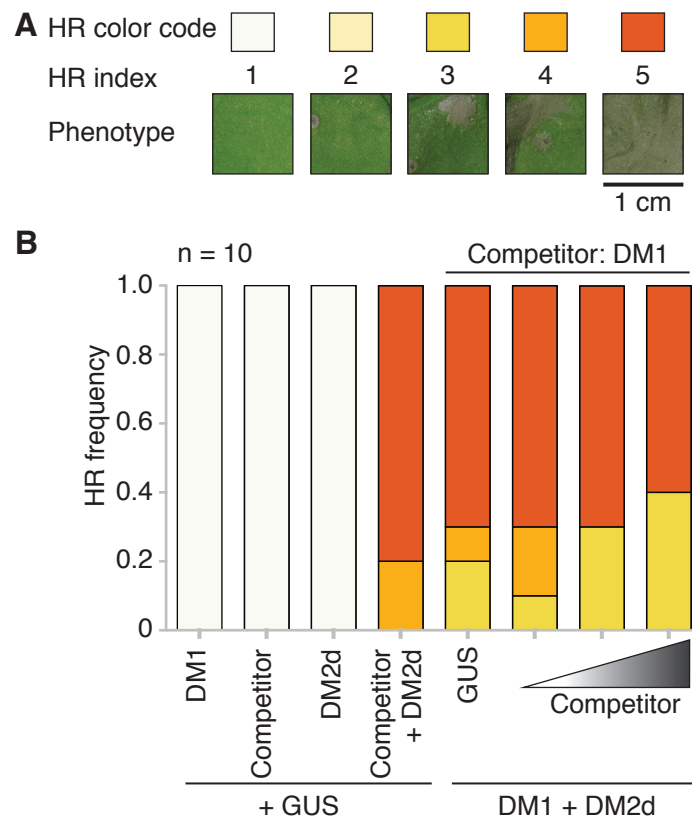


Figure R13. HR scoring and the competition assay using wild-type DM1 in *N. benthamiana*

(A) Semi-quantitative scoring scheme for HR confluency in *N. benthamiana*. The HR index was scored as a percentage of leaf area exhibiting HR in the total infiltrated area ranging from 1 (no HR), 2 (less than 5% HR), 3 (5 to 20% HR), 4 (20 to 60% HR), and 5 (more than 60% HR). n represents number of replicates.

(B) Increasing amount of wild-type DM1 does not greatly affect DM1/DM2d signaling.

I also tested P-loop mutant DM2d^{G259A K260A} and the inactive DM2d paralog, DM2g, as competitors. DM2g, which shares 93% amino acid similarity with DM2d and resides also at *DM2* locus on chromosome 3 of *Uk-1* (Chae et al., 2014), is discussed in more detail below. DM2g also interacted with DM1 in yeast (**Fig. R19B-C**), but was unable to trigger HR when co-expressed with DM1 (**Fig. R20**), as expected from *A. thaliana* genetics (Chae et al., 2014). I found that elevated amounts of the DM2d^{G259A K260A} or DM2g competitors caused only a mild suppression of HR – different than what I observed with DM1 competitors (**Fig. R15**). This suggests that

small amounts of DM2d are sufficient to initiate robust HR signaling, while DM1 is needed in comparatively larger amounts.

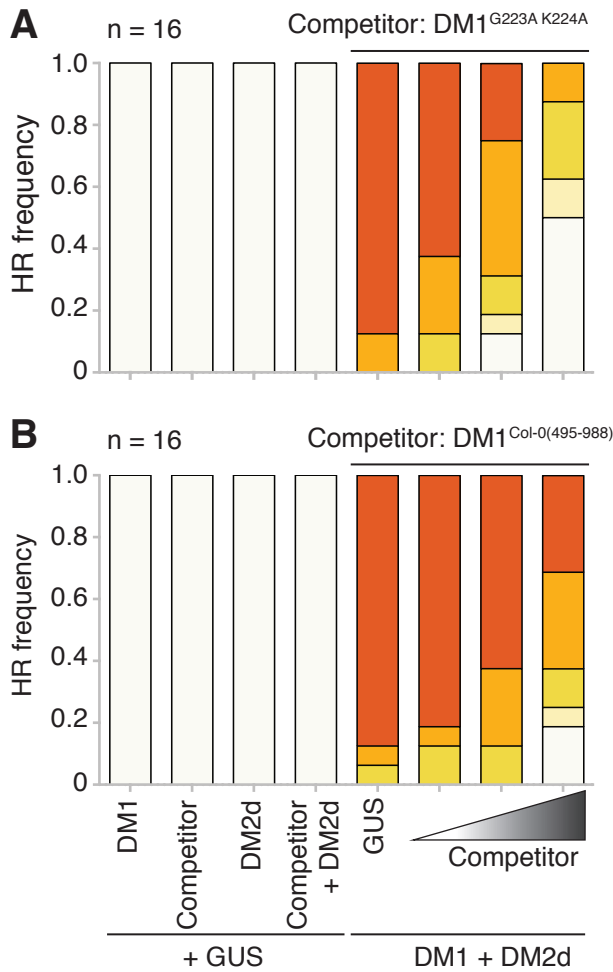


Figure R14. Competition assays using DM1 variants in *N. benthamiana*

Competition assays using the P-loop mutant DM1^{G223A K224A} (A) and DM1^{Col-0 (495-988)} (B) as competitors for DM1^{WT}. The HR was scored at 4 dpi. n indicates the number of replicates in each panel. See the legends in Figure R13A for color code and HR index.

The different degrees of HR that I observed in the presence of different competitors indicate that the signaling competency of each participating NLR can modulate the summation of signaling intensity. Given DM1 and DM2 competitors show different outcomes, the data supports that DM2d functions as a switch, whose function is similar to a catalyst in an enzymatic reaction, i.e. a small amount of wild-type DM2d is sufficient to trigger signaling; while DM1 plays a major role in executing signaling.

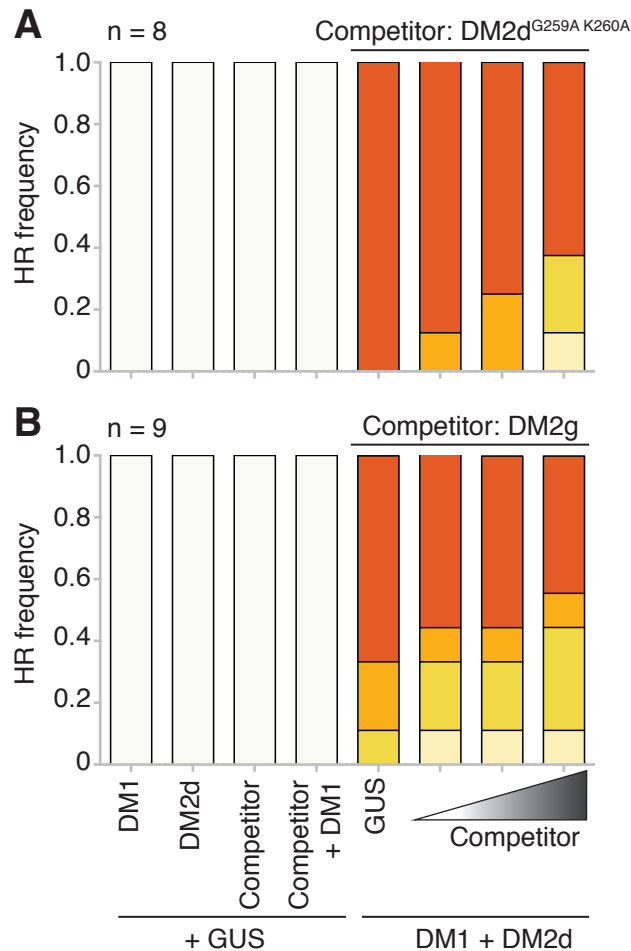


Figure R15. Competition assays using DM2d variants in *N. benthamiana*

Competition assays using the P-loop mutant DM2d^{G259A K260A} (A) and DM2g (B) as competitors for DM2d^{WT}. The HR was scored at 4 dpi. n indicates the number of replicates in each panel. See the legends in Figure R13A for color code and HR index.

2. Asymmetric contribution of the MHD motifs in DM1 and DM2d to the signaling

The MHD motif, as mentioned above, is located in the ARC2 subdomain of NB-ARC domain, and is believed to cooperate with the P-loop in forming the nucleotide-binding pocket. Mutations in either the MHD motif or P-loop or both might not only affect ADP/ATP binding and/or exchange, but might also affect the conformation of the entire receptor (Lukasik and Takken, 2009; Takken et al., 2006).

In both DM1 and DM2d, the MHD motif does not conform to the consensus found in most plant NLRs (Howles et al., 2005), being MHH in DM1 and paralogs, and MHT in DM2d and paralogs. One might hypothesize that the changes could contribute to structural alterations modifying the requirements for protein activation, given that, for example, MHS and MHV variants of flax L6 are autoactive (Howles et al., 2005).

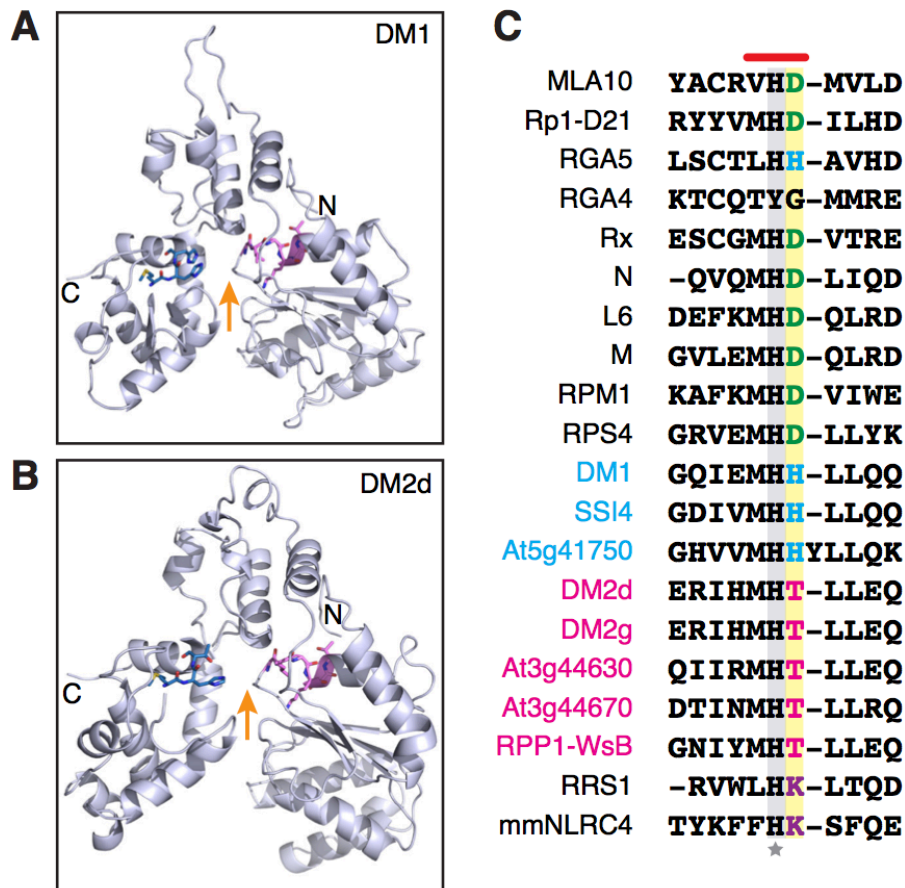


Figure R16. Modeling visualization of the NB-ARC domain of DM1 and DM2d and amino acid sequence alignment of the MHD motif among plants NLRs

(A-B) Homologous topology of NB-ARC domain of DM1 (A) and DM2d (B) based on that of mNLRC4 (Hu et al., 2013). Predictions were performed using PHYRE2 (Kelley et al., 2015). P-loop and MHD motifs are indicated as amino acid sticks highlighted in pink and blue. ATP/ADP binding pocket is indicated by an arrow.

(C) Sequence alignments of the MHD motif of plant NLRs as well as NLRC4 from mouse (mNLRC4). The MHD motif is marked under the red bar. The conserved Histidine residue at the second position is shaded in grey and variable residues at the third position in yellow. Different text colors indicate different residues at the third position. DM1 homologs are labeled by cyan and DM2 homologs in magenta. The asterisk below the mNLRC4 sequence indicates a residue that causes autoimmunity when mutated (Hu et al., 2013).

Because crystal structures of plant NB-ARC domain were not available, I used PHYRE2 to search for published structural homology of the NB-ARC domains of DM1 and DM2d. The NB-ARC domains of both DM1 and DM2d share stereo-similarities to the previously crystalized central NOD domain of animal NLR receptors including mouse NLRC4 that serves as co-receptor for different NAIP receptors sensing distinct pathogen effectors (Hu et al., 2013). The modeled NB-ARC structures of DM1 and DM2d are shown in **Fig. R16A-B**. Both place the P-loop (in

pink) and the MHD motif (in blue) in close proximity, and form a nucleotide-binding pocket.

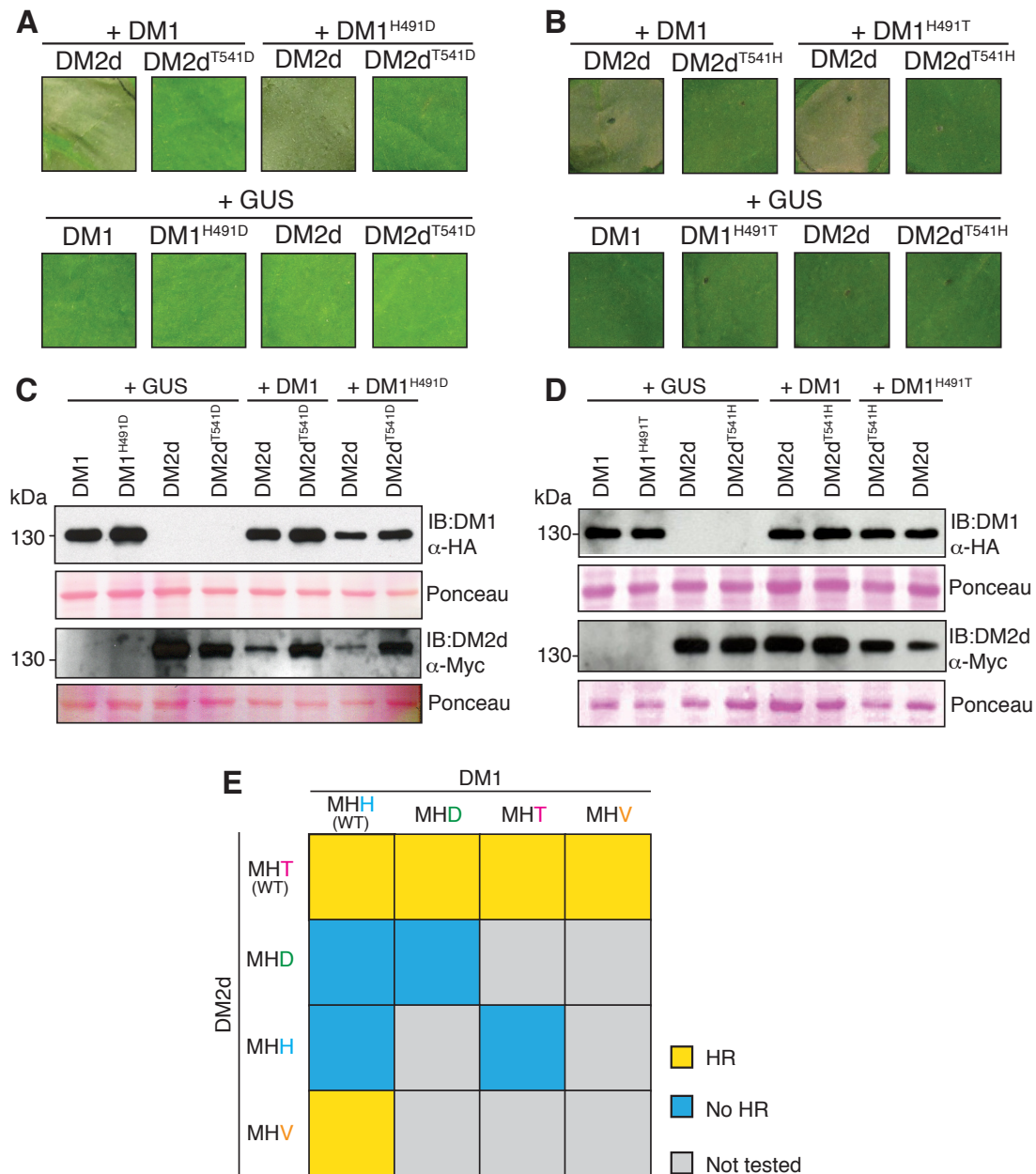


Figure R17. Differential effects of MHD substitutions in DM1 and DM2d

(A, B) DM1 and DM2d MHD mutants were transiently co-expressed in *N. benthamiana* in all combinations with respective partners. GUS served as a negative control. Representative HR phenotypes at 4 dpi are shown.

(C-D) Protein blot analyses of proteins expressed in (A) and (B). Leaf samples for protein extraction were collected at 2 dpi. Ponceau-S staining shown to indicate loading.

(E) Summary diagram of the MHD motif mutagenesis shown in A and B. Each square in the diagram represents HR phenotype scored at 4 dpi. HR phenotypes are color-coded: 100% HR is in yellow, no HR is in blue, and combinations that were not test are in grey.

Because of the close proximity of the P-loop and the MHD motif in the NB-ARC domain, I assessed the predicted conformation changes in P-loop GIGKTT to GIAATT mutants (DM1^{G223A K224A} and DM2d^{G259A K260A}) based on the mouse NLRC4 crystal structure (Hu et al., 2013). In both cases (**Fig. R18**), only minor alterations were observed. This suggests that the coordination of the MHD motif in relation to P-loop is intact in the P-loop-dead variants of DM1 and DM2d, and loss of signaling ability is independent of the proximity to the MHD motif.

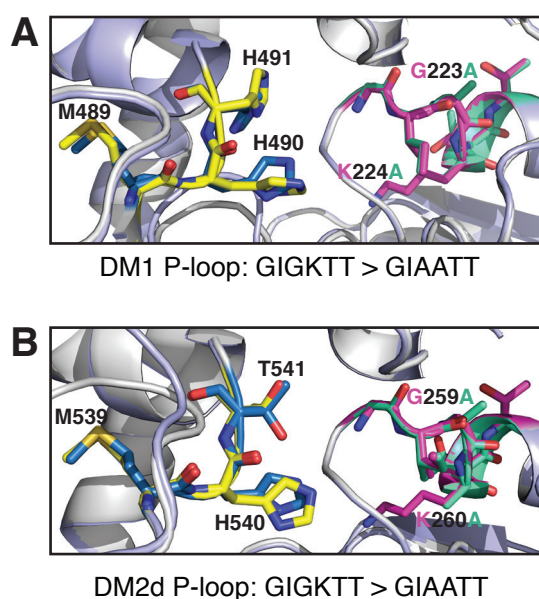


Figure R18. Structure simulation of P-loop mutants.

Superimposed homologous structure shows relative spatial position of P-loop and the MHD motif in DM1 (A) and DM2d (B). For wild-type proteins, P-loop residues are highlighted in pink and MHD residues in blue. For P-loop mutant proteins, P-loop residues are highlighted in green and MHD residues in yellow. Glycine and lysine residues of P-loop motifs and three residues of MHD motifs in each protein are indicated in the figures.

Alignment of various NLRs around the MHD motif revealed that the third position (D) is most variable. Particularly in those proteins known as sensors with integrated domains whose activities do not depend on functional P-loops, such as RRS1 and RGA5 (Césari et al., 2013), the motif is degenerate. (**Fig. R16C**). Substitution of the residues in RGA5 did not alter the activity, while the motif in RGA4, despite high degeneracy, is required for proper signaling (Césari et al., 2014b), pointing to relative importance of the motif in relation to P-loop activity.

I already observed that valine substitutions in DM1 and DM2 (DM1^{H491V} and DM2d^{T542V}) did not render the proteins autoactive, different from what has been observed for other NLRs (Howles et al., 2005) (**Fig. R3**). Consistently, the predicted protein structures appear to barely change (**Fig. R19C and F**).

To further assess the role of the third residue of the MHD motif in DM1 and DM2d function, I introduced more substitutions and tested their effect on DM1/DM2d-dependent HR. To retrieve the 'usual' MHD sequence, I engineered an aspartate in both proteins (DM1^{H491D} and DM2d^{T542D}), and I also generated the reciprocal version DM1^{H491T} and DM2d^{T542H}. When co-expressed in *N. benthamiana* leaves with DM2d^{WT}, none of the DM1 variants affected the HR outcome (**Fig. R17**). On the contrary, both DM2d^{T542D} and DM2d^{T542H} abrogated HR signaling completely when co-expressed with DM1^{WT} (**Fig. R17**). This demonstrates that unlike DM1, DM2d is sensitive to changes at the MHD motif, and it supports a model in which the signaling competency of the heteromeric DM1/DM2d complex relies more on the conformation or activity status of DM2d rather than DM1.

Because of the close proximity of the P-loop motif and the MHD motif in the NB-ARC domain, I sought to assess the conformational effect caused by P-loop motif mutations on the MHD motif, and *vice versa*, for DM1 and DM2d. Indeed, structural simulation of the NB-ARC domains of DM1 and DM2d based on that of the crystalized NLRC4 from mouse (Hu et al., 2013) revealed that mutations of the P-loop motif did not drastically affect the conformation of the MHD motif of both DM1 and DM2d (**Fig. R18**). This result suggests that DM1 and DM2d P-loop mutants lose their activity not merely because of structural alterations, but rather because of P-loop activity.

In line with this idea, structure predictions suggested that in the DM2d^{T542D} variant, an amine tail of K260 in the P-loop would bend approximately 90°, which in turn might disturb its contact to H541 and binding to ATP/ADP (Hu et al., 2013) (**Fig. R19D**). I did not find such a drastic change for any of the DM1 variants (**Fig. R19A-C**) or DM2d^{T542H} (**Fig. R19E-F**).

Based on these findings, I speculate that the third residue of DM2d MHD motif is sensitive to changes. This suggests that alterations in the DM2d molecule that (mildly or strongly) affect the T541 residue, maybe induced by close contact to DM1, could easily induce larger (possibly structural) changes and subsequent initiation of HR signaling, likely via DM1.

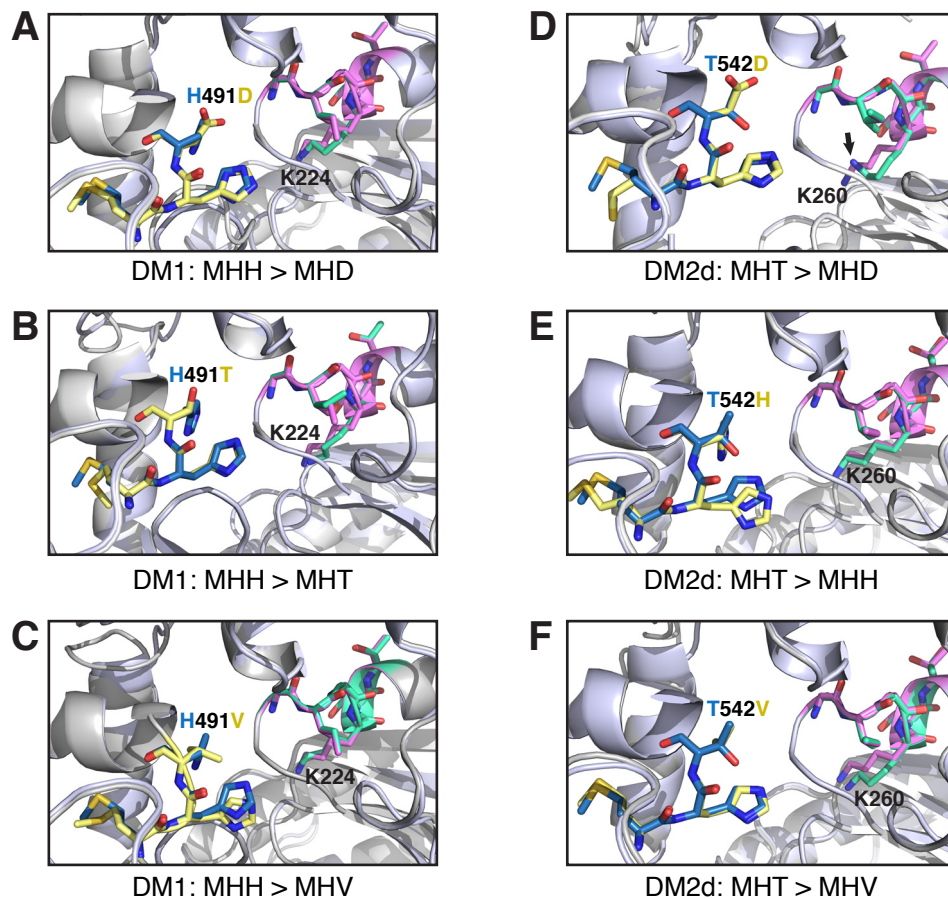


Figure R19. Structure simulation of MHD mutants

Superimposed homologous structure of the MHD motif and its third-residue mutants in relation to the P-loop in DM1^{H491D} (A), DM1^{H491T} (B), DM1^{H491V} (C), DM2d^{T541D} (D), DM2d^{T541H} (E) and DM2d^{T541V} (F). For wild-type proteins, P-loop residues are highlighted in pink and MHD motif residues in blue. For mutated proteins, P-loop residues are highlighted in green and MHD motif residues in yellow. Glycine and lysine residues of P-loop and three residues of MHD motif in each protein are indicated in the figures. Black arrow in (D) indicates the distortion of amine tail of K260 in mutated DM2d.

CHAPTER 4.

Analysis of Natural Variants of DM2

The *DM2d* gene is part of an NLR gene cluster that contains *RPP1*-like genes, several of which confers race-specific resistance to the oomycete *Hpa* (Botella et al., 1998; Chae et al., 2014; Krasileva et al., 2011). Corresponding gene clusters from various *A. thaliana* accessions show high variability not only in sequence but also in *NLR* copy number (Alcázar et al., 2009; Bomblies et al., 2007; Chae et al., 2014). *DM2* is an ‘incompatibility hotspot’, with different causal alleles for number of *A. thaliana* hybrid necrosis cases (Chae et al., 2014; Stuttmann et al., 2016). Proteins encoded at the *DM2* locus are often highly similar, possibly due to gene duplications and conversion events (Chae et al., 2014). Nevertheless, a single *DM2* allele is usually responsible for hybrid incompatibility and also for race-specific *Hpa* resistance. Studying the limited differences between closely related *DM2* variants provides a unique entry point for understanding their molecular modes of action.

1. Polymorphisms in *DM2* variants

In the Uk-1 accession, the *DM2* cluster contains eight *DM2* paralogs, *DM2a* to *DM2h* (**Fig. R20A**), all of which except *DM2f* have N-terminal TIR and a central NB domain (Chae et al., 2014). The C-termini vary in length and in LRR consensus motifs (Chae et al., 2014). Among the eight paralogs in the *DM2*^{Uk-1} cluster, *DM2d* and *DM2g* not only show the highest similarity (93.4% amino acid identity), but also share an N-terminal indel (prior to TIR) that generates a potential membrane localization signal (Chae et al., 2014). Despite being closely related in sequence (**Fig. S7**), *DM2g* does not trigger HR when co-expressed with *DM1*, either in *A. thaliana* hybrids, or in *N. benthamiana* (**Fig. R21**). The NB-ARC domains are almost identical, with scattered differences in the TIR domain, and most polymorphisms in the LRR repeats (at LRR1, 3, 4, and 8) (**Fig. S7**) as well as at the extended C-terminus following the LRRs (Chae et al., 2014). In addition, *DM2d* contains a duplicated LRR7 repeat compared to *DM2g* (Chae et al., 2014).

In the Col-0 accession, the *DM2* subcluster of the *RPP1* supercluster contains only two *RPP1* paralogs, *At3g44630* and *At3g44670*. Upstream are two paralogs,

At3g44400 and *At3g44480* that might have originated through an inverted segmental duplication event (Chae et al., 2014). Amino acid sequence similarity between DM2d^{Uk-1} and *At3g44400*, *At3g44480*, *At3g44630* and *At3g44670* are 70.8%, 72.3%, 69.7% and 65.3%, respectively, while *At3g44400* and share the N-terminal indel with DM2d and DM2g (**Fig. S8**).

Like DM2g, *At3g44400* is unable to trigger HR in combination with DM1. In order to assign functional differences to individual or short stretches of amino acids, I investigated the functional properties of DM2 paralogs and homologs.

2. Physical interaction between DM1 and the DM2d paralog (DM2g)

As described in the previous chapters, I had hypothesized that DM1 may function as the signaling executor, while DM2d as a ‘trigger’. Given the great sequence similarity of the two DM2^{Uk-1} paralogs, DM2d and DM2g, it would not be surprising if they had similar properties, but this is not the case. Therefore, I wanted to identify which features of the DM2 variants, specifically ability to physically interact with DM1 or protein sequence differences, prevent DM1 activation by DM2d and other DM2 paralogs.

I first performed Y2H assays as described before, with TIR-pNB fragment of DM1 (DM1¹⁻³⁰⁸) and various DM2g fragments (amino acid 1-234, 1-359, 1-582, 583-1190) and full-length DM2g. Similar to DM2d, DM2g fragments that containing the TIR domain (DM2g¹⁻²³⁴) and TIR plus 125 amino acids of the NB domain (DM2g¹⁻³⁵⁹) could interact with DM1¹⁻³⁰⁸ (**Fig. R20B**). In contrast, DM2g¹⁻⁵⁸² (TIR domain with whole NB domain), DM2g⁵⁸³⁻¹⁹¹⁰ (LRR domain) and the full-length DM2g did not interact with DM1¹⁻³⁰⁸ in yeast (**Fig. R20B**), as was observed for DM2d (**Fig. R5**). The interaction strengths, as inferred from yeast growth rate, were similar between DM1-DM2g and DM1-DM2d (**Fig. R20C**).

To determine the functionally relevant differences between DM2d and DM2g, I tested whether DM2g inactivity *in planta*, as deduced from *A. thaliana* genetics and transient expression in *N. benthamiana*, is due to its low protein accumulation compared to DM2d. I cloned a genomic *DM2d* coding region and placed it under the control of different promoters: a 1.5-kb fragment upstream of the *DM2g* locus (*pDM2g*), the previously used *DM2d* promoter (*pDM2d*), and the cauliflower mosaic virus 35S promoter (*p35S*).

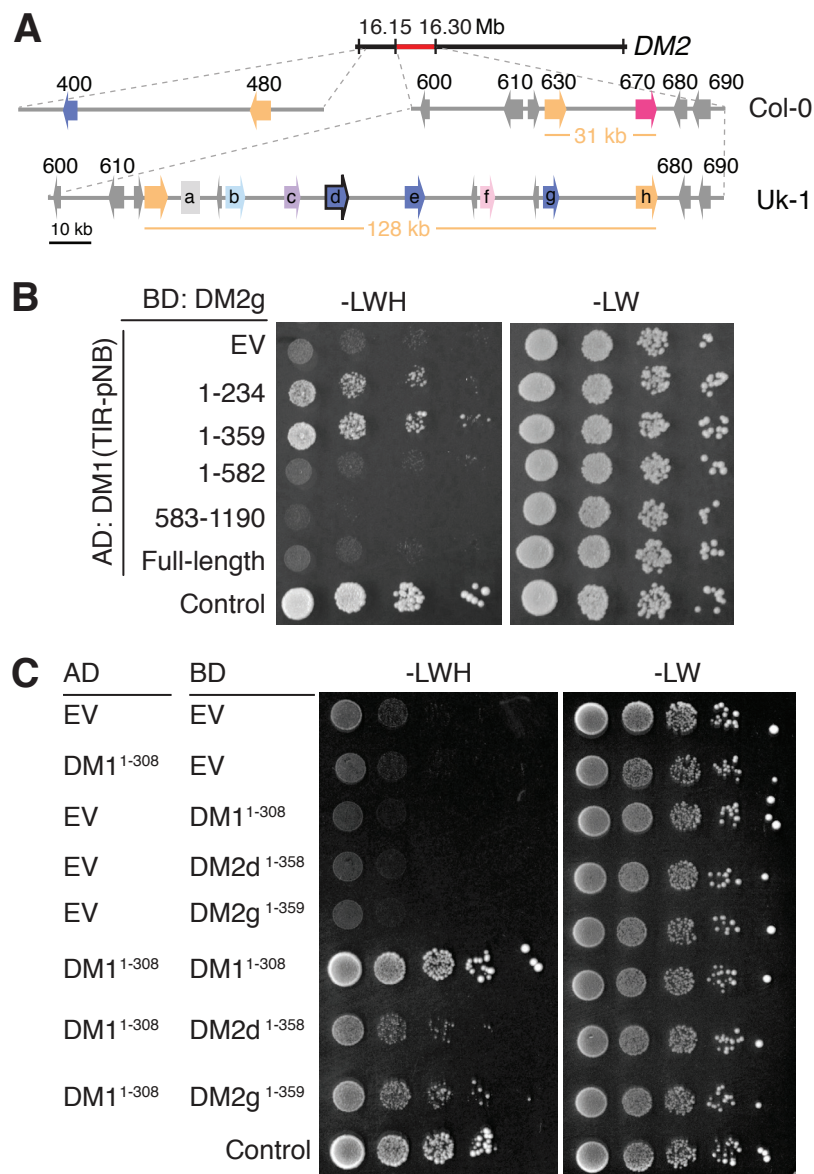


Figure R20. The DM2 gene cluster in *A. thaliana* and physical interaction of TIR containing fragments of DM1 and DM2g in yeast

(A) Schematic illustration of DM2 clusters in *A. thaliana* accession Col-0 and Uk-1 (adapted from Chae et al., 2014). The genomic interval for DM2 is indicated in red (Upper panel). Genes are shown as arrows; NLR genes are in colors and non-NLR genes are in grey. Numbers above the arrows indicate the last three digits of At3g44xxx. The DM2d incompatibility gene is outlined in black. The size in kilobase pairs (kb) of each DM2 cluster is indicated in orange text (Chae et al., 2014).

(B) Y2H analysis using TIR-pNB truncations of DM1 and different lengths of DM2g fragments showing DM1-DM2g interaction interface locates at the TIR domain. (The yeast panel was prepared by Monika Demar).

(C) Y2H analysis showing that the TIR-pNB fragments of DM2g (DM2g¹⁻³⁵⁹) and DM2d (DM2d¹⁻³⁵⁸) can associate with DM1¹⁻³⁰⁸.

DM2g constructs was tagged with 4xMyc epitope at the C-terminus (*pDM2g::gDM2g-Myc*, *pDM2d::gDM2g-Myc*, *p35S::gDM2g-Myc*). In transient infiltration assays in *N. benthamiana*, none of the three *gDM2g-Myc* versions were able to initiate cell death when co-expressed with the full-length DM1 (**Fig. R21A**), similar to what had been reported for the untagged DM2g version (Chae et al., 2014). Protein blot analysis showed that DM2g accumulated to very high levels when expressed from *p35S*, higher than DM2d under its own promoter (**Fig. R21B**). This indicates that the absence of cell death in *N. benthamiana* is not due to insufficient accumulation of DM2g.

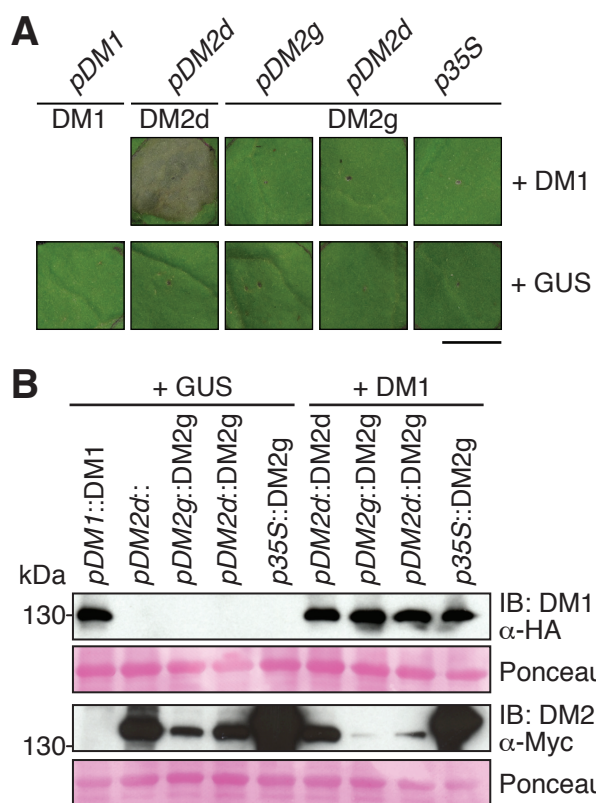


Figure R21. Inactivity of DM2g in HR-triggering in *N. benthamiana*

(A) Despite the driven promoter, DM2g did not trigger HR when transiently co-expressed with DM1 in *N. benthamiana*. The HR phenotype was scored at 4 dpi. Scale bar equals 1 cm.

(B) Western blot analysis of the promoter-chimeric DM2g constructs shown in (A). Leaf samples for protein extraction were collected at 2 dpi. Ponceau-S staining shown to indicate loading.

To summarize, my findings suggest that in DM1 can in principle associate with at least one other DM2 paralog, DM2g, but this association does not trigger HR *in planta*. This prompted me to identify which polymorphic domains determine the functional differences between the two DM2 paralogs.

3. Polymorphisms in TIR and LRR domains determine DM2 activity

The previous experiments confirmed that specific changes in the DM2d protein are responsible for triggering HR in combination with DM1 (Chae et al., 2014). To identify the causal sequence differences, I generated a series of *pDM2d*-driven chimeric constructs of *DM2d-Myc* and *DM2g-Myc* and co-expressed these in *N. benthamiana* with DM1. Since most polymorphisms between DM2d and DM2g are in the TIR domain or at the C-terminus including some of the LRR domain (upper panel, **Fig. R22A-C**), I divided the proteins into three parts: the N-terminus including the TIR domain (amino acids 1-184 in DM2d), the middle region including the NB-ARC domain (amino acids 185-581), and the C-terminus including the LRR repeats (amino acids 582-1216), and generated all six possible chimera (**Fig. 22A**). HR was only observed with wild-type DM2d and the chimera NB-ARC swap I, in which the middle region was from DM2g (**Fig. R22A**). This suggests that residues in both TIR and LRR domains are necessary for DM2d activity.

To narrow down the sequences in the LRR domain that contribute to the DM2d activity in cooperation with the TIR domain, I used the NB-ARC swap I chimeric construct (**Fig. R22A**) as backbone for three additional chimeras with extended contributions from DM2g, expanding from the end of NB-ARC domain towards the C-terminal end (LRR swap1, 2, and 3) (**Fig. R22B**). HR was still observed when the fragment from DM2g included a fragment from the NB-ARC domain to the LRR repeat 4 (LRR4), but was abolished when the DM2g sequences extended further (**Fig. R22B**). This indicates that the domains from LRR5 to LRR8 in DM2d, including the duplicated LRR7 and polymorphisms in LRR8, are critical for DM2d function. However, a chimera of the LRR7 and 8 of DM2d along with N-terminus from DM2d in a DM2g background did not trigger HR (**Fig. S9**, LRR swap 7), indicating that residues in the second half of the LRR domain and in the extended C-terminal are important for DM2d activity.

To further dissect the role of the extended C-terminal region, I introduced into the NB-ARC swap I chimera different lengths of DM2g C-terminal regions, generating LRR swap 4, 5 and 6 (**Fig. R22C**). None of these induced HR when co-expressed with DM1 (**Fig. R22C**). Different from the set of chimeras described above, they all carried the DM2g version of the protein at the very C-terminus, thereby implicating a role of this segment in DM1/DM2-triggered cell death. Protein blot analyses revealed that the chimeras accumulated to the same level as the original, active NB-ARC swap I (**Fig. R22F**). LRR swap 6 chimera was least abundant, suggesting that the very C-terminus region contributes to stabilization of DM2 protein. In summary, the

analysis of chimeric DM2 proteins revealed that more than one region of the protein determines its competence to initiate cell death signaling in combination with DM1, and the different, in particular the TIR domain and the C-terminal end of DM2 proteins cooperate.

In summary, the analysis of chimeric DM2 proteins revealed that more than one region of the protein determines its competence to initiate cell death signaling in combination with DM1. My finding is in agreement with those from other studies on NLRs, suggesting that intramolecular interactions among different NLR domains likely contribute to govern the activity of the receptor (Bernoux et al., 2016; Sloatweg et al., 2013; Steinbrenner et al., 2015; Wang et al., 2015).

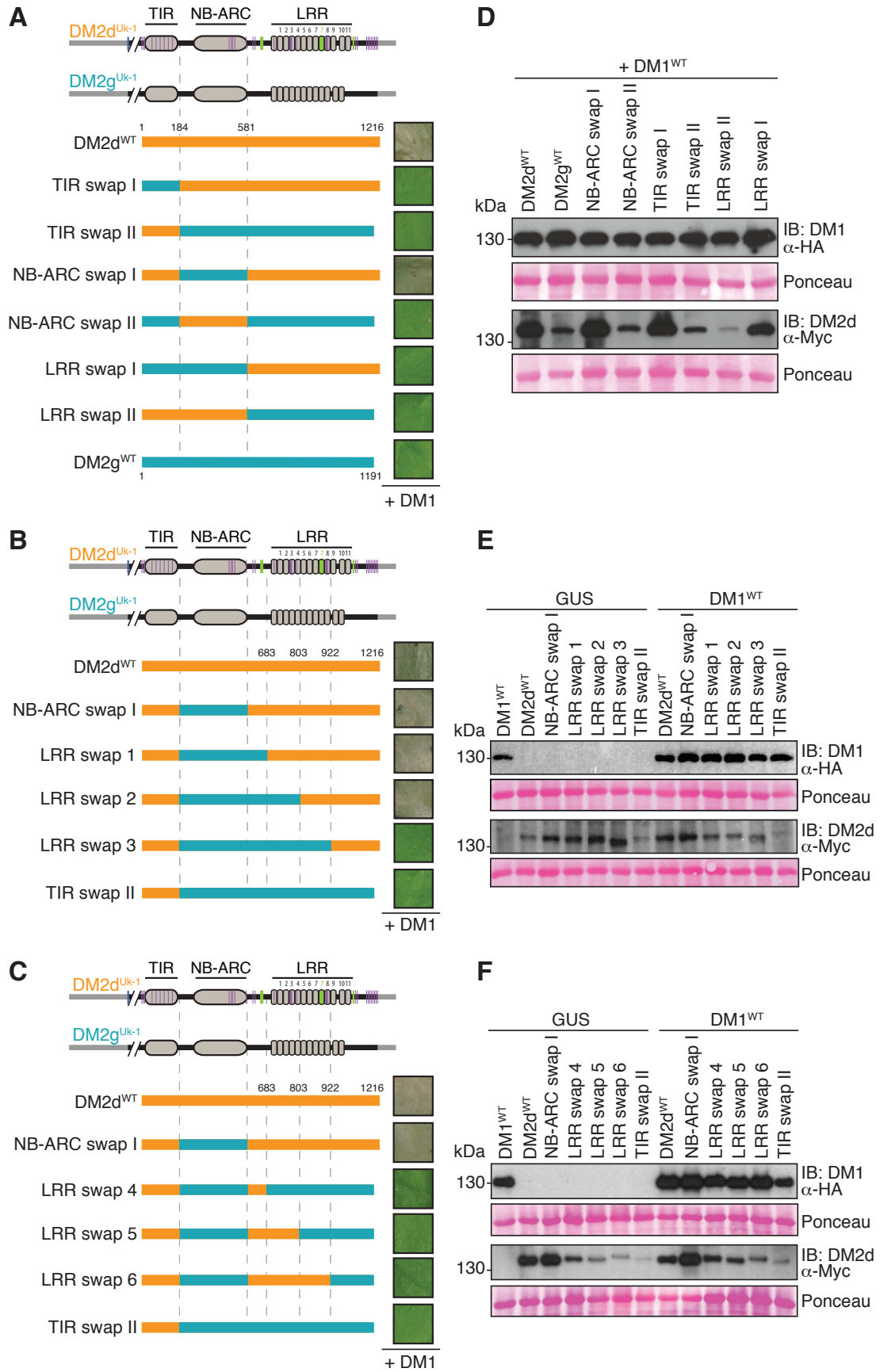


Figure R22. Residues in the TIR domain and C-terminus of DM2d determine its activity

Figure R22 (cont.)

(A-C) Schematic diagram of the domain swapping experiments between DM2d and DM2g. Domain structures of DM2d/g and polymorphisms in DM2d relative to DM2g are indicated in the top two diagrams. Purple vertical lines represent amino acid changes; and green bars, indels. In chimeric DM2d-DM2g proteins, orange indicates DM2d and turquoise DM2g sequences. The numbers indicate amino acid positions in DM2d. A representative HR phenotype of each chimeric protein when co-expressed with wild-type DM1 in *N. benthamiana* is presented in the black-lined square on right. HR was scored at 4 dpi. WT: wild-type.

(D-F) Protein blot analyses of the chimeric DM2d-DM2g proteins used in (A-C), respectively. Leaf samples for protein extraction were collected at 2 dpi. Ponceau-S staining shown to indicate loading.

4. Polymorphisms in the center of LRR domain determine DM1 activity

Similar to DM2, other paralogs, such as At5g41750 from Col-0, cannot substitute for DM1 from Uk-3 in triggering hybrid necrosis in combination with DM2d from Uk-1 (Bomblies et al., 2007).

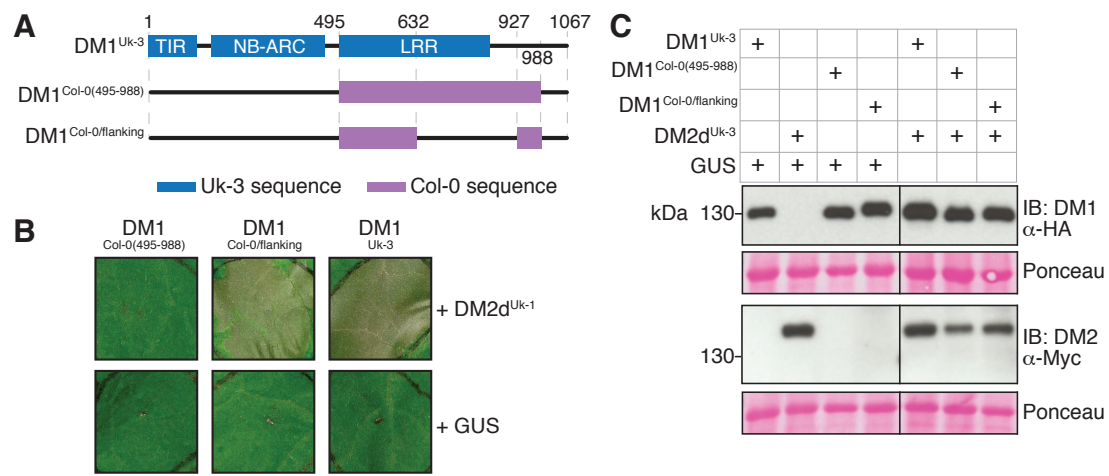


Figure R23. Residues in the central LRR domain define DM1 specificity

(A) Schematic diagram of the domain swapping experiments between DM1 and At5g41750. Domain structure of DM1 is indicated in blue. DM1 sequences in black, At5g41750 sequences in purple. Numbers indicate amino acid positions in DM1.

(B) Representative HR phenotypes (4 dpi) in *N. benthamiana* upon co-expression of DM1 variants described in (A) and DM2d^{Uk-1}. Scale bar equals 1 cm.

(C) Protein blot analysis of the experiments in (B). Leaf samples for protein extraction were collected at 2 dpi. Ponceau-S staining shown to indicate loading.

To determine residues in DM1 responsible for DM2d-triggered signaling, I first examined amino acid polymorphisms between DM1^{Uk-3} and its Col-0 homolog. Most

of them were found in the LRR domain (**Fig. S10**). To identify whether residues in the LRR domain were important for DM1 function, I made use of chimeric *DM1* constructs previously generated by Kirsten Bomblies (**Fig. R23A**), adding a C-terminal HA tag. DM1 chimera contained either an extended LRR segment from the Col-0 homolog At5g41750 in the DM1 background ($DM1^{Col-0(495-988)}$), or a Col-0 segment of similar length with the second half of the LRR domain from DM1 ($DM1^{Col-0/flanking}$) (**Fig. R23A**). Both were expressed in *N. benthamiana* under the *DM1* promoter in combination with DM2d. HR was observed with $DM1^{Col-0/flanking}$, but not with $DM1^{Col-0(495-988)}$ (**Fig. R23B**), although proteins were expressed at comparable levels, with DM2d accumulating to slightly lower levels when co-expressed with the two chimeric variants compared to wild-type DM1 (**Fig. R23C**). These findings suggest that polymorphisms in the C-terminal half of the LRR domain contribute to DM1 activity, and that DM1 may stabilize DM2d.

DISCUSSION

In this study, I have described a biochemical mechanism of the autoimmune activation triggered by the two TNL receptors, DM1 and DM2d, previously identified as causal proteins for the necrotic *A. thaliana* hybrid Uk-3 x Uk-1. I found that DM1/DM2d-mediated autoimmune signaling utilizes typical downstream components shared with other examples of TNL-triggered ETI. Using the heterologous *N. benthamiana* system, where DM1/DM2d-dependent signaling is recapitulated as HR (Chae et al., 2014), I further investigated the requirements of the signaling. Full-length proteins of DM1 and DM2d, their heteromeric association, as well as the P-loops of both proteins are required for the signaling. Using Y2H assays and co-immunoprecipitation assays *in planta*, I discovered that DM1 and DM2d engaged not only in heterotypic but also homotypic associations (DM1-DM1 and DM2d-DM2d). Both types of associations utilize the same interaction interface including the N-terminal TIR domain. I examined the functional contributions of DM1 and DM2d to signaling and found that both are required but each partner has its own role in signaling. While DM1 may act as primary signal transducer, DM2d may function as a signal trigger that is required at a lower level than DM1. In support of this hypothesis, the unequal contribution of the two TNLs to signaling was demonstrated by different effectiveness in competition assays as well as differential sensitivity to mutations that supposedly affect protein conformation. I propose that physical association of different NLRs, as shown for DM1 and other DM2 non-risk variant, may be quite common and that the sum of activation status of participating NLRs in a signaling complex is a critical parameter for signaling.

1. DM1/DM2d NLRs signal through EDS1

Downstream signaling of a number of TNL receptors is EDS1 dependent (Bhattacharjee et al., 2011; Heidrich et al., 2011; Hu et al., 2005; Parker et al., 1996; Wirthmueller et al., 2007). EDS1, in a protein complex with PAD4, not only regulates PTI to biotrophic and hemi-biotrophic pathogens (Bhattacharjee et al., 2011; Heidrich et al., 2011; Parker et al., 1996), but is also required for SA accumulation during TNL-mediated ETI (Clarke et al., 2001; Feys et al., 2001). In addition, EDS1 has been

shown to interact with both effectors and TNL receptor (Bhattacharjee et al., 2011; Heidrich et al., 2011). It is note that DM1 and DM2d are TNL proteins as well. Although DM1/DM2d-dependent cell death occurs in the absence of an effector, *EDS1* is also required for DM1/DM2d-mediated autoimmunity. This is consistent with the involvement of *EDS1* in other cases of autoimmunity triggered by mutant TNLs, such as *chs2*, *slh1*, *snc1*, and *ssi4* (Huang et al., 2010; Li et al., 2001; Noutoshi et al., 2005; Shirano et al., 2002). It will be interesting to investigate whether *EDS1* can interact with DM1 or DM2d or both and how these interactions affect DM1/DM2d-mediated signaling.

EDS1 appears to transduce TNL signals by modulating nuclear localization of TNL receptors (Bhattacharjee et al., 2011; García et al., 2010; Heidrich et al., 2011; Stuttmann et al., 2016; Wirthmueller et al., 2007). Therefore, it will in future be interesting to see whether *EDS1* also leads to nuclear translocation of DM1 and DM2d, either alone or in combination with each other. Wirthmueller and colleagues (2007) found that RPS4-mediated resistance to AvrRps4 requires RPS4 nuclear localization, whereas in the absence of the effector, RPS4 mainly associates with endomembranes. However, because total RPS4 overexpression level in different transgenic lines in *eds1* background was different from each other and neither evidence of whether the absence of *EDS1* affects RPS4 nuclear accumulation nor of the correlation between *EDS1* and RPS4 accumulations in cytoplasm and nucleus was provided (Wirthmueller et al., 2007), I suggest that the role of *EDS1* in regulating TNL nucleocytoplasmic trafficking deserves further study.

There is also evidence of increased nuclear *EDS1* accumulation upon AvrRps4 treatment (García et al., 2010). Although *EDS1* is located both in the cytoplasm and nucleus, forced exclusion of *EDS1* from the nucleus with a nuclear export signal (NES) leads to a reduction in disease resistance mediated by RPS4 and RPP4 (García et al., 2010). The opposite experiment, forcing nuclear *EDS1* accumulation with a nuclear localization signal (NLS) tag, leads to different levels of autoimmunity, with severity positively correlating with *EDS1*-NLS protein levels (Stuttmann et al., 2016). The *EDS1*-NLS transgenic lines that have no or intermediate autoimmune syndrome successfully mount RPS4- and RPP4-dependent immune responses. The authors propose that a low dose of nuclear *EDS1* is sufficient for ETI activation and that the nuclear-cytoplasmic balance of *EDS1* plays a

critical role not only in ETI (Bhattacharjee et al., 2011; Heidrich et al., 2011), but also for immune autoactivation (Stuttman et al., 2016).

Stuttman and colleagues (2016) have found that EDS1-NLS induces autoimmunity apparently through association with the RPP1-like DM2h NLR of *A. thaliana* accession Landsberg *erecta* (*Ler*) (Stuttman et al., 2016). DM2h from *Ler* is also causal in other cases of hybrid necrosis (Alcázar et al., 2010; Stuttman et al., 2016). DM2h from the Bla-1 accession is another hybrid necrosis risk allele that triggers autoimmune responses, in this case in interaction with an allele of DM3, a peptidase containing an alpha/beta hydrolase domain similar to EDS1 (Chae et al., 2014). Given that DM1/DM2d-dependent autoimmunity requires *EDS1*, as shown in my study, and RPP1-*WsA*-mediated resistance against different *Hpa* isolates also signals through *EDS1* (Botella et al., 1998), it is likely that *EDS1* may function as a common immune signaling hub for DM2/RPP1 responses. It will be interesting to test whether an increase in EDS1 nuclear accumulation selectively enriches DM2 accumulation in the nucleus over DM1 in an EDS1-NLS background, and at the same time whether DM1/DM2d-mediated autoimmunity depends on EDS1 localization. Detection of nuclear accumulation of DM2 proteins, however, might be difficult in the native condition because DM1-DM2d association often leads to rapid cell death, which might be further enhanced in an EDS1-NLS background. These challenges could be negotiated using high-temperature suppression of autoimmunity or ethanol-inducible DM1 constructs.

2. RAR1 and SGT1b regulate DM1/DM2d protein accumulation

In plants, several studies have confirmed the important role of HSP90-SGT1-RAR1 chaperone complex to positively regulate NLR accumulation (Azevedo et al., 2006; Belkhadir et al., 2004a; Bieri et al., 2004; Böter et al., 2007; Holt et al., 2005; Mestre and Baulcombe, 2006). RAR1 is required for accumulation of several NLRs such as barley MLA1, MLA6 (Bieri et al., 2004), *A. thaliana* RPM1 (Tornerio et al., 2002), RPS5 (Holt et al., 2005), and RPS2 (Belkhadir et al., 2004a); while SGT1 for Rx (Azevedo et al., 2006; Böter et al., 2007) and N protein (Mestre and Baulcombe, 2006). My study additionally provides evidence of RAR1 and SGT1b contributions to NLR-dependent autoimmunity.

Loss of *RAR1* impairs NLR dependent resistance, such as recognition of *P. syringae* DC3000 effector AvrPphB by RPS5 (Warren et al., 1999), of downy mildew

oomycete *Hpa* isolate Noco2 by RPP5 (Muskett et al., 2002), and *P. syringae* DC3000 effector AvrRpm1 by RPM1 (Tornero et al., 2002). In these other cases, decrease in resistance is highly correlated with reduction of NLR protein accumulation (Belkhadir et al., 2004a; Bieri et al., 2004; Tornero et al., 2002). However, RAR1 seems to only affect the protein abundance of NLR receptors that function as effector recognizing sensors, and it is dispensable for the accumulation of helper CNL ADR1-L2 (Roberts et al., 2013). I have proposed that DM1 and DM2d play different roles in their signaling complex, with DM1 as primary signal transducer and DM2d as a signal trigger. I therefore asked whether the functional relationship between the two DM receptor resembles the helper/sensor duality. A preliminary experiment in my study indicates that both DM1 and DM2d protein levels were greatly reduced in the *rar1-21* background (**Fig. D1**). This result suggests that similar to other sensor NLRs, RAR1 also positively regulates DM1 and DM2d protein accumulation, even though in this case an effector is not required for their activity.

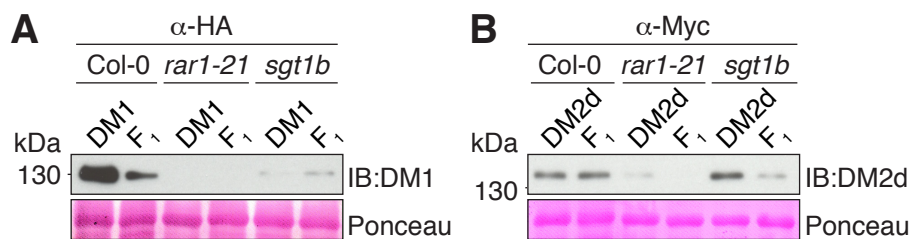


Figure D1. Protein blot for DM1-HA (A) and DM2d-Myc (B) in Col-0 wild-type, *rar1-21* and *sgt1b* backgrounds. Ponceau-S staining shown to indicate loading.

As an interacting partner of RAR1 (Zhang et al., 2010), SGT1 is also essential for plant immunity as shown for various NLR receptors including MLA, N, Rx, RPS4, and I2 (Shirasu, 2009). Similar to RAR1, SGT1 positively controls effector-induced accumulation of several NLRs, such as Rx and N, and disease resistance mediated by these NLRs (Azevedo et al., 2006; Mestre and Baulcombe, 2006). However, SGT1 and RAR1 can function antagonistically to fine-tune NLR protein accumulation. For example, in RPS5 mediated resistance against *P. syringae* DC3000, RPS5 protein level is elevated in the *sgt1b* mutant, but reduced in the *rar1* mutant, demonstrating that RAR1 is a positive regulator while SGT1b is a negative regulator of RPS5 accumulation (Holt et al., 2005). In the indicated preliminary experiment, I also found that RAR1 and SGT1b differently regulate DM1 and DM2d protein levels

in parental lines and in F_1 [*gDM1-HAxgDM2d-Myc*] hybrids (**Fig. D1**). Specifically, DM1 in *rar1-21* was not detectable in either the DM1-carrying parent or F_1 progeny (**Fig. D1A**). However, DM2d protein accumulation turned out to be less dependent on chaperone function. In the parental lines, DM2d level rather accumulated more in *sgt1b* than in Col-0 background, while it reduced, but still detectable in *rar1-21* (**Fig. D1B**). Nonetheless, the suppression of the hybrid phenotype in both mutant backgrounds is paralleled by considerable reduction in protein levels of both DM1 and DM2d.

These results may provide first insights into the different roles of DM1 and DM2d in signaling that I deduced from my experiments. Future experiments to investigate this further could include surveying the protein levels of DM1 and DM2d in different temperature regimes (which affect immune signaling), and in the presence of proteasome-inhibitors.

3. Signaling interdependency of DM1 and DM2d and physical associations

Physical association between NLR receptor molecules upon effector perception, either with the same or different NLR partner, is observed in both plants and animals (Césari et al., 2014a; Liu and Xiao, 2015; Yuan and Akey, 2013). Here, I showed that an NLR physical association could occur in the absence of effector. DM1 and DM2d formed different types of associations: homotypic associations of DM1 with DM1 and of DM2d with DM2d, and heterotypic association of DM1 and DM2d, adding one more example of the collection from the plant side. Different types of NLR interactions have been also found in other plant NLR hetero-complexes such as the CNL pair RGA4/RGA5 (Césari et al., 2014b) and the TNL pair RPS4/RRS1 (Williams et al., 2014), independently of the presence of their cognate effectors. In all three RGA4/RGA5, RPS4/RRS1, and DM1/DM2d pairs, the NLR interactions utilize the N-terminal domain of each member for both homotypic and heterotypic associations (Césari et al., 2014b; Williams et al., 2014; and my study). My experiments showed that the TIR-TIR interface involving SH motif identified by RPS4/RRS1 crystallography (Williams et al., 2014) also contributes to DM1/DM2d association. However, in RPS4/RRS1 pair, the TIR-mediated heterotypic association allows RRS1 to suppress the activation of the signaling executor RPS4 in the absence of an effector (Williams et al., 2014). The suppressive association is apparently reversed in the presence of the effector, releasing RPS4 for homotypic

association, which in turn results in immune responses. In contrast, the heterotypic association between DM1 and DM2d leads to functional cooperation of the two NLRs to trigger autoimmune response when there is no effector. In my study, I showed that neither homotypic interaction of DM1 and DM1 nor of DM2d and DM2d alone could cause cell death. However, evidence from the DM1 competition assays pointed out that the functional integrity of DM1-DM1 association was necessary for effective signaling, possibly pointing to DM1-DM1 homotypic interactions contributing to DM1-DM2d signaling.

The TIR domain has been shown to mediate self-associations of several TNL receptors, such as tobacco N (Mestre and Baulcombe, 2006) and flax L6 (Bernoux et al., 2011). I compared the TIR sequence of DM1 and DM2d with the characterized TIR of L6 (Bernoux et al., 2011) and found that the overall TIR structure of DM1 and DM2d was predicted to resemble that of L6.

This leads to the question whether self-association of the N-terminal domain is a prerequisite for NLR-triggered cell death. The answer is “it depends”. Several examples have demonstrated that the TIR or CC self-association is important for transducing signals upon NLR activation. For examples, TIR self-associations of L6 and RPS4 and CC self-associations of NRG1 and MLA10 initiate spontaneous cell death without an effector trigger, and disruption of the TIR-TIR or CC-CC associations correlates with reduced HR (Bai et al., 2012; Bernoux et al., 2011; Collier et al., 2011; Maekawa et al., 2011; Williams et al., 2014). However, there are also examples where TIR or CC self-association does not confer autoactivation, such as RRS1 TIR (Williams et al., 2014) and RGA5 CC (Césari et al., 2014b). Particularly, the CC domain of potato Rx neither forms homodimers (Hao et al., 2013) nor can it cause autoactivation (Rairdan et al., 2008). Possible explanations for some N-terminal domains not being autoactive are due to lack of self-association (Rx CC) or having differentiated function in the signaling when cooperating with another NLR partner (RRS1 TIR, RGA5 CC). My study showed that the TIR domains of DM1 and DM2d did not cause cell death when expressed alone or together, even though TIR-TIR associations between DM1/DM1 and between DM1/DM2d were observed. Therefore, the lack of TIR-mediated autoactivation in DM1 and DM2d is not due to the lack of TIR physical association, but there are additional requirements for signaling. Autoimmune activation was observed only when DM1 and DM2d are both

present as full-length proteins, indicating functional cooperation of all domains in the proteins.

Although DM1/DM2d and RPS4/RRS1 utilize a similar TIR-TIR interface for physical association, DM1/DM2d signaling is distinct from RPS4/RRS1 signaling in several ways. First, RPS4/RRS1 requires effector recognition to initiate signaling (Le Roux et al., 2015; Sarris et al., 2015; Williams et al., 2014), while DM1/DM2d does not. As discussed, in the absence of effector, RRS1 through TIR/TIR interaction with RPS4 suppresses RPS4 activity and therefore conferring inactivation of the complex (Williams et al., 2014), while in DM1/DM2d the TIR/TIR interactions facilitate the cooperation of both proteins to reach activation status. Second, the requirement of P-loops from both DM1 and DM2d is essential for DM1/DM2d-dependent signaling. However, in RPS4/RRS1, the P-loop of RPS4 is indispensable (Williams et al., 2014). Third, the aspartic acid-to-valine substitution in the MHD motif of DM1 and DM2d did not lead to individual autoactivation, confirming the interdependency of the two TNLs for signaling. Therefore, I believe that not all NLR pairs act in the same manner. The nature of N-terminal-mediated physical associations between NLR receptors might imply different functions; in some cases associations underlie signaling initiation, while in others they serve as a signaling inhibition. This raises the possibility that in many NLRs, not only one domain but also other domains participate in signaling through changes in intramolecular conformation. This may also be the reason why not all N-terminal NLR fragments are autoactive. Other cases of hybrid necrosis in *A. thaliana* are likely also caused by NLR-NLR interactions (Chae et al., 2014). Once the causal genes of these cases are characterized, it will be interesting to see whether only the N-terminal domains or the full-length proteins are required for immune signaling.

4. Functional significance of NLR conformation

NLR activation/inactivation has been postulated to involve conformation changes dependent on ATP/ADP exchange (Lukasik and Takken, 2009; Sukarta et al., 2016; Takken et al., 2006). The importance of NLR conformation has been supported by structural simulation studies using mammalian NOD receptors, whose domain structures have been extensively characterized (Hu et al., 2013; Lukasik and Takken, 2009; Riedl et al., 2005; Sukarta et al., 2016; Takken et al., 2006). Analyses of mouse NLRC4 lacking the N-terminal CARD domain has shown that the receptor

in the inactive state binds to ADP and has a closed conformation formed by interactions between NB and HD2 and between NB and LRR domains (Hu et al., 2013). In plant NLRs, data from physical association between domains of potato Rx and *Arabidopsis* RPS5 in the absence of effectors (Ade et al., 2007; Moffett et al., 2002) indicate that the inter-domain interactions may constrain receptor conformation and inhibit its activation by preventing ADP/ATP exchange. Despite the lack of structural information of NB and LRR domains in plant NLRs, increasing functional knowledge about NLR domains has begun to elucidate mechanisms of plant NLR regulation. Domain swaps between closely related NLRs have been used to investigate intramolecular autoinhibition and activation mechanisms (Bernoux et al., 2016; Luck et al., 2000; Rairdan and Moffett, 2006; Ravensdale et al., 2012; Slootweg et al., 2013; Steinbrenner et al., 2015; Wang et al., 2015). Depending on the NLRs, different domain regions have been shown to contribute to receptor activity. In potato Rx, *Arabidopsis* RPP1 and maize Rp1D variants, the LRR domain plays a role in allele-specific recognition and the ARC2 subdomain contribute to regulate the receptor activation and the matching between the two domains is important to initiate receptor activation (Slootweg et al., 2013; Steinbrenner et al., 2015; Wang et al., 2015). My study showed that TIR and LRR domains together contribute to differentiate the autoimmune triggering function between two closely related DM2 variants, DM2d and DM2g. These data could be interpreted to imply that association between two different domains might regulate NLR activation through their conformation. This suggests that the strength of intramolecular interaction might determine the closed or relaxed conformation of inactive or active NLR variants (Slootweg et al., 2013; Steinbrenner et al., 2015; Wang et al., 2015; and this study). In addition, I noted that without DM1, DM2d couldn't trigger cell death autoactivation, even the MHV variant. Therefore, DM2d domain conformation, though relatively relaxed, might not be at a fully open status, which might be only reached when associated with DM1. This suggests NLRs might have different degrees of conformational relaxedness, which determines their activation potential.

The conventional view is that NLRs are activated by effector recognition (Lukasik and Takken, 2009; Sukarta et al., 2016; Takken et al., 2006). NLR activation can, however, also be induced by point mutations, or by interaction with NLR or other plant proteins, in the absence of an effector (See **Table 2**). NLR conformational change is proposed to be coupled to ATP/ADP exchange to regulate NLR activity (Lukasik and Takken, 2009; Sukarta et al., 2016; Takken et al., 2006). It is clear from

examples of animal NOD receptors and plant NLR receptors that NOD or NLR active status correlates with ATP binding, while inactive status with ADP binding (Riedl et al., 2005; Tameling et al., 2002; Tameling et al., 2006; Williams et al., 2011). Given that NLRs in the inactive state have a tightly closed conformation and bind to ADP, one emerging question is whether the default for all NLR molecules is the ADP-bound status. If so, how can ATP have access to turn on NLR activity? An answer to the second question is that effector binding to the LRR domain of an NLR triggers a conformational change and leads to exchanging ADP with ATP (Lukasik and Takken, 2009; Takken et al., 2006). However, to date it is unknown how effector recognition at the LRR surface can induce overall NLR domain re-arrangement, given that the tightly folded NLR structure in the inactive state might interfere with the effector finding its LRR interaction interface.

In the case of DM1/DM2 autoimmune response, I showed that signaling outputs by DM1 and DM2d were differently affected by amino acid substitutions in MHD motifs of each NLR. Changes in DM2d caused more dramatic loss of signaling than those in DM1 did. In addition, DM2d T542 mutations were predicted to alter spacious arrangement of the histidine residue in the MHD motif and lysine residue in the P-loop motifs, while changes in DM1 H491 did not result in such conformation modification. This leads me to hypothesize that the ARC2 subdomain, where the MHD motif is located, might involve in differentiating DM1 and DM2d function via their conformation coupled with nucleotide-binding status. The more sensitizing of DM2d ARC2 subdomain might endow the receptor a peculiar conformation, which might enable DM2d to have a higher affinity with ATP than ADP. DM1, on the other hand, carries a more stable ARC2 subdomain, bringing it to a less flexible or closed conformation, which might cause the protein to preferentially bind to ADP. Presumably different nucleotide-binding preference and protein conformation between DM1 and DM2d in the absence of effector therefore could not be explained by the conventional hypothesis of NLR activation. Recent evidence from difference in activity of flax L6 and L7 due to the polymorphisms in the TIR and NB domain has shown that combination of these polymorphisms in L7 causes the protein to have a higher ADP-bound status, which in turn leading L7 to have a less efficient effector recognition and therefore a milder defense response, than L6. L6-type amino acid substitutions into L7 that make L7 become active in effector binding and defense response also lower its ADP-bound status to L6-similar level (Bernoux et al., 2016). This data suggests that, unlike previously proposed, effector tends to have a higher

binding affinity to ATP-bound NLRs than ADP-bound molecules, stabilizing this ATP-bound state and hence activating NLRs. It leads to the model of ATP/ADP “equilibrium-based switch”, stating that both ATP- and ADP-bound states exist in NLR population, and the shift of the equilibrium to either ATP- or ADP- bound states is correlated with NLR activation or inactivation (Bernoux et al., 2016). This model, in my opinion, provides a more reasonable explanation for both effector dependent and independent activation of NLRs. It seems better to imagine that effector may access more easily to an ATP-bound, relaxed conformation than an ADP-bound, closed conformation. This model can also illustrate for the dynamic yet subtle regulation of NLR activity that at the same time guarantee an effective defense response when needed and avoid an inappropriate activation.

In the case of DM1 and DM2d, their presumably different sensitivity at the MHD motifs suggested that DM2d might have a more relaxed conformation than DM1. This leads to a scenario that each NLR might have a different threshold in their ATP/ADP equilibrium status, in which DM2d might be more likely ATP-bound. That DM1 on its own is not active supports the view that DM1 is more likely to be ADP-bound. Interaction of DM1 with DM2d might lead to a stronger shift toward ATP-binding and signaling. This speculation is consistent with my finding of the unequal contribution of DM1 and DM2d to signaling, in which DM2d at a low dosage is sufficient for signaling while DM1 is not. However, to confirm the ATP/ADP equilibrium shift of DM1 or DM2d, one needs to measure the nucleotide occupancy level of DM1 and DM2d using their wild-type forms and MHD variants.

In addition, P-loop mutations in both DM1 and DM2d did not abrogate DM1-DM1 and DM1-DM2d associations, unlike in human APAF-1 (Hu et al., 1998) and tobacco N protein (Mestre and Baulcombe, 2006), further supporting the major role of ATP- versus ADP-bound status of DM1 and DM2d signaling.

DM2d belongs to the RPP1 cluster, whose members confer resistance to different strains of the oomycete *Hpa* (Botella et al., 1998; Krasileva et al., 2010; Krasileva et al., 2011). By swapping of the ARC2 domains between RPP1 proteins with different recognition specificities, Steinbrenner and colleagues (2013) have shown that the ARC2 domain is likely responsible for expanding recognition specificity by facilitating receptor activation. The authors hypothesized that different *RPP1* alleles might adopt different conformations based on intramolecular interaction strength between the ARC2 and LRR domains, which are responsible for effector

recognition. The difference in recognition specificity of RPP1 alleles might be determined by a stepwise relaxing in each receptor conformation (Steinbrenner et al., 2015). I speculate that RPP1 proteins with low activity might preferentially hold ADP and their close conformation might prevent ADP-to-ATP exchanges, while those with high activity might be prone to engage ATP. Their flexible conformation may allow nucleotide exchange more easily once the effector is present. Although cognate effectors for DM2d are unknown, I hypothesize that DM2d might have gained a peculiar conformation during evolution, determined by intramolecular interaction and ATP/ADP bound status, of which the nucleotide equilibrium is shifted closer to active status than is the case for other homologs. It would be interesting to test the ATP/ADP occupancy of the DM2d/DM2g chimeras I have generated and examine the correlation between nucleotide binding status and signaling.

5. Preformed DM1 complex and higher-order DM1/DM2d oligomerization

In animals, the formation of higher-order NOD complexes during NOD receptor activation have been demonstrated in several cases, such as *Drosophila* DARK, *C. elegans* CED-4, human APAF-1 apoptosome, and mouse NAIP2/NLRC4 inflammasome (Hu et al., 2015; Qi et al., 2010; Riedl et al., 2005; Yu et al., 2006; Zhang et al., 2015). Apoptosome and inflammasome share a common feature in the wheel-like structure made up by multiple individual NOD receptors, with the N-terminal domain gathering in the center of the wheel and the C-terminal domain pointing outward. In the inactive state, these animal NOD receptors exist as monomer and only assemble into higher-order oligomer complexes upon an external trigger (Hu et al., 2015; Qi et al., 2010; Riedl et al., 2005; Yu et al., 2006; Zhang et al., 2015). In plants, although the oligomerization state has been suggested to occur with activated NLRs (Césari et al., 2014a), there is a lack of extensive experimental evidence. CoIP and Y2H assays have suggested physical association between an NLR either with the same NLR or with a different NLR, both in the presence or absence of effectors (Ade et al., 2007; Bernoux et al., 2011; Césari et al., 2014b; Gutierrez et al., 2010; Maekawa et al., 2011; Mestre and Baulcombe, 2006; Williams et al., 2014). Similarly, my study showed that DM1 and DM2d could associate both in Y2H experiments (as partial TIR-containing fragments) and in *in planta* coIP assays (as full-length proteins). The crystal structures of N-terminal domains (TIR or CC) of several receptors, such as L6, MLA10, RPS4 and RRS1, suggest TIR or CC domains

can form homodimers (L6-L6, MLA10-MLA10, RPS4-RPS4 and RRS1-RRS1) or heterodimers (RPS4-RRS1), but not higher oligomers, at least not *in vitro* (Bernoux et al., 2011; Maekawa et al., 2011; Williams et al., 2014). However, different types of physical associations have been demonstrated with full-length proteins of RGA4 and RGA5 (Césari et al., 2014b) and of RPS4 and RRS1 (Williams et al., 2014), suggesting that these receptors might associate in a higher-order oligomeric complex.

I observed that the DM1/DM1 and DM1/DM2d associations differ in interaction strength in Y2H and coIP assays in *N. benthamiana*. While DM1/DM1 interaction is quite strong, DM1/DM2d interaction is much weaker. This result led me to propose two alternative scenarios for the oligomeric states of DM1 and DM2d. The first possibility is that DM1/DM1 and DM1/DM2d exist as dimers and DM1/DM1 complexes might have to be dissociated so that monomeric DM1 can interact with monomeric DM2d. In the second scenario, signaling does not involve a simple one-to-one competition for the same interaction interface, but both types of associations might be accommodated in the same hetero-complex, with unequal stoichiometry, to activate signaling. Given that DM1 and DM2d utilize the same interface for both homotypic and heterotypic interactions and DM1/DM2d interaction is weaker than DM1/DM1 interaction, it is difficult to explain why DM2d can one-to-one compete with DM1 for the same interaction interface, as proposed in the first hypothesis. Using competition assays, I showed that the functional integrity of both DM1 and DM2d was important to induce cell death. This is supported by the evidence that association of wild-type and P-loop mutant DM1 reduces cell death signaling. The additional requirement of DM2d for signaling is obvious, as no cell death is triggered by DM1 without DM2d. More importantly, as also shown in my competition assays, a small amount of DM2d is sufficient to initiate cell death, implying uneven stoichiometry of DM1 and DM2d in the DM1/DM2d signaling complex.

In collaboration with Eui-Hwan Chung (Dangl lab, Department of Biology, University of North Carolina, Chapel Hill, USA), I am currently investigating the composition of DM1 complexes and DM1/DM2d in *A. thaliana* using Blue-Native PAGE. Chung (personal communication) found that DM1-HA alone was able to form homomeric complexes with a range of molecular weights, all larger than the monomeric state (ca. 130 kDa). The range of DM1 complex molecular weights varies from dimeric (ca. 250 kDa) to larger (ca. 500 kDa) states, suggesting that DM1

potentially forms at least homodimeric complexes, independent from DM2d (**Fig. D2**). In other words, DM1 might exist as a preformed NLR complex in *A. thaliana*. Co-localization of DM1-HA and DM2d-Myc extracted from F₁ *A. thaliana* plants carrying *gDM1-HA* and *gDM2d-Myc* confirmed the hetero-association of DM1-DM2d. Importantly, different from the DM1/DM1 complex, the migration range of DM1/DM2d hetero-complex cumulated more sharply at the higher molecular weight area (ca. 500 kDa) (**Fig. D2**). These observations suggest that the presence of DM2d might cause a shift in size of DM1 oligomeric complex *in planta*, implying that the preformed DM1 complex might accommodate DM2d when the latter becomes available, generating a hetero-oligomeric complex that is competent for signaling.

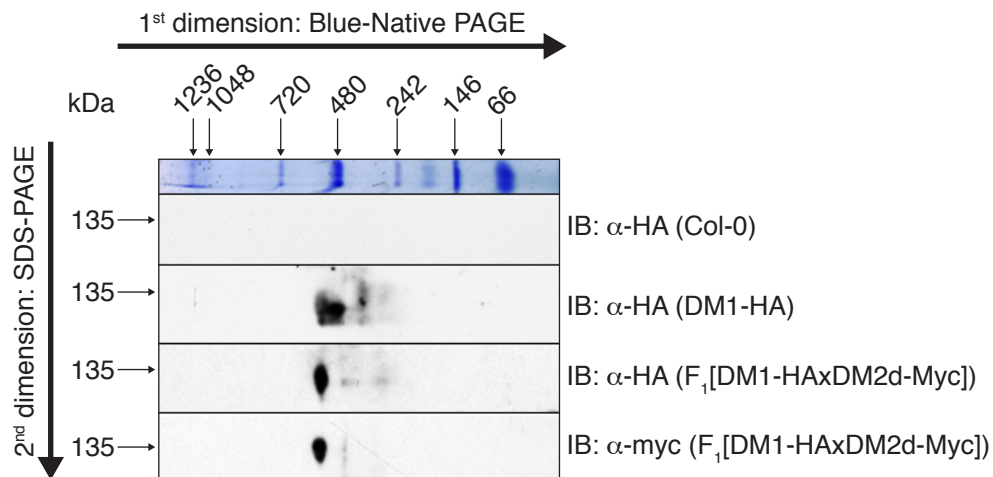


Figure D2. Blue-Native PAGE showing higher-order oligomerization of DM1 complex and DM1/DM2d complex. Proteins were extracted from *A. thaliana* leaves of non-transgenic plants (uppermost panel), transgenic plants expressing DM1-HA (the second panel), and F₁[*gDM1-HAxgDM2d-Myc*] hybrids (the last two panels) using Blue-Native PAGE extraction buffer containing 30 mM HEPES pH 7.5, 150 mM potassium acetate, 10% glycerol and 0.5% DDM. The picture was provided by Eui-Hwan Chung (Dangl lab, University of North Carolina, Chapel Hill, NC, USA).

These data, consistent with the observation of unequal functional contribution of DM1 and DM2d to signaling, support that only a small number of DM2d molecules needs to be integrated into preformed DM1 complexes to trigger signaling. To rule out the possibility that the higher-order DM1/DM2d complexes observed in blue-native PAGE might also involve other non-NLR proteins, it is necessary to perform more intensive biochemical assays such as gel filtration of purified proteins of DM1

and DM2d to identify more precisely the size of the NLR complex, or mass spectrometry of isolated complexes. Nevertheless, it is tempting to speculate that DM1/DM2d complex exists in a higher-order oligomeric state.

As aforementioned, animal NOD-derived apoptosomes and inflammasomes often adopt a wheel-like structure upon activation (Hu et al., 2015; Qi et al., 2010; Riedl et al., 2005; Yu et al., 2006; Zhang et al., 2015). Uneven stoichiometry of DM1 and DM2d in the signaling complex might resemble that of the active NAIP2/NLRC4 inflammasome. The formation of NAIP2/NLRC4 complex upon effector recognition by NAIP2 is reminiscent of a domino effect, in which activated NAIP2 primes the recruitment of subsequent NLRC4 molecules in a consecutive manner to complete the complex (Hu et al., 2015; Zhang et al., 2015). In the DM1/DM2d complex, however, DM2d-independent existence of the DM1 complex in a wide range of sizes suggests a different assembly mechanism of the DM1/DM2d hetero-complex. These DM1 complexes presumably serve as a pre-formed scaffold that can associate with DM2d when the latter becomes available to complete and switch on the signaling complex. To complete the signaling complex, two scenarios can be envisioned: more DM1 molecules could be successively recruited to the complex upon binding to DM2d, or DM2d association simply fills a gap in the preformed DM1 complex. I favor the second possibility, since DM1 was shown to be predominant in a dimer or higher oligomer state (**Fig. D2**). In addition, filling the gap in DM1 incomplete complex by DM2d association might explain the rapid induction of cell death when DM1 and DM2d are co-expressed in *N. benthamiana* and the early necrosis onset in the *A. thaliana* hybrids. Under either scenario, the heteromeric interaction between DM1 and DM2d greatly facilitates full activation of the complex.

The independence of preformed DM1 complexes from DM2d presence leads me to hypothesize that the DM1 complex is able to interact with not only DM2d but also other NLRs and that the immune activation of the hetero-complex depends on the 'trigger' potential of the partner NLR. Supporting this hypothesis, I showed DM1 could also associate with the highly similar but inactive paralog of DM2d (DM2g). However, it remains to be investigated whether DM1 also interacts with other DM2/RPP1 variants such as RPP1-WsA, RPP1-WsB, RPP1-NdA or RPP1-ZdrA, which have known effectors, or are at least known to recognize molecules from specific *Hpa* strains.

6. Functional diversification of DM2 variants

The DM2/RPP1 locus is highly polymorphic in *A. thaliana* populations, which presumably undergo different evolutionary processes (Alcázar et al., 2010; Botella et al., 1998; Chae et al., 2014). *RPP1* is among the minority of plant NLRs that directly binds to pathogen effectors (Krasileva et al., 2010; Krasileva et al., 2011). Distinct *RPP1* alleles show race-specific recognition of *Hpa* isolates and the specificity appears to be largely determined by polymorphisms in the LRR domain (Botella et al., 1998; Krasileva et al., 2010; Steinbrenner et al., 2015). The *DM2* locus recurrently spawns incompatibility alleles in several natural *A. thaliana* accessions, leading to different cases of hybrid necrosis (Alcázar et al., 2010; Bomblies et al., 2007; Chae et al., 2014). Fast evolution of *DM2/RPP1* alleles due to an arms-race selection imposed by pathogen effectors might make it a necrosis risk locus, in which the sequence variation, especially at the C-terminal LRR domain, could also determine their potential autoimmune activity.

I showed in this study that different DM2 paralogs from the Uk-1 accession share the same physical association property. DM2d and DM2g both interact with DM1 with similar strength and using a similar interface. However, only the DM1/DM2d pair triggers cell death, while DM1/DM2g does not. The cooperation between the C-terminal LRR domain and the N-terminal TIR domain determines the discrepancy in activity between the two DM2 paralogs. I found that DM2d and DM2g are polymorphic in the TIR domain, LRR repeats as well as the extended C-terminal region, perhaps reflecting co-evolution of recognition and signaling functions within the same NLR. In addition, since both DM2d and DM2g utilize similar TIR-containing interfaces to associate with DM1, it is likely that polymorphisms in the LRR domain and the C-terminal region modulate different intramolecular conformations in relation with the TIR domain, thereby differentiating activities among DM2 paralogs. Likewise, extensive analyses using effector-binding NLRs, such as L6 and RPP1, have suggested that the sensor domain coevolves with other domains within the molecule to generate multiple variants in populations, each of which would occupy a distinct position in an incremental step toward full NLR activity (Ravensdale et al., 2012; Steinbrenner et al., 2015).

Members within the *DM2/RPP1* cluster have been hypothesized to evolve from tandem duplication, gene conversion events, and a disproportionate amount of mutational changes (Chae et al., 2014). Diversifying selection particularly acting on

the LRR region might give rise to sequence polymorphisms and variation in activity of DM2 paralogs (Chae et al., 2014). In agreement, I showed that polymorphisms at the C-terminal ends of the LRR domain (in combination with TIR domain) are involved in fine-tuning functional activities of DM2d and DM2g. Particularly, the C-terminal part of DM2 variants seems to involve in regulating the protein accumulation. Chimeric DM2 proteins with the C-terminal part from DM2g tended to accumulate less than those carry DM2d C-terminal part. This suggests that polymorphisms in the LRR region, which affect signaling function, work together with polymorphisms affecting protein accumulation level to subtly differentiate the activation threshold of DM2 variants. The multi-layer functional regulation of DM2 variants therefore might normally avoid inappropriate immune activation. One question remains is why, despite the potential danger of autoimmunity, these risk alleles are still maintained during evolution. A possibility could be that the polymorphisms although incurring a cost of autoimmune risk might become particularly quickly beneficial when plants encounter new pathogens, since risk alleles carrying these polymorphisms might adopt a peculiar “near-active” conformation. The presence of inactive but closely related DM2 variants suggests that these variants could serve as a reservoir for defense against future pathogens.

PERSPECTIVES

I have provided insights into the biochemical basis of autoimmunity caused by a pair of *A. thaliana* NLR proteins, showing that new mechanistic aspects of immune signaling in plants can be revealed by the study of hybrid necrosis. While physical interaction between different NLR receptors had been shown before for effector-triggered defense responses, such interactions underlying autoimmune responses in the absence of pathogens had not yet been reported. Similar to the receptors co-acting in pairs that have differentiated functional roles, I also observed an asymmetrical contribution of two NLRs in the case I investigated. In addition, the activity differences between closely related NLRs point to a cooperative function and possible co-evolution of different NLR domains to fine-tune NLR activity by modulating protein conformation. In combination with information on effector recognition specificity, breeders can apply such knowledge to generate an NLR reservoir of “risk variants” with a graded spectrum of potential activities and effector sensitivities by modifying the intramolecular interactions in the protein structure, arming plants for future infections. Given that intramolecular cooperation of different domains defines NLR activation status, it will be informative to study directly the 3D structure of domain arrangement of each NLR in inactive and active states.

The application of structural techniques including crystallization and today cryo-electron microscopy provides us with powerful tools to resolve protein structures at high resolution. Major problems in solving full-length or at least the NB-ARC and LRR domains of plant NLRs are insolubility, instability and lack of proper post-translation modifications when expressing the proteins *in vitro* (Bostjan Kobe, personal communication). The DM1/DM2d hetero-complex, in which each partner as full-length protein accumulates stably when co-expressed in *N. benthamiana*, and whose accumulation can be effectively induced *in planta* using an ethanol-inducible system, could provide a new opportunity with which to overcome the above technical problems for structural studies.

In this study, the activation mechanism of DM1/DM2d signaling was explained in terms of a newly proposed “equilibrium-based switch” model. This hypothesis is based on the functional requirement of the P-loop of both proteins and the sensitivity of protein activity to MHD mutations. An experiment that could confirm my hypothesis

is to measure directly the nucleotide occupancy of DM1 and DM2d as individual proteins and when in the complex. Insight into ATP/ADP binding status and their balance in NLR pools could then be exploited to modulate the receptor inactivation/activation shift, which could improve the ability of NLRs to rapidly respond to pathogens and at the same time lower fitness cost.

Knowledge of the 3D structure of DM1/DM2d complex, and other NLR in general, will advance our understanding of NLR activation and regulation, while detailed biochemical evidence of NLR-mediated autoimmunity helps to answer how inappropriate activation of the immune system arises in plants and how NLR activity is regulated in the absence of pathogens. They also helps us to understand how different potential activities of closely related NLR variants are influenced by their conformation. Such knowledge in turn might be harnessed to engineer NLR variants with new properties.

MATERIALS AND METHODS

General equipment and reagents

I used the following standard laboratory equipment: pipettes (Gilson, Inc., Middleton, WI, USA), shakers (HTC Infors Multitron, Einsbach, Germany), nanodrop spectrophotometer (Thermo Scientific, Wilmington, DE, USA), PerfectBlue Gel System Mini (PeqLab, Bruchsal, Germany), MJ Research DNA Engine PTC-200 thermo cycler (Bio-Rad, Foster City, CA, USA), Mini-PROTEAN[®] system (Bio-Rad, Foster City, CA, USA), Mini Trans-Blot[®] Electrophoretic Transfer Cell system (Bio-Rad, Foster City, CA, USA), X-ray cassettes (Kodak, Rochester, NY, USA), X-ray developer machine AGFA CP 1000 LC 50 (AGFA, Mortsel, Belgium), CFX384 Real-Time PCR system (Bio-Rad, Foster City, CA, USA), Orion Star[™] Conductivity Meter for conductivity measurement (Thermo Scientific, Beverly, MA, USA), Biophotometer (Eppendorf, Hamburg, Germany), digital camera (Canon, Tokyo, Japan).

Standard chemicals and solvents were purchased from Sigma-Aldrich (Steinheim, Germany), Carl Roth (Karlsruhe, Germany), Invitrogen (Carlsbad, CA, USA), Merck (Darmstadt, Germany), Bio-Rad (Foster City, CA, USA), Roche (Mannheim, Germany), Clontech (Mountain View, CA, USA), if not otherwise mentioned. Compositions for yeast media were from MP Biomedicals, LLC (Strasbourg, France).

Standard enzymes were purchased from Thermo Scientific or NEB Biolabs. I used *Taq* polymerase (NEB) for genotyping and Phusion *Taq* polymerase (Thermo Scientific, Vilnius, Lithuania) for specific gene amplification and cloning.

Oligonucleotides were purchased from Eurofins Genomics (Ebersberg, Germany). Prestained protein ladder (Cat #26616) was purchased from Thermo Scientific (Vilnius, Lithuania)

Information of bacterial and yeast strains, antibodies and beads, and oligonucleotides can be found in **SUPPLEMENTARY MATERIAL** section.

Growth media (for bacteria, yeast, and plants)

Bacterial media

LB media for growing bacteria were prepared according to (Sambrook et al., 1989).

For bacterial selection, antibiotics were used with the following concentrations:

For all bacteria	Spectinomycin	100 µg/mL
	Kanamycin	25 µg/mL
For <i>E. coli</i>	Ampicillin	50 µg/mL
For Agrobacteria	Chloramphenicol	25 µg/mL
	Tetracycline	5 µg/mL

Yeast media

YPD medium (pH 6.5): 20 g/L Bacto peptone, 10 g/L Yeast extract, 20 g/L agar (for solid medium only), and 2% Glucose.

LW- or LWH-lacking selective media (pH 5.6 – 5.8): 7.6 g/L Yeast nitrogen base (YNB) without amino acids, 0.72 g/L amino acid supplement lacking LW or LWH, 20 g/L agar (for solid medium only), and 2% Glucose.

Plant media

Murashige and Skoog (MS) medium (pH 5.8): 2.15 g/L 1xMS salts, 0.5 g/L MES, 8 g/L agar (for solid medium only), 0.1% MS vitamin solution.

To select transgenic plants, add 25 g/L Kanamycin or 0.1% glufosinate ammonium (BASTA, Sigma-Aldrich, Steinheim, Germany).

Oligonucleotides

All the oligonucleotides used in this study are listed in the **Table S3** and **S4**.

Overlapping PCR to generate chimeric constructs

Chimeric constructs of *DM2d* and *DM2g* were generated using overlapping PCR. Individual fragments were amplified separately such that short overlaps (from 20 – 50 base pairs (bp)) were generated at conserved positions between *DM2d* and *DM2g*. 250 ng of the individual (purified) PCR products were mixed in a fusion reaction, whereby the initial five cycles were performed without flanking

oligonucleotides and ramping of the annealing temperature from 60 to 55°C (-1°C per cycle). After adding flanking oligonucleotides, PCR reaction was performed for another 25 cycles at the annealing temperature of 60°C. The final PCR products were size-selected and purified from agarose gels using GeneJET Gel Extraction Kit (Thermo Scientific, Vilnius, Lithuania). It is noted that in all PCR steps, Phusion *Taq* DNA polymerase (Thermo Scientific, Vilnius, Lithuania) was used.

DNA plasmid cloning

DNA fragments were cloned by conventional cloning using restriction endonucleases or via Gateway LR Clonase II system (Invitrogen). See **Table 4** for detail information.

Table 4. *Cloning systems*

Plasmid	Selection marker*	Cloning system	Purpose	Provider
pGEM-T Easy	Amp	TA cloning	Subclone a gene amplified by PCR	Promega
pBlueScript SK(-)	Amp	Restriction enzymes	Subclone a gene amplified by PCR	Stratagene
pJL-Blue	Kan	Restriction enzymes	Entry vector for Gateway LR Clonase II system	Yant et al., 2010
pFK vectors	Bacteria: Spec Plant: Kan or BASTA	Gateway LR Clonase II system	Binary vector (derived from pGREEN vector) for plant transformation	Hellens et al., 2005 with in-house modifications
pGWB	Bacteria: Spec Plant: Kan	Gateway LR Clonase II system	Binary vector for plant transformation	Nakagawa et al., 2007
pZZ006	Bacteria: Spec Plant: BASTA	Gateway LR Clonase II system	Ethanol-inducible expression vector	Zhao et al., 2010
pSOUP	Tet	-	Helper plasmid for <i>Agrobacteria</i> transformation	BRAC T John Innes Centre
pGADT7 (GAL4-AD)	Amp	Restriction enzymes	Transcription activating fusion protein for Y2H assay	Clontech
pGBKT7 (GAL4-BD)	Kan	Restriction enzymes	Bait protein for Y2H assay	Clontech

* *Amp: Ampicillin, Kan: Kanamycin, Spec: Spectinomycin, Tet: Tetracyclin*

DNA isolation and purification

Purification of DNA fragments from agarose gel was performed using the GeneJET Gel Extraction Kit (Thermo Scientific). Isolation and purification of DNA plasmids was performed using GeneJET Plasmid Miniprep Kit (Thermo Scientific). Molecular cloning was conducted according to the standard protocol (Sambrook et al., 1989) using *E. coli* DH5 α . The cloning systems are described in Table 4.

Plant materials and growth conditions

In this study, I used the *A. thaliana* Col-0, Ws-0, Uk-1 and Uk-3 accessions. The Col-0 reference accession was used as background for most transgenic lines, otherwise mentioned. A list of mutants is shown in Table 5. *Arabidopsis thaliana* seeds were frozen at -80°C overnight, surface-sterilized with 70% EtOH and 0.5% (v/v) Triton X-100, and stratified for 3 days in 0.1% agar in the dark. Plants were sown and grown in growth rooms with controlled temperature (16°C or 23°C) in long-day condition (fluorescent lights with intensity of 125 to 175 $\mu\text{mol m}^{-2} \text{s}^{-1}$, photoperiod of 16hour light/ 8hour dark) and humidity of 65%. Plant transformation was performed using the floral dip method (Clough and Bent, 1998). Transgenic lines were selected on 0.1g/L of glufosinate (BASTA SL, Bayer Crop Science, Leverkusen, Germany) treated soil. For phenotyping, F₁ hybrids and their corresponding parents were grown at 16°C, all other plants were grown at 23°C.

Table 5. *A. thaliana* mutants used in the study

Mutant	Background	Type of mutation	Mean of validation	Reference
<i>eds1-1</i>	Ws-0	Loss-of-function mutation of <i>EDS1</i> (E466K)	Sequencing of alleles	Parker et al., 1996
<i>rar1-21</i>	Col-0	Missense mutation of <i>RAR1</i> (Q52*)	Sequencing of alleles	Tornero et al., 2002
<i>sgt1b</i>	Col-0	Deletion of SGT1b in Col-0 (<i>edm</i> mutant)	qRT	Tör et al., 2002
<i>rbohD</i> (SALK_074825)	Col-0	T-DNA insertion in third intron of <i>RBOHD</i> (At5g47910) (position on chromosome 5 19398763)	T-DNA insertion verification	Alonso et al., 2003

(*) indicating premature stop codon

Nicotiana benthamiana seeds were frozen at -80°C overnight, surface-sterilized with 70% EtOH and 0.5% (v/v) Triton X-100, and stratified for 3 days in

0.1% agar in the dark. *N. benthamiana* plants were grown at 23°C in long-day conditions. Plants of 4-5 week-old were used for *Agrobacterium tumefaciens*-mediated transient expression assays (see below).

RNA extraction

RNA extraction from *A. thaliana* leaf tissue was carried out as previously described (Box et al., 2011). Fine powder of 100 mg leaf tissue was homogenized in 300 µL of pre-warmed to 60°C isolation buffer (0.1M Tris pH 8.0, 5 mM EDTA pH 8.0, 0.1M NaCl, 0.5% SDS, and freshly added 1% β-mercaptoethanol). The mixture was vigorously mixed with 300 µL of 5:1 acidic phenol:chloroform pH 4.5. After centrifuging at 20000 *g* for 15 min at room temperature (RT), 300 µL of the upper aqueous phase was transferred to a new tube containing 240 µL of isopropanol and 30 µL of 3 M sodium acetate (NaOAc) pH 5.2. The nucleic acids were precipitated at -80°C for 30 min and collected by centrifuging at 20000 *g* for 30 min at RT. The RNA pellet then was washed twice with 600 µL of 70% ethanol and air-dried for 20 min at RT. After dissolving the pellet in 50 – 100 µL of nuclease-free water, RNA samples were incubated at 65°C for 5 min to dissolve completely. The RNA samples were used directly for cDNA synthesis or stored at -80°C until further use.

cDNA synthesis

1 µg of total RNA was used for cDNA synthesis. The cDNA synthesis was carried out using RevertAid RT Kit (Thermo Scientific, Vilnius, Lithuania) according to the manufacturer's instructions with minimal modifications. Genomic DNA was removed from RNA sample (in the volume of 8 µL) by treating with 1 µL of 1U of DNase I (Thermo Scientific, Vilnius, Lithuania) at 37°C for 30 min. The DNase I was deactivated by adding 1 µL of 50 mM EDTA at 65°C for 10 min. The first strand of cDNA was synthesized by adding 1 µL of 100 µM Oligo(dT)₁₈ following by incubation at 65°C for 5 min. The reverse strand of cDNA was synthesized by adding 1 µL of 20 U/µL RiboLock RNase Inhibitor, 2 µL of 10 mM dNTP mix and 1 µL of 200 U/µL RevertAid reverse transcriptase (RT). The reaction was incubated in a thermal cycler at 16°C for 30 min, followed by 60 cycles of (30°C for 30 sec, 42°C for 30 sec and 50°C for 1 min). Enzymes were heat-inactivated by incubating at 85°C for 5 min.

Reverse transcription followed by quantitative real-time PCR (qRT-PCR)

I used qRT-PCR to quantify the transcript levels of several ETI marker genes (*PR1*, *NPR1*, *WRKY46*). β -Tubulin 2 (*TUB2*, *At5g05620*) was used as an internal control for all samples. Specific oligonucleotides for amplifying *PR1*, *NPR1*, *WRKY46* and *TUB2* in qPCR reactions are listed in Table S3. The qPCR reaction consisting of 2 μ L of 1:5 diluted cDNA template (see above), 0.25 μ L of 100 pM each oligonucleotide, and 5 μ L of Maxima SYBR Green 2X Master Mix (Thermo Fisher Scientific, Vilnius, Lithuania) in a total volume of 10 μ L was performed in a Bio-Rad CFX384 Real-Time PCR system. The qPCR reactions were performed at 95°C for 15 sec, 60°C for 30 sec and 72°C for 30 sec for 40 cycles. The emission of the fluorescence was read at the end of each cycle. A single melting curve of each reaction was observed, indicating that only single PCR product was produced for each gene.

All experiments were carried out with 3 biological replicates (3 independent lines of F₁ hybrids and parents) and 3 technical replicates for each biological replicate. Each data point shown in the figures represents the mean of $\Delta\Delta$ CT values of 3 technique replicates. The $\Delta\Delta$ CT values is calculated as followed:

$$\Delta\text{CT}_{\text{hybrid}} = \text{CT}_{\text{target}}^{(*)} - \text{CT}_{\text{reference}}^{(**)}$$

$$\Delta\text{CT}_{gDM1-HA \text{ parent}} = \text{CT}_{\text{target}} - \text{CT}_{\text{reference}}$$

$$\Delta\Delta\text{CT} = \Delta\text{CT}_{\text{hybrid}} - \Delta\text{CT}_{gDM1-HA \text{ parent}}$$

(*) $\text{CT}_{\text{target}}$ indicates the CT value of qPCR for *PR1*, *NPR1* or *WRKY46*

(**) $\text{CT}_{\text{reference}}$ indicates the CT value of qPCR for *TUB2*

Agrobacterium-mediated transient expression assays in *N. benthamiana*

Agrobacterium tumefaciens strains carrying *DM1*, *DM2*, or *GUS* or *GFP* for control were grown overnight at 28°C in an orbital shaker at 200 rpm/min in 50 mL of LB medium containing appropriate antibiotics to OD₆₀₀ of approximate 1.2 to 1.8. *Agrobacterium* cells were harvested by centrifugation at 3000 *g* and resuspended in induction medium containing 10 mM MES pH 5.6, 10 mM MgCl₂ and 150 μ M acetosyringone. The cells were incubated at 28°C for 2 to 3 h in the orbital shaker at 200 rpm/min prior to adjusting bacterial density. The bacterial density was then normalized to an OD₆₀₀ of 0.35 with the induction medium. For co-infiltrations, the

normalized bacterial cultures carrying each construct were mixed in a 1:1 (v/v) ratio before infiltration. P19 culture at a ratio of 1:10 of total volume was added to each bacterial mixture to enhance the transient expression system. The bacterial mixtures were manually infiltrated using a 1-mL needleless syringe into the abaxial side of 4- to 5-week-old *N. benthamiana* leaves, which were slightly punctured with a pipette tip before infiltration. The infiltrated leaves were kept in dark by covering with aluminum foil at 23°C in the growth room for two days. Leaf sample for protein extraction were collect at 2 days post-infiltration (dpi). The cell-death phenotypes were visually observed and recorded at 3 to 4 dpi.

For competition assays, elevating amounts of competitor cultures were co-infiltrated with a constant amount of cultures containing the wild-type partners (DM1 and DM2d). Before mixing, the bacterial densities (OD_{600}) of the constant partners were adjusted to 0.525 and those of the competitors were adjusted to 0.525, 1.05 and 2.1. To prepare the infiltration mixture, the cultures were mixed at a ratio of 1:1:1 (v/v/v) right before infiltration. It is noted that P19 was not used in the competition assays.

Conductivity assays

Kinetics of HR signaling was quantified with a conductivity assay (Dellagi et al., 1998) that records the level of cell death by measuring ion leakage from cells in leaf samples. *DM1* variants were cloned into an ethanol-inducible (AlcA) system (Zhao et al., 2010), in which protein expression could be induced by irrigating plants with 1% (v/v) aequos ethanol. In *Agrobacterium*-mediated infiltration assay, bacterial cultures carrying the ethanol-inducible *DM1* (*indDM1*) constructs (OD_{600} of 0.13) were mixed with non-inducible DM2d constructs (OD_{600} of 0.33) in a ratio of 1:1 (v/v). Induction was carried out at 18 h post-infiltration (hpi) by irrigating plants with 1% ethanol and keeping them under a transparent dome for 18 h. To measure conductivity or ion leakage from infiltrated leaves, 5 leaf discs of each sample with a diameter of 0.8 mm were cut out with a leaf puncher and floated in 15 mL water for 30 min. The leaf discs then were transferred into 6 mL water. The conductivity (μ Siemens/cm or μ S/cm) of the 6 ml-water samples was measured using a Thermo Scientific Orion StarTM Conductivity Meter at indicated time points. Each assay was carried out with 8 replicates per samples, and was independently repeated twice.

Yeast-two hybrid assays and yeast crude protein extraction

To analyze protein-protein interaction in yeast, I used the Matchmaker GAL4 Two-Hybrid Systems (Clontech, Mountain View, CA, USA). *S. cerevisiae* strain AH109 was co-transformed with GAL4-activation domain (AD)-containing vectors (pGADT7) carrying truncated *DM1* fragments and DNA-binding domain (BD)-containing vectors (pGBKT7) carrying truncated *DM2d* fragments according to the manufacturer's instruction. Three independent yeast colonies after co-transformation were selected on SD agar medium lacking Leucine (L), Tryptophan (W) and Histidine (H) for testing interaction.

Yeast cells were resuspended in YNB medium and serial dilutions (OD_{600} of 5×10^{-1} , 5×10^{-2} , 5×10^{-3} , 5×10^{-4} , and 5×10^{-5}) were spotted on the LWH-lacking selective media (Clontech, Mountain View, CA, USA) to visualize the strength of interactions after 4-5 days of incubation at 30°C.

For crude protein extraction, a yeast colony was picked and grown in 3 mL of YPD medium at 30°C overnight. Yeast cells were lysed by subjecting the yeast pellet to 3 successive freeze-thaw cycles by dipping tubes containing yeast cells into liquid N_2 , then thawing them at room temperature for 2 min. Yeast protein extract was resuspended in 50 μ L of 3X Urea Laemmli buffer (240 mM Tris-HCl pH 6.8, 6% SDS, 30% Glycerol, 16% β -mercaptoethanol, 0.006% Bromophenol blue, 10 M Urea) and denatured by boiling at 100°C for 15 min. The extracted protein was separated on a 10% SDS-PAGE (in a volume of 8 mL gel: 2 mL of 40% Acrylamide, 2 mL of 1.5 M Tris pH 8.8, 80 μ L of 10% SDS, 80 μ L of 10% APS, 8 μ L of TEMED) and immunoblotted on a PVDF membrane (Bio-Rad, Foster City, CA, USA). AD- or BD-binding proteins were detected by anti-HA or anti-c-Myc antibody at the indicated dilution (**Table S2**).

Plant protein extraction and co-immunoprecipitation assays

Protein expression of DM1 and DM2 in *N. benthamiana* samples from transient assays as well as in *A. thaliana* transgenic plants was assayed using the microsomal fractionation method reported previously (Boyes et al., 1998) with minor modifications. 100 mg of leaf tissue was ground into fine powder in liquid nitrogen, and homogenized in 210 μ L of lysis buffer (0.33 M sucrose, 20 mM Tris-HCl pH 7.5, 1 mM EDTA, 10 mM DTT and 1 x cComplete ULTRA Tablets Mini, EDTA-free protease inhibitor cocktail (Roche, Mannheim)). The lysate was cleared by

centrifugation at 5000 *g* for 10 min at 4°C. Microsomal pellet fractions were collected by centrifugation at 20000 *g* for 1 h at 4°C. Proteins were resuspended in 4 x Laemmli sample buffer (240 mM Tris-HCl pH 6.8, 8% SDS, 40% Glycerol, 5% B-mercaptoethanol, 0.04% Bromophenol blue), boiled for 10 min at 95°C, separated on a 7% SDS-PAGE (in a volume of 8 mL gel: 1.4 mL of 40% Acrylamide, 2 mL of 1.5 M Tris pH 8.8, 80 µL of 10% SDS, 80 µL of 10% APS, 8 µL of TEMED) and immunoblotted on PVDF membrane (Bio-Rad, Foster City, CA, USA). The membranes were incubated with anti-HA or anti-c-Myc antibodies at the indicated dilution (**Table S2**)

Co-immunoprecipitation assays were performed using total protein extract as described by Mackey et al., (2002) with some modifications. 500 mg of leaf tissue was ground into fine powder in liquid nitrogen, and homogenized in 1 mL of extraction buffer (50 mM HEPES-KOH pH 7.5, 50 mM NaCl, 10 mM EDTA pH 8.0, 10 mM MgCl₂, 0.5% Tween-20, 5 mM DTT, 1x cOmplete ULTRA Tablets Mini, EDTA-free protease inhibitor cocktail (Roche, Mannheim, Germany)). The lysates were cleared by centrifugation at 10000 *g* for 10 min at 4°C. 25 µL of Pierce™ anti-c-Myc magnetic beads (Thermo Scientific) after equilibrating in the extraction buffer were mixed with the supernatants. After incubation for 4 h at 4°C, the magnetic beads were collected using a magnetic stand and washed 3 times with washing buffer (similar to extraction buffer but containing only 0.2% Tween-20). Immunoprecipitated proteins were collected by adding 50 µL of pre-heated (to 95°C) elution buffer (50 mM Tris-HCl pH 6.8, 50 mM DTT, 1% SDS, 1 mM EDTA pH 8.0, 0.005% bromophenol blue, 10% glycerol). The immunoprecipitated proteins from anti-c-Myc were loaded on a 7% SDS-PAGE and subjected for western blot analysis with anti-c-Myc and anti-HA antibodies at the indicated dilution (**Table S2**).

Other tools

Conductivity was plotted using GraphPad Prism v6.0c.

Structural modeling used the PHYRE2 server (<http://www.sbg.bio.ic.ac.uk/phyre2/>).

Amino acid alignment was performed using the Uniprot server (<http://www.uniprot.org/align/>).

SUPPLEMENTARY MATERIAL

Table S1. Bacterial and yeast strains

Bacterial or yeast strain	Purpose
<i>Escherichia coli</i> strain DH5 α (bacteria) (Life Technology Inc, Darmstadt, Germany)	Amplification of plasmid DNA
<i>Agrobacterium tumefaciens</i> strain ASE (bacteria)	Shuttle for (transient and stable) plant transformation
<i>Saccharomyces cerevisiae</i> AH109 (yeast) (Clontech, Mountain View, CA, USA)	Yeast-two hybrid (Y2H) assays

Table S2. Antibodies and beads

Antibody/Beads	Cat No.	Company	Dilution
Anti-HA-Peroxidase	12013819001	Roche (Mannheim, Germany)	1:5000 ^(*)
Anti-c-Myc-Peroxidase	A5598	Sigma-Aldrich (Saint Louis, Missouri, USA)	1:15000 ^(*)
Pierce Anti-HA magnetic beads	88836	Thermo Scientific (Rockford, IL, USA)	50 μ L beads/1 g leaf tissue ^(**)
Pierce Anti-c-Myc magnetic beads	88842	Thermo Scientific (Rockford, IL, USA)	50 μ L beads/1 g leaf tissue ^(**)

(*) for Western blot

(**) for immunoprecipitation (IP)

Table S3. Oligonucleotides for amplification of *TUB2*, *PR1*, *NPR1* and *WRKY46*

Oligo name	Target gene	Orientation	Sequence (5'-3')	qPCR size
N-0078	<i>TUB2</i>	Forward	GAGCCTTACAACGCTACTCTGTCTGTC	167 bp
N-0079	<i>TUB2</i>	Reverse	ACACCAGACATAGTAGCAGAAATCAAG	
G-13182	<i>PR1</i>	Forward	CGTTCACATAATTCCCACGA	275 bp
G-13183	<i>PR1</i>	Reverse	AAGAGGCAACTGCAGACTCA	
G-13184	<i>NPR1</i>	Forward	CGTTTCTCAGCAGTGTCTGTC	213 bp
G-13185	<i>NPR1</i>	Reverse	CCGTCTCACTGGTACGAAGA	
G-38254	<i>WRKY46</i>	Forward	CGTGCATCTGTAATATGCTCTAGG	81 bp
G-38255	<i>WRKY46</i>	Reverse	GATGATGGTCACTGCTGGAG	

Table S4. Oligonucleotides for DM2d/DM2g chimeric amplification and site-directed mutagenesis

Oligo name	Purpose	Orientation	Sequence (5'-3')
G-23330	DM2d-Myc	Forward	CACCAAGCGAGCATGAGATA
G-31100	DM2d-Myc	Reverse	CTAAGCGCTACCGTTCAAGTCT
G-38231	NB-ARC swap II	Forward	ATGAGATTGCTTGGGAAGTTACCTGCTTA GCTGGTAAACTCCCTTTGGGAT
G-38232	NB-ARC swap II	Reverse	ATCCCAAAGGGAGTTTACCAGCTAAGCAG GTAACTTCCCAAGCAATCTCAT
G-38233	NB-ARC swap II	Forward	TGAAGTGCTCAATGATGATACAATAGTAA GTTTTTCA
G-38234	NB-ARC swap II	Reverse	TGAAAAAACTTACTATTGTATCATCATTGA GCACTTCA
G-38410	NB-ARC swap I	Forward	CACGAAGGTTTTCGATGAGATTGCAAGGGA AGTTATGGCCCTTGCTGGTGAAGTCCCTT TGGGATTGAAGTTCTAGGC
G-38411	NB-ARC swap I	Reverse	GCCTAGAACCTTCAATCCCAAAGGGAGTT CACCAGCAAGGGCCATAACTTCCCTTGCA ATCTCATCGAAACCTTCGTG
G-38412	NB-ARC swap I	Forward	GAAAGGGATATATGTGAAGTACTCGATGA CGATACAACAGTAAGTTTTTTCATTGCATC TC
G-38413	NB-ARC swap I	Reverse	GAGATGCAATGAAAAAACTTACTGTTGTA TCGTCATCGAGTACTTCACATATATCCCTT TC
G-38521	TIR and LRR swap	Forward	CTAATGGATTCTTCTTTTTTCTTGTCTTA GT
G-38522	TIR and LRR swap	Reverse	ACTAAGACAAGGAAAAAAGAAGAATCCAT TAG
G-38523	TIR and LRR swap	Forward	ATGGTTTTGTTGGGATGACACCTCATATG G
G-38524	TIR and LRR swap	Reverse	CCATATGAGGTGTCATCCCAACAAAACCA T
G-39654	LRR swap 1-6	Forward	CTTGATAATTGAGTTTATTTGATAAC
G-39655	LRR swap 1-6	Reverse	GTTATCAAATAAACTCAATTATCAAG
G-39656	LRR swap 1, 4	Forward	CTAAAGTAAGTAGTTTTGATGAAAAC
G-39657	LRR swap 1, 4	Reverse	AGTTTTCATCAAACTACTTACTTTAG
G-39658	LRR swap 2, 5	Forward	GTCTCTAAGAAATTGTTACGTGTTGT
G-39659	LRR swap 2, 5	Reverse	ACAACACGTGAACAATTTCTTAGAGAC
G-39660	LRR swap 3, 6	Forward	GCTAGAGACTCTTCCAATCAACATC
G-39661	LRR swap 3, 6	Reverse	GATGTTGATTGGAAGAGTCTCTAGC
G-39662	LRR swap 4, 5, 6	Reverse	GAATTGGGTAGCGGCCGCCCTCGAGC

Table S5. Binary T-DNA constructs

Construct	Backbone	Promoter	Coding region
pDT010	pZZ006*	<i>palcA</i>	<i>DM1-2xHA</i>
pDT077	pGREENIIS (BAR)**	<i>pDM2d</i>	<i>TIR(DM2d)-NB(DM2g)-LRR(DM2d)-4xMyc</i>
pDT081	pGREENIIS (BAR)	<i>pDM2d</i>	<i>TIR(DM2g)-NB(DM2d)-LRR(DM2d)-4xMyc</i>
pDT092	pGREENIIS (BAR)	<i>p35S</i>	<i>DM2g-4xMyc</i>
pDT100	pGREENIIS (BAR)	<i>pDM2d</i>	<i>DM2g-4xMyc</i>
pDT101	pGREENIIS (BAR)	<i>pDM2d</i>	<i>TIR(DM2g)-NB(DM2d)-LRR(DM2g)-4xMyc</i>
pDT103	pGREENIIS (BAR)	<i>pDM2d</i>	<i>TIR(DM2d)-NB(DM2g)-LRR(DM2g)-4xMyc</i>
pDT105	pGREENIIS (BAR)	<i>pDM2d</i>	<i>DM2d¹⁻⁵⁸¹-4xMyc</i>
pDT134	pGREENIIS (BAR)	<i>pDM1</i>	<i>DM1^{H491V}-2xHA</i>
pDT135	pGREENIIS (BAR)	<i>pDM1</i>	<i>DM1^{G223A K224A H491V}-2xHA</i>
pDT137	pGREENIIS (BAR)	<i>pDM1</i>	<i>DM1^{G31R}-2xHA</i>
pDT138	pGREENIIS (BAR)	<i>pDM1</i>	<i>DM1^{G31T}-2xHA</i>
pDT139	pGREENIIS (BAR)	<i>pDM1</i>	<i>DM1^{G31D}-2xHA</i>
pDT140	pGREENIIS (BAR)	<i>pDM1</i>	<i>DM1^{G31E}-2xHA</i>
pDT143	pGREENIIS (BAR)	<i>pDM2d</i>	<i>DM2d^{T66A}-2xHA</i>
pDT144	pGREENIIS (BAR)	<i>pDM2d</i>	<i>DM2d^{T66G}-2xHA</i>
pDT157	pGREENIIS (BAR)	<i>pDM1</i>	<i>DM1¹⁻²¹⁸-2xHA</i>
pDT158	pGREENIIS (BAR)	<i>pDM2d</i>	<i>DM2d¹⁻²⁵⁴-4xMyc</i>
pDT164	pZZ006	<i>palcA</i>	<i>DM1^{G223A K224A}-2xHA</i>
pDT165	pZZ006	<i>palcA</i>	<i>DM1^{H491V}-2xHA</i>
pDT166	pZZ006	<i>palcA</i>	<i>DM1^{G223A K224A H491V}-2xHA</i>
pDT182	pGREENIIS (BAR)	<i>pDM1</i>	<i>DM1^{Col-0(495-988)}-2xHA</i>
pDT186	pGREENIIS (BAR)	<i>pDM1</i>	<i>DM1^{H491T}-2xHA</i>
pDT187	pGREENIIS (BAR)	<i>pDM2d</i>	<i>DM2d^{T541H}-4xMyc</i>
pDT192	pGREENIIS (BAR)	<i>pDM1</i>	<i>DM1¹⁻⁵²⁸-2xHA</i>
pDT193	pGREENIIS (BAR)	<i>pDM2d</i>	<i>DM2d/g (LRR swap 1)-4xMyc</i>
pDT194	pGREENIIS (BAR)	<i>pDM2d</i>	<i>DM2d/g (LRR swap 2)-4xMyc</i>
pDT195	pGREENIIS (BAR)	<i>pDM2d</i>	<i>DM2d/g (LRR swap 3)-4xMyc</i>
pDT196	pGREENIIS (BAR)	<i>pDM2d</i>	<i>DM2d/g (LRR swap 4)-4xMyc</i>
pDT197	pGREENIIS (BAR)	<i>pDM2d</i>	<i>DM2d/g (LRR swap 5)-4xMyc</i>
pDT198	pGREENIIS (BAR)	<i>pDM2d</i>	<i>DM2d/g (LRR swap 6)-4xMyc</i>
pDT204	pGREENIIS (BAR)	<i>pDM2d</i>	<i>DM2d/g (LRR swap 7)-4xMyc</i>
pDT207	pGREENIIS (BAR)	<i>pDM2d</i>	<i>TIR(DM2d)-NB(DM2d)-LRR(DM2g)-4xMyc</i>
pDT208	pGREENIIS (BAR)	<i>pDM2d</i>	<i>TIR(DM2g)-NB(DM2g)-LRR(DM2d)-4xMyc</i>

Table S5 (continue)

pEC300	pGWB420	p35S	DM2d ¹⁻³⁵⁸ -10xMyc
pEC301	pGREENIIS (BAR)	pDM1	DM1 ^{H491D} -2xHA
pMD324	pGREENIIS (BAR)	pDM2d	DM2d-2xHA
pMD325	pGREENIIS (BAR)	pDM2d	DM2d-4xMyc
pMD341	pGWB414 ^{***}	p35S	DM1 ⁵²⁹⁻¹⁰⁶⁷ -3xHA
pMD344	pGWB420	p35S	DM1 ⁶⁸⁷⁻¹²¹⁶ -10xMyc
pMD347	pGWB420	p35S	DM2g-10xMyc
pMD365	pGREENIIS (BAR)	pDM1	DM1 ^{G223A K224A} -2xHA
pMD366	pGREENIIS (BAR)	pDM2d	DM2d ^{G259A K260A} -4xMyc
pMD444	pGREENIIS (BAR)	pDM1	DM1 ¹⁻³⁰⁸ -2xHA
pMD445	pGREENIIS (BAR)	pDM2g	DM2g-4xMyc
pMD447	pGWB416	pDM1	DM1-4xMyc
pMD469	pGREENIIS (BAR)	pDM2d	DM2d ^{T541V} -4xMyc
pMD470	pGREENIIS (BAR)	pDM2d	DM2d ^{T541D} -4xMyc
pMD471	pGREENIIS (BAR)	pDM2d	DM2d ^{G259A K260A T541V} -4xMyc
pMD477	pGREENIIS (BAR)	pDM1	DM1 ^{S34A H35A} -2xHA
pMD478	pGREENIIS (BAR)	pDM2d	DM2d ^{S69A H70A} -4xMyc

* pZZ006 vector was generated by incorporating ethanol-inducible AlcR transcription factor-alcA promoter system in *Aspergillus nidulans* (Caddick et al., 1998) into pMLBart binary backbone (Zhao et al., 2010).

** pGREENIIS vector (Hellens et al., 2005) carries a gene conferring Basta resistance in plants.

***pGWB vectors are from (Nakagawa et al., 2007).

SUPPLEMENTARY FIGURES

Figure S1. Phenotypic representation of progeny from $F_1[gDM1-HA \times gDM2d-Myc]$ in indicated mutant backgrounds crossed with Col-0. Plants were grown at 16°C. Pictures are taken at 19 days after sowing. Scale bar equals 1 cm.



Figure S2. Phenotypic representation of F₁[*gDM1-HA*x*gDM2d-Myc*] in Col-0, *eds1-1*, *rar1-21*, *sgt1b*, and *rbohD* backgrounds. Plants were grown at 16°C. Pictures are taken at 55 days after sowing. Scale bar equals 1 cm.

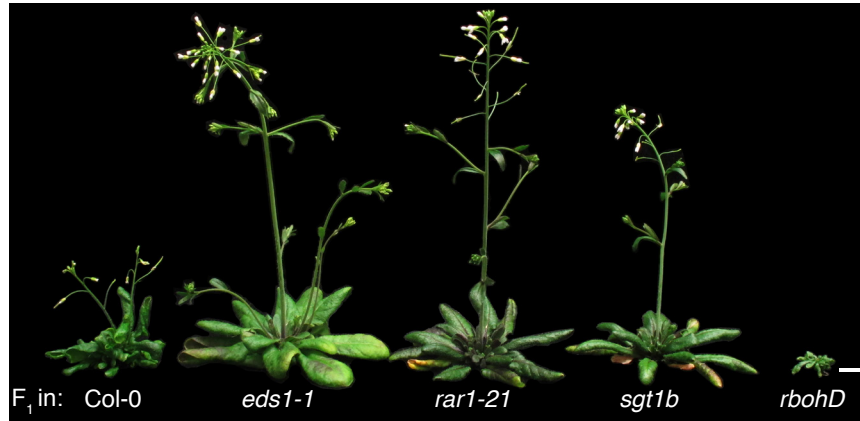


Figure S3. Representative HR in *N. benthamiana* results from co-expression of full-length DM1 and DM2d fused with different tags at the C-terminal regions. The phenotype was captured at 4 days post-infiltration. Scale bar equals 1 cm.

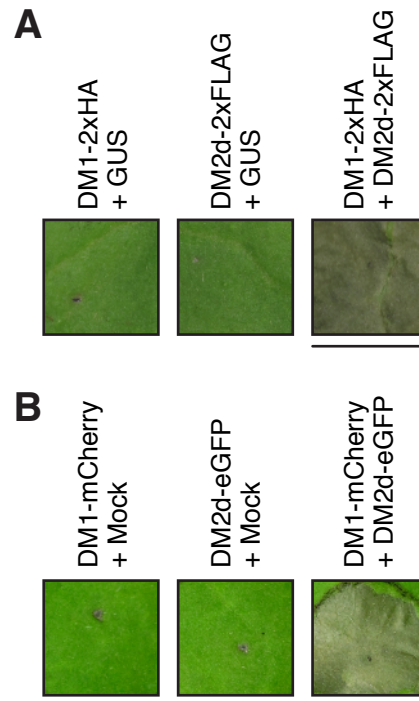


Figure S4. Optimization of ethanol inducible system in *N. benthamiana*. Combinations of indDM1-HA and DM2d-Myc at indicated OD₆₀₀ are indicated in the figure. (A) Pictures of *N. benthamiana* leaves were taken at 4 days post-infiltration. (B) Conductivity assays of indicated combinations without and with ethanol treatment. Scale bar equals 1 cm.

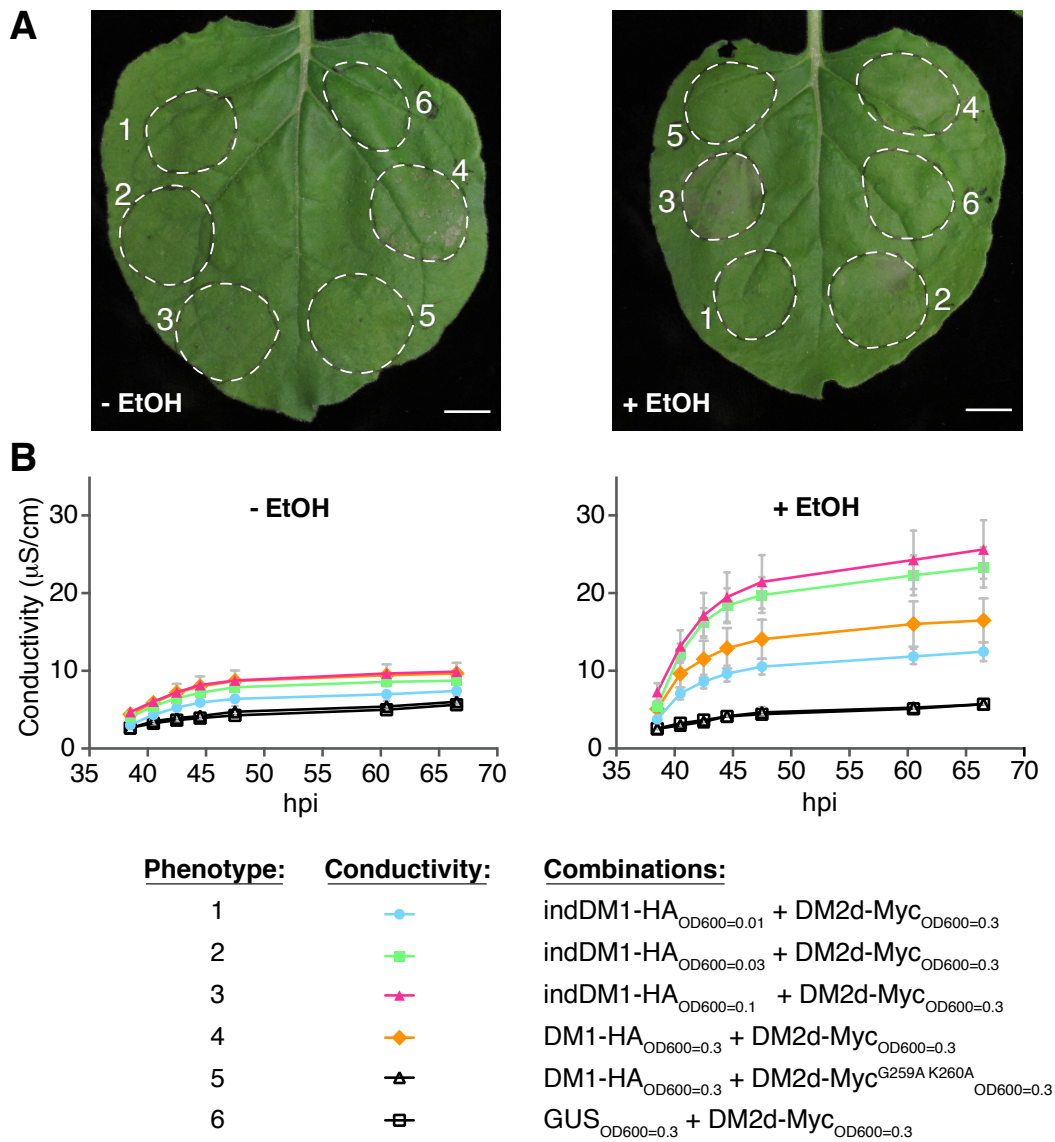


Figure S5. A full set of recapitulated DM1/DM2d-dependent necrosis in $F_1[indDM1-HAxDM2d-Myc]$. Ethanol induction was performed with 15-day-old seedlings by irrigating with 1% EtOH and covering the flat for 3 days with a transparent dome. Red arrows indicate onset of cell death at 3 days after induction.

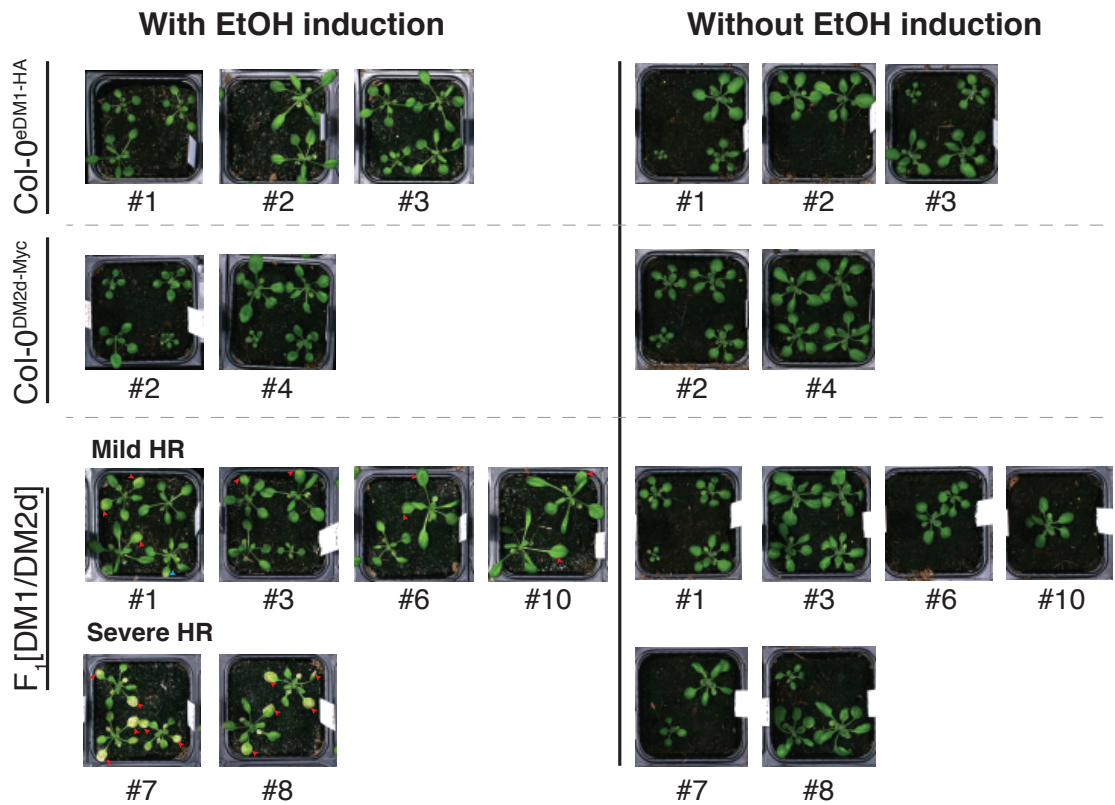


Figure S6. CoIP analysis of DM1 and DM2d from *A. thaliana* samples shown in Fig.R8A. CoIP condition was performed by using an extraction buffer containing 0.5% NP-40. Total protein extracts from the pooled leaf tissues collected at 18 days after induction were used for CoIP. Input indicates 10% of total protein extract. Ponceau-S staining shown to indicate loading.

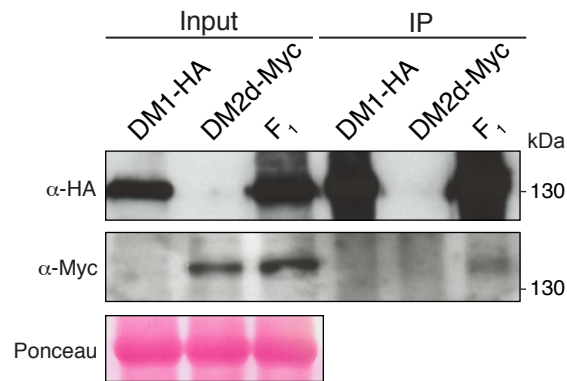


Figure S7. Amino acid alignment between DM2d and DM2g. Asterisk, colon, or dot below the sequence indicates positions with fully conserved, strongly similar, or weak similar properties, respectively. Dash indicates amino acid deletion (www.uniprot.org). The TIR, NB-ARC, and LRR domains are highlighted in magenta, turquoise, and yellow, respectively. The SH motif, P-loop and MHD motif are marked as white, blue, and red texts, respectively.

```

DM2d MDSSFFLVLVVA--AATGFFMLFRKFRFHQDNKESNSSLSLSPATSVSRNWKHDVFPSPFH 59
DM2g MDSSFFLVLVAAAAVGVFFILYRKFRFQDNQESNSSALSPLSPPTSVSRIWKHQVFPSPFH 60
***** * * . * * * : * : * * * * : * * * : * * * * * * * * * * * * * * * * * * *

DM2d GADVRRRTFLSHILESFRRKIDTFIDNNIERSKSIGPELKEAIKGSKIAIVLLSRKYASS 119
DM2g GADVRRRTFLSHIMESFRRKIDTFIDNNIERSKSIGPELKKAIKGSKIAIVLLSRKYASS 120
***** * * . * * * * * * * * * * * * * * * * * * * * * * * * * * * * * * * * * * *

DM2d SWCLDELAEIMKCREMVGQIVMTIFYEVEPTDIKKQTSEFGKAFKTCRCGKTKEHIERWR 179
DM2g SWCLDELAEIMICREVLGQIVMTIFYEVEPTDIKKQTSEFGKAFKTCRCGKTKEHVERWR 180
***** * * * : * : * * * * * * * * * * * * * * * * * * * * * * * * * * * * *

DM2d KALEDVATIAGYHSHKWSNEAEMIEKISTDVSNILNLSIPSRDFDGFVGMTPHMEMMEKY 239
DM2g KALEDVATIAGYHSHKWSNEAEMIEKISTDVSNILNLSIPSRDFDGFVGMTPHMEMMEKY 240
*****

DM2d LRLDLDEVRMVGIWGPPIGIGKTTIATCVFNRFSSRPFFAAIITDIRECYPRLCLDERSAQ 299
DM2g LRLDLDEVRMVGIWGPPIGIGKTTIATCVFNRFSSRPFFAAIITDIRECYPRLCLDERSAQ 300
*****

DM2d LKLQAQMLSQMINHKDIMISHLGVAPERLKDKKVFLVLEVDHLGQLDALAKDTRWFGPG 359
DM2g LKLQAQMLSQMINHKDIMISHLGVAPERLKDKKVFLVLEVDHLGQLDALAKDTRWFGPG 360
*****

DM2d SRIIITTEDLGVLKAHGINHVYKVGYPNDEAFQIFCMNAFGQKQPHEGFDEIAREVMAL 419
DM2g SRIIITTEDLGVLKAHGINHVYKVGYPNDEAFQIFCMNAFGQKQPHEGFDEIAWEVTCL 420
***** * * . *

DM2d AGELPLGLKVLGSALRGSKPEWERTLPRLRTSLDGKIGSIIQFSFDALCEEDKYLFLYI 479
DM2g AGKLPLGLKVLGSALRGSKPEWERTLPRLRTSLDGKIGSIIQFSFDALCEEDKYLFLYI 480
* * : * * * * * * * * * * * * * * * * * * * * * * * * * * * * * * * * * * *

DM2d ACLFNKESTTKVEGLLGKFLDVRQGLHILAQKSLISIEYGNIFYFTLLAQSAFDGERIHM 539
DM2g ACLFNKESTTKVEGLLGKFLDVRQGLHILAQKSLISIEYGNIFYFTLLAQSAFDGERIHM 540
*****

DM2d HTLLEQFGRETSRKQFVHHGYRKHQLLVGERDICEVLDDDTTDSRRFIGINLDRNNEE 599
DM2g HTLLEQFGRETSRKQFVHHGYRKHQLLVGERDICEVLNDDTI DSRRFIGINLDRNNEE 600
***** * : * * * * * * * * * * * * * * * * * * * * * * * * * * * * * * *

DM2d LNISEKALQRIHDFQFVRINDKNHAQHERLQAVLQGLIYQSPQIRSLHWKCYQNICLPST 659
DM2g LNISEKALQRIHDFQFVRINDKNHAQHERL---QGLIYQSPQIRSLHWKCYQNICLPST 656
***** * * * * * * * * * * * * * * * * * * * * * * * * * * * * * * *

DM2d FNSEFLVELDMSDSNLRKRWEGTKQLRNLKWMDSLDCEDLKELPNLSTATNLEELKLRNC 719
DM2g FNSEFLVELDMSDSNLRKRWEGTKQLRNLKWMDSLSEDLKELPNLSTATNLEELKLRNC 716
***** * . * * * * * * * * * * * * * * * * * * * * * * * * * * * * * * *

DM2d SSLVELPSSIEKLTSLQRLDLHSCSSLVELPSFGNATKLEKLDLGNCRSLVKLPPSINAN 779
DM2g SSLVELPSSIEKLTSLQRLDLHSCSSLVELPSFGNATKLVILDVGYCSSLVKLPPSINAN 776
***** * * : * * * * * * * * * * * * * * * * * * * * * * * * * * * * * * *

DM2d NLQELSLRNCNRVVKLPAIENATKLRKLLQNCSSLIELPLSIGTATNLKKNISGCSL 839
DM2g NLQKLSLRNCNRVVKLPAIENATKLRKLLQNCSSLIELPLSIGTATNLKKNISGCSL 836
* * * : * * * * * * * * * * * * * * * * * * * * * * * * * * * * * * *

```

DM2d VKLPSSIGDMTNLEVFDSLNCNSLVLPSSIGDITDLEVFNLDNCSSLVTLPSSIGNLQN 899
DM2g VKLPSSI-----GDITDLEVFNLDNCSSLVTLPSSIGNLQN 872

DM2d LSELLMCGCSKLETLPININLKALSTLDLTDSCQLKSFPEISTHIDSLSLIGTAIKEVPL 959
DM2g LIVLTMHGCSKLETLPININLKALSTLDLTDSCQLKSFPEISTHIDSLSLIGTAIKEVPL 932
* * *

DM2d SIMSWSRLAEFQISYFESLKEFPHALDIITGLWLSKSDIEEVPPWVKRMSRLHRLTLNNC 1019
DM2g SIMSWSRLAEFQISYFESLKEFPHALDIITGLWLSKSDIEEVPPWVKRMSRLHRLTLNNC 992

DM2d>NNLVSLPQLPDSLDIYADNCKSLERLDCCFNNRWITLHFPKCFKLNQEARDLIMHTST- 1078
DM2g>NNLVSLPQLPDSLDIYADNCKSLERLDCCFNNRWITLHFPKCFKLNQEARDLIMHTSPC 1052

DM2d RSFAMFPGTQVHACFIHRATSGDSLKIKLKESPLPTTLRFKACIMLVKVNEELMSYDQTP 1138
DM2g IDLIMLPGTQVPACFNHRATSGDSLKIKLKESPLPTTLRFKACIMLVKVNEELMSYDQTP 1112
.: *:***** **

DM2d ISMSVGIVIRDEHNDLIVHCTPSEHEIYPVLT--EHIYTFELEMSTSTELVFEFIL 1196
DM2g ISMSVGIVIRDEHNDLIVHCTPSEHEIYPVLTSEHIYTFELEV--EEVTSTELVFEFTL 1170
*****: : ***** *

DM2d DNESNWKIGECGILQIVEVP 1216
DM2g DNESNWKIGECGILQIVEVP 1190

Figure S8. Amino acid alignment between DM2d^{Uk-1} and its Col-0 homologs. See Figure S7 for domain annotation.

```

DM2dUk-1 -----MDSSFFLVLVAAAT 14
At3g44400 -----MDSSFFLVVVAAAI 14
At3g44480 MGSVMSLGC SKRKATNQDV DSES RKRK ICSTNDAENCRFIQDESSWKHPWSLCANRVIS 60
At3g44630 MGSAMSLC SKRKATSQDV DSES CKRRK TCSTNDAENCIFIPDESS----WSLCANRVIT 56
At3g44670 MGSVMSLGC SKRKATSQDV DSES RKRK ICSTNDAENCRFIQDESSWKHPWSLCVNV--- 57
                                     : *

DM2dUk-1 GFFMLFRKFRFHQDNKESNSSLSLSPATSVSRNWKHDVFPFSGADVRRRTFLSHILES 74
At3g44400 GFFILFRKFRFQE----SNSSLSLSPATSVSRNWKHDVFPFSGADVRRRTFLSHIKES 70
At3g44480 VAAVALTNFRFQODNQESNSSLSLSPATSVSRNWKHDVFPFSGADVRRRTFLSHIMES 120
At3g44630 VAAVALTNFRFQODNQESNSSLSLPSLATS SVSRNWKHDVFPFSGADVRRRTFLSHIMES 116
At3g44670 -AAAF TKFRFQODNKYTKSSALS LSPPTSVSRIWKHHVFPFSGADVRKTI LSHILES 116
          : :***: : :*:***** ***** ** .***** :*:***** **

DM2dUk-1 FRRKGIDTFIDNNIERSK SIGPELKEAIKGSKIAIVLLSRKYASSSWCLDELAEIMKCRE 134
At3g44400 FRRKGIDTFIDNNIERSK SIGPELKEAIKGSKIAIVLLSRKYASSSWCLDELAEIMKCRE 130
At3g44480 FRRKGIDTFIDNNIERSK SIGPELKEAIKGSKIAIVLLSRKYASSSWCLDELAEIMKCRQ 180
At3g44630 FRRKGIDTFIDNNIERSK SIGPELKEAIKGSKIAIVLLSRKYASSSWCLDELAEIMKCRQ 176
At3g44670 FRRKGIDPFIDNNIERSK SIGHELKEAIKGSKIAIVLLSKNYASSSWCLDELAEIMKCRE 176
          ***** ***** ***** :*****:*****:

DM2dUk-1 MVGQIVMTIFYEVEPTDIKKQTSEFGKAF TKTCRGKTKEHIERWRKALEDVATIAGYHSH 194
At3g44400 MVGQIVMTIFYEVEPTDIKKQTGEFGKAF TKTCRGKTKEHIERWRKALEDVATIAGYHSH 190
At3g44480 MVGQIVMTIFYEVDPTDIKKQTGEFGKAF TKTCRGKPKQEVRWRKALEDVATIAGYHSH 240
At3g44630 MVGQIVMTIFYEVEPTDIKKQTGEFGKAF TKTCRGKPKQEVRWRKALEDVATIAGYHSH 236
At3g44670 LLGQIVMTIFYEVDPTDIKKQTGEFGKAF TKTCCKGKTKEYVERWRKALEDVATIAGEHSR 236
          :*:*****:***** .*****:*** ** :***** ***** **

DM2dUk-1 KWSNEAEMIEKISTDVSNI LNLSIPSRDFDGFVGMTPHMEMMEKYLRLDLDEVRMVG IWG 254
At3g44400 KWCDEAEMIEKISTDVS-----KDFDDFVGMMAHMERTEQLLRLDLDEVRMIG ILG 241
At3g44480 SWRNEADMIEKISTDVS NMLNSFTPSRDFDGLVGMRAHMDMLEQLLRLDLDEVRMIG IWG 300
At3g44630 SWRNEADMIEKIATDVS NMLNSFTPSRDFDGLVGMRAHMDMLEQLLRLDLDEVRI IGIWG 296
At3g44670 NWRNEADMIEKIATDVS NMLNSFTPSRDFDGLVGMRAHMDMLEQLLRLDLDEVRMIG IWG 296
          .* :*:*****:***** :*** :*** **: :* :*****:*** *

DM2dUk-1 PPGIGKTTIATCVFNRFSSRFPFAAIITDIRECYPR LCLDERSAQLKLOA QMLSQMINHK 314
At3g44400 PPGIGKTTIATCMFDRFSRRFPFAAIMTDIRECYPR LCLNERN AQLKLOEQMLSQIFNQK 301
At3g44480 PPGIGKTTIARFLFNQVSDRFQLSAIMVNIKGCYPRPCFDEYSAQLQ LQNLQMLSQMINHK 360
At3g44630 PPGIGKTTIARFLFNQVSDRFQLSAIMVNIKGCYPRPCFDEYSAQLQ LQNLQMLSQMINHK 356
At3g44670 PPGIGKTTIARFLFNQVSDRFQLSAIIVNIRGIYPRPCFDEYSAQLQ LQNLQMLSQMINHK 356
          ***** :::.* ** :*:*:*: ** ** :*:*.***:*** :*:**

DM2dUk-1 DIMISHLGVAPERLKD KKVFLVLD EVDHLGQLDALAKDTRWF GPGSRI IITTEDLGVLKA 374
At3g44400 DTMISHLGVAPERLKD KKVFLVLD EVGHLGQLDALAKETRWF GPGSRI IITTEDLGVLKA 361
At3g44480 DIMISHLGVAQERLRD KKVFLVLD EVDQLGQLDALAKETRWF GPGSRI IITTEDLGVLKA 420
At3g44630 DIMISHLGVAQERLRD KKVFLVLD EVDQLGQLDALAKETRWF GPGSRI IITTEDLGVLKA 416
At3g44670 DIMISHLGVAQERLRD KKVFLVLD EVDQLGQLDALAKETRWF GPGSRI IITTEDLGVLKA 416
          * ***** ** :***** :*****:*****:*****:

DM2dUk-1 HGINHVYKVGYP SNDEAFQIFCMNAFGQKQPHEGFDEIAREVMALAGELPLGLKVLGSAL 434
At3g44400 HGINHVYKVGYP SNDEAFQIFCMNAFGQKQPCEGFCDLAWEVKALAGELPLGLKVLGSAL 421
At3g44480 HGINHVYKVEYP SNDEAFQIFCMNAFGQKQPHEGFDEI AWEVTC LAGELPLGLKVLGSAL 480
At3g44630 HGINHVYKVEYP SNDEAFQIFCMNAFGQKQPHEGFDEI AWEVKALAGK LPLGLKVLGSAL 476
At3g44670 HGINHVYKVKYP SNDEAFQIFCMNAFGQKQPHEGFDEI AWEVMALAGELPLGLKVLGSAL 476
          ***** ***** ***** ** :* ** .***:*****

DM2dUk-1 RGKSKPEWERTL PRLR TSLDGKIGSIIQFSYDALCEDDKYLFLYIACL FNKESTTKVEGL 494
At3g44400 RGMSKPEWERTL PRLR TSLDGKIGNIIQFSYDALCEDDKYLFLYIACL FNVESTTKVKEL 481
At3g44480 RGKSKREWERTL PRLK TSLDGKIGSIIQFSYDVLCD EDDKYLFLYIACL FNGESTTKVKEL 540
At3g44630 RGKSKPEWERTL PRLR TSLDGKIGGIQFSYDALCEDDKYLFLYIACL FNGESTTKVKEL 536
At3g44670 RGKSKPEWERTL PRLK TSLDGNIGSIIQFSYDGLCEDDKYLLLYIACL FNVESTTKVEEV 536
          ** ** *****:*****:*** *****:* **:*****:***** *****: :

```

DM2dUk-1 L-GKFLDVRQGLHILAQKSLISIEYGNIFYFTLL-----AQKSAFDGERIHMHTL 542
At3g44400 L-GKFLDVKQGLHVLAQKSLIS-----FYGETIRMHHTL 513
At3g44480 L-GKFLDVKQGLHLLAQAQKSLISFDGE-----RIHMHTL 572
At3g44630 L-GKFLDVRQGLHVLAQKSLISFDEEISWKQIVQVLLLNKFSHVRHTKRNSQIIRMHHTL 595
At3g44670 LANKFLDVKQGLHVLAQKSLISIDENS-----LYGDTINMHHTL 574
* *****:****:***** * .****

DM2dUk-1 LEQFGRETSRKQFVHHGYRKHQLLVGERDICEVLDDDTTDSRRFIGINLDRNNVEELNI 602
At3g44400 LEQFGRETSCKQFVHHGYRKHQLLVGERDICEVLDDDTTRNRRFIGINLDRKNEKELKI 573
At3g44480 LEQFGRETSRKQFVHHGFTKRQLLVGARGICEVLDDDTTDSRRFIGIHLELNTTEELNI 632
At3g44630 LEQFGRETSRKQFVHHRYTKHQLLVGERDICEVLDDDTTDSRRFIGINLDLYKNEELNI 655
At3g44670 LROFGRETSRKQFVYHGFTRKQLLVGERDICEVLSDDTIIDRRFIGITFDLFGTQDYLNI 634
*.***** *****: * :*:***** * *****.* * .***** :*: * . . *:*

DM2dUk-1 SEKALQRIHDFQFVRINDKNH-----AQHERLQAVLQGLIYQSPQIRSLHWK 649
At3g44400 SEKTLERMHDFQFVRINDVFTHKERQKLLHFKIIHQPERVQLALEDLIYHSPRIRSLKWF 633
At3g44480 SEKVLERVHDFHFVRIDASF-----QPERLQALQDLIYHSPKIRSLNWX 677
At3g44630 SEKALERIHDFQFVKINYVFT-----HQPERVQLALEDLIYHSPRIRSLKWF 702
At3g44670 SEKALERMNDFEFVRINAL-----IPTERLQALQDLICHSPKIRSLKWX 679
.*:*.**.*:*: **:* .*: ** :*:**.*

DM2dUk-1 CYQNICLPSTFNSEFLVELDMSDNSLRKRWEGTKQLRNLKWMDSLDCEDLKELPNL-STA 708
At3g44400 GYQNICLPSTFNPEFLVELDMSSSKLRKRWEGTKQLRNLKWMDSLSDSEDLKELPNL-STA 692
At3g44480 GYESLCLPSTFNPEFLVELDMRSSNLRKRWEGTKQLRNLKWMDSLSSYSSYLKELPNL-STA 736
At3g44630 PYQNICLPSTFNPEFLVELDMRCSKLRKRWEGTKQLRNLKWMDSLSDRDLKELPSSIEKL 762
At3g44670 SYQNICLPSTFNPEFLVELHMSFSKLRKRWEGTKQLRNLKWMDSLNSSEDLKELPNL-STA 738
*.:***** *****.* *:***** . ***** . .

DM2dUk-1 TNLEELKLRNCSSLVELPSSIEKLTSLQRLDLHSCSSLVELPSFGNATKLEKLDLGNCRS 768
At3g44400 TNLEELKLRRCSSLVELPSSIEKLTSLQILDHSCSSLVELPSFGNATKLEKLDLENCSS 752
At3g44480 TNLEELKLRNCSSLVELPSSIEKLTSLQ----- 764
At3g44630 TSLQILDLRDCSSLVKLPPSINA-NNLQ----- 789
At3g44670 TNLEELKLRDCSSLVELPSSIEKLTSLQRLYLQRCSSLVELPSFGNATKLEELYLENCSS 798
.: :*.** *****:* ** : .**

DM2dUk-1 LVKLPSSINANNLQELSLRNCSSRVVKLPAIENATKLRKLLKQNCSSLIELPLSIGTATNL 828
At3g44400 LVKLPSSINANNLQELSLRNCSSRVVLPALAIENATNLRELKLLKQNCSSLIELPL----- 804
At3g44480 -----ILDLENCSSLEKLPALAIENATKLRKLLKQNCSSLIELPLSIGTATNL 810
At3g44630 -----GLSLTNCSSRVVKLPAIENVNTNLHQLKLLKQNCSSLIELPLSIGTANNL 835
At3g44670 LEKLPSSINANNLQQLSLINCSRVVLPALAIENATNLQKLDLGNCSLIELPLSIGTATNL 858
. *** : :*****.*:*.**.* *****

DM2dUk-1 KKLNISGCSSLVVKLPSSIGDMTNLEVFDSLNCSSNLVELPSSIGDITDLEVFNLDCSSSLV 888
At3g44400 ----- 849
At3g44480 KQLNISGCSSLVVKLPSSIGDITDLEVFDSLNCSSSLVTLPL----- 849
At3g44630 WKLDIRGCSSLVVKLPSSIGDMTNLKEFDSLNCSSNLVELP----- 874
At3g44670 KELNISGCSSLVVKLPSSIGDITNLKEFDSLNCSSNLVEL----- 896

DM2dUk-1 TLPSSIGNLQNLSELLMCGCSKLETLPININLKALSTDLTDCSQLKSFPEISTHIDSLS 948
At3g44400 ----- 906
At3g44480 ---SSIGNLQNLCKLIMRGCSKLEALPININLKSLDTLNLTDCSQLKSFPEISTHISELR 906
At3g44630 ---SSIGNLQKLFMLRMRGCSKLETLPNTINLISLRILDLTDCSQLKSFPEISTHISELR 931
At3g44670 -----PININLKFLDTLNLGCSQLKSFPEISTKIFT-- 928

DM2dUk-1 LIGTAIKEVPLSISWSRLAEFQISYFESLKEFPHALDIITGLWLSKSDIEVPPVWKRM 1008
At3g44400 -----SWVKRM 810
At3g44480 LKGTAIKEVPLSISWSPLADFQISYFESLMEFPHALDIITKLH-LSKDIQEVPPVWKRM 965
At3g44630 LKGTAIKEVPLSISWSRLAVYEMSYFESLKEFPHALDIITDLLVSEDIQEVPPVWKRM 991
At3g44670 -----DCYQRM 934
: **

DM2dUk-1 SRLHRLTLNCCNNLVSLPQLPDSLDIYADNCKSLERLDCCFNNRWITLHFPKCFKLNQE 1068
At3g44400 SRLRVLTLNCCNNLVSLPQLPDSLDIYADNCKSLERLDCCFNNPEISLYFPNCFKLNQE 870
At3g44480 SRLRDLTLNCCNNLVSLPQLPDSLDIYADNCKSLERLDCCFNNPEIRLYFPKCFKLNQE 1025
At3g44630 SRLRALRNLNCCNNLVSLPQLPDSLDIYADNCKSLERLDCCFNNPEIRLYFPKCFKLNQE 1051
At3g44670 SRLRLRNLNCCNNLVSLPQLPDSLAYLYADNCKSLERLDCCFNNPEISLNFPKCFKLNQE 994
: * :**.* ***** * *:***** . * * ** :*****

DM2dUk-1 ARDLIMHTSTRSFAMFPGTQVHACFIHRATSGDSLKIKLKESPLPTTLRFKACIMLVKVN 1128
 At3g44400 ARDLIMHTSTRSFAMLPGTQVPACFIHRATSGDYLKIKLKESFPPTTLRFKACIMLVKVN 930
 At3g44480 ARDLIMHTCI--DAMFPGTQVPACFIHRATSGDSLKIKLKESPLPTTLRFKACIMLVKVN 1083
 At3g44630 ARDLIMHTSTRKYAMLPSIQVPACFNHRATSGDYLKIKLKESLPTTLRFKACIMLVKVN 1111
 At3g44670 ARDLIMHTTCI-NATLPGTQVPACFNHRATSGDSLKIKLKESLPTTLRFKACIMLVKVN 1053
 ***** * : . ** ** ***** ***** :*****

DM2dUk-1 EELMSYDQTP--ISMSVGIVIRDEHNDLIVHCTPSEHEI--YPVLTEHIYTFEELMSYD 1184
 At3g44400 EE-MSYDQRS--MSVDIVI---SVHQAIVQCTPSYHHI--YPVLTEHIYTFELEVVEE-- 980
 At3g44480 EELMSYDQTP----MIVDIVIRDEHNDLKEKIYPSIY-PSIYPLLTEHIYTFELDVEE-- 1136
 At3g44630 EEMRDDEMWP----SVL-IAIRVKQNDLKVL----CT-ASIYPVLTEHIYTFELEVVEE-- 1159
 At3g44670 EEMSSDLKSMIFDPMRVDIVIRDEQNDLKVQCTPSYHFINYFIISTEHIYTFELEVVEE-- 1111
 ** . : * :: : : : *****: .

DM2dUk-1 QTSTELVFEFILDNES----NWKIGECGILQIVEVP----- 1216
 At3g44400 VTSTELVFEFI-SFRS----NWKIGECGILQR----- 1007
 At3g44480 VTSTELVFEFPQLN----KRNWKIGECGILQRETRSLRRSSSPDLSPESSRVSSYDHCLR 1192
 At3g44630 VTSTELVFEFTPFH----KSNWKIGECGILQRETRSFCSRSSPDLPPESSRAFSLSLSHS 1215
 At3g44670 VTSTELVFEFILDKESNWKRNWKIGECGILQRETRSLRRSSSPDLSPESSRVSSYDHCLR 1171
 ***** *****

DM2dUk-1 -----
 At3g44400 -----
 At3g44480 GD----- 1194
 At3g44630 PFLSLCLMDW----LMIRFLLMGFRVSS----- 1240
 At3g44670 GKNHGFDFSLSHSMDSIIGFILCEWELAVKYGFCDMFSFVVFVYLER 1219

Figure S9. Domain swapping experiment indicated that LRR motif 7 and 8 of DM2d alone were not sufficient to alter TIR^{DM2d}-containing DM2g activity. Domain structures of DM2d/g and polymorphisms in DM2d relative to DM2g are indicated in the top two diagrams. Purple vertical lines represent amino acid changes; and green bars, indels. In chimeric DM2d-DM2g proteins, orange bars indicate fragments from DM2d; and turquoise bars, those from DM2g. The numbers indicate amino acid positions in DM2d. A representative HR phenotype of each chimeric protein when co-expressed with wild-type DM1 in *N. benthamiana* is presented in the black-lined square on right. HR was scored at 4 dpi. Ponceau-S staining shown to indicate loading.

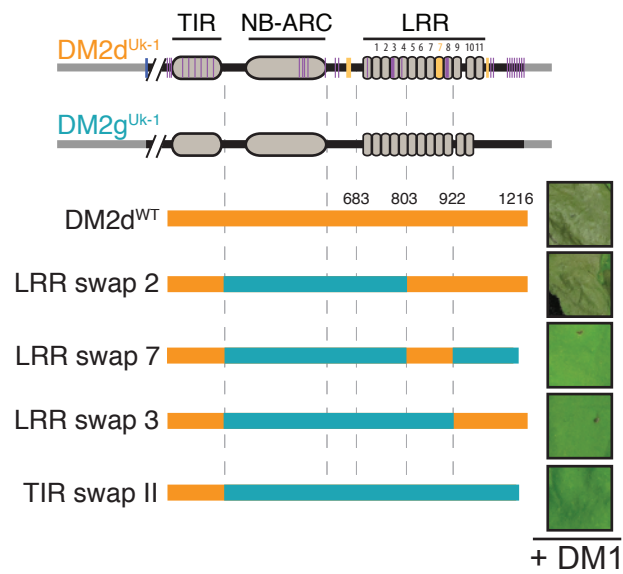


Figure S10. Amino acid alignment between DM1^{Uk-3} and its Col-0 homolog. See Figure S7 for domain annotation.

```

DM1Uk-3  MASSSSSSSSSSSHIRRHVFSFFHGPVDRKGFLSHLHSVFASKGITNFNDQKIERGQTIG 60
At5g41750 ---MALSSSLSCIKRYQVFSSFHGPVDRKGFLSHLHSVFASKGITTFNDQKIDRGQTIG 56
      :  *** * * : * : : ***** . ***** : *****

DM1Uk-3  PELIQGIREARVSIVVLSKKYASSWCLDELVEILKCKEALGOIVMTVFYEVDPDVKKQ 120
At5g41750 PELIQGIREARVSIVVLSKKYASSWCLDELVEILKCKEALGOIVMTVFYEVDPDVKKQ 116
      *****

DM1Uk-3  SGFGEAFEKTCQGKNEEVKIRWRNALAHVATIAGEHSLNWDNEAKMIQKIATDVSDKLN 180
At5g41750 SGVFGEAFEKTCQGKNEEVKIRWRNALAHVATIAGEHSLNWDNEAKMIQKIATDVSDKLN 176
      ** *****

DM1Uk-3  LTPSRDFEGMVGMEAHLTELNSLLSLESDEVKMIGIWGPAGIGKTTIARTLFNKLSSIFP 240
At5g41750 LTPSRDFEGMVGMEAHLKRLNSLLCLESDEVKMIGIWGPAGIGKTTIARTLFNKISSIFP 236
      ***** . ***** . ***** : *****

DM1Uk-3  FKCFMENLKGSIKGGAEHYSKLSLQKQLLSEILKQENMKIHHLGTIKQWLHDQKVLIIID 300
At5g41750 FKCFMENLKGSIKGGAEHYSKLSLQKQLLSEILKQENMKIHHLGTIKQWLHDQKVLIIID 296
      *****

DM1Uk-3  DVDDLEQLEVLAE DP SWFGSGSRIIVTTEDKILKAHRIQDIYHVDFPSEEEALEILCLS 360
At5g41750 DVDDLEQLEVLAE DP SWFGSGSRIIVTTEDKNILKAHRIQDIYHVDFPSEEEALEILCLS 356
      ***** : *****

DM1Uk-3  AFKQSSIPDGFEE LANKVAELCGNPLGLSVVGASLRRKSKNEWERLLSRIESSLDRDID 420
At5g41750 AFKQSSIPDGFEE LANKVAELCGNPLGLCVVGASLRRKSKNEWERLLSRIESSL DKNID 416
      ***** . ***** : : **

DM1Uk-3  DILRIGYDRLSKEDQSLFLHIACFFNYAKVDNVTALLADSNLDVRNGFNILADRSLVRIS 480
At5g41750 NILRIGYDRLSTEDQSLFLHIACFFNNEKVDYLTALLADRKL DVVNGFNILADRSLVRIS 476
      : ***** . ***** ***** ** : ***** : ** *****

DM1Uk-3  TFDVGQIEMHH-LLQQLGKQIVLEQ-SKEPGKREFIIEPEEIRDVLTNETGTGTSVKGISF 538
At5g41750 TD--GHVVMHHYLLQKLGRRIVHEQWPNEPGKROFLIEAEEIRDVLTTKGTGTESVKGISF 534
      *   * : : *** ** : * : * : ***** : * : * ***** : *** *****

DM1Uk-3  DTSNIGEVS SVSKGAFEGMRNLRFLRIYRVLEYFNYELPSEGTLOISEDMEYLPPLRLLDW 598
At5g41750 DTSNIEEVS SVKGFEGMRNLQFLRIYRD-----SFNSEGTLOIPEDMEYIPVRLLLHW 588
      ***** ** . ***** : ***** . : ***** ***** : * : * . *

DM1Uk-3  DRYPRKSLPTKFQPERLVEIHMPRSKLEKLWGGIQPLPNLKSIDLNRSHKLEIPNLSKA 658
At5g41750 QNYPRKSLPQRFNPEHLVKIRMPSSKLLWGGIQPLPNLKSIDMSFSYSLEIPNLSKA 648
      : . ***** : * : * : * : * : * : * : * : * : * : * : * : * : * : * : * : *

DM1Uk-3  TNLETNLNTHCENLVELPSSISNLHKLEILNVEYCSMLKVIPTNINLASLEEVQMSGCWE 718
At5g41750 TNLEILSLEFCKSLVELPFSILNLHKLEILNVENCSMLKVIPTNINLASLERLDMTGCSE 708
      **** * . * . * : ***** * ***** ***** . : * : * *

DM1Uk-3  LRTFPDISSNIKKLNLNLENTMIKDVPVSVGCWSRLDHL YIRSRSLKRLMHVPPCITVLVLS 778
At5g41750 LRTFPDISSNIKKLNLGDTMIEDVPPVSVGCWSRLDHL YIGSRSLKR-LHVPPCITSLVLW 767
      ***** : * : * : ***** ***** : ***** **

DM1Uk-3  GSYIERIPESFIGLTRLHRLHVKRCIKLKSILGLPSSLQFLDANDCVSLKRVRF SFHNPM 838
At5g41750 KSNIESIPESIIGLTRLDWLVNNSCRKLSILGLPSSLQFLDANDCVSLKRVCF SFHNPI 827
      * ** *** : ***** . * : * ***** ***** *****

DM1Uk-3  DTLGFNNCLKLDEEAKRGIMQRPVSR YICLPCKKIPEEFTHKATGRSITIPSPGTLSAS 898
At5g41750 RALSFN NCLNLDEEARKGI IQOSVYRYICLPGKKIPEEFTHKATGRSITIPSPGTLSAS 887
      : * . ***** : ***** : * : * : * ***** *****

DM1Uk-3  SRFKASILILLVESYEIKGISCSIRT KGGVEVHCCGRGYLD-RDLRSEHLFIFHDDLFPQ 957
At5g41750 SRFKASILILPVESYETDDISCSLRTKGGVEVHCCELPYHFLRSRSEHLFIFHGDLFPQ 947
      ***** ***** . ***** : ***** * ***** *****

```

```

DM1Uk-3  GNKYHEVDVTMREITFEFSHTKIGDKIIECGVQIMTEGAEGDSSRELDSFETESSSSQVG 1017
At5g41750 GNKYHEVDVTMSEITFEFSHTKIGDKIIECGVQIMTEGAEGDSSRELDSFETESSSSQVD 1007
*****

DM1Uk-3  NFEFGNHHHTDGNNGDGNIEAEGSKFSQDENIKTSKRTGFMSWLRKLGQ----- 1067
At5g41750 NFETGGNHHHTDGNNGDGNIEAEGFKFFQDENIKTSKHTGFRSWLRELGLKVKKMNSHG 1067
***

```


REFERENCES

- Aarts, N., Metz, M., Holub, E., Staskawicz, B.J., Daniels, M.J., and Parker, J.E. (1998). Different requirements for *EDS1* and *NDR1* by disease resistance genes define at least two R gene-mediated signaling pathways in *Arabidopsis*. *Proc Natl Acad Sci U S A* *95*, 10306-10311.
- Ade, J., DeYoung, B.J., Golstein, C., and Innes, R.W. (2007). Indirect activation of a plant nucleotide binding site-leucine-rich repeat protein by a bacterial protease. *Proc Natl Acad Sci U S A* *104*, 2531-2536.
- Alcázar, R., García, A.V., Kronholm, I., de Meaux, J., Koornneef, M., Parker, J.E., and Reymond, M. (2010). Natural variation at Strubbelig Receptor Kinase 3 drives immune-triggered incompatibilities between *Arabidopsis thaliana* accessions. *Nat Genet* *42*, 1135-1139.
- Alcázar, R., García, A.V., Parker, J.E., and Reymond, M. (2009). Incremental steps toward incompatibility revealed by *Arabidopsis* epistatic interactions modulating salicylic acid pathway activation. *Proc Natl Acad Sci U S A* *106*, 334-339.
- Alonso, J.M., Stepanova, A.N., Leisse, T.J., Kim, C.J., Chen, H., Shinn, P., Stevenson, D.K., Zimmerman, J., Barajas, P., Cheuk, R., *et al.* (2003). Genome-wide insertional mutagenesis of *Arabidopsis thaliana*. *Science* *301*, 653-657.
- Arai, M., Sugase, K., Dyson, H.J., and Wright, P.E. (2015). Conformational propensities of intrinsically disordered proteins influence the mechanism of binding and folding. *Proc Natl Acad Sci U S A* *112*, 9614-9619.
- Ashikawa, I., Hayashi, N., Yamane, H., Kanamori, H., Wu, J., Matsumoto, T., Ono, K., and Yano, M. (2008). Two adjacent nucleotide-binding site-leucine-rich repeat class genes are required to confer *Pikm*-specific rice blast resistance. *Genetics* *180*, 2267-2276.
- Austin, M.J., Muskett, P., Kahn, K., Feys, B.J., Jones, J.D., and Parker, J.E. (2002). Regulatory role of SGT1 in early R gene-mediated plant defenses. *Science* *295*, 2077-2080.
- Ausubel, F.M. (2005). Are innate immune signaling pathways in plants and animals conserved? *Nat Immunol* *6*, 973-979.
- Azevedo, C., Betsuyaku, S., Peart, J., Takahashi, A., Noel, L., Sadanandom, A., Casais, C., Parker, J., and Shirasu, K. (2006). Role of SGT1 in resistance protein accumulation in plant immunity. *EMBO J* *25*, 2007-2016.
- Baecher-Allan, C., and Hafler, D.A. (2006). Human regulatory T cells and their role in autoimmune disease. *Immunol Rev* *212*, 203-216.
- Bai, S., Liu, J., Chang, C., Zhang, L., Maekawa, T., Wang, Q., Xiao, W., Liu, Y., Chai, J., Takken, F.L., *et al.* (2012). Structure-function analysis of barley NLR immune receptor MLA10 reveals its cell compartment specific activity in cell death and disease resistance. *PLoS Pathog* *8*, e1002752.
- Bartsch, M., Gobbato, E., Bednarek, P., Debey, S., Schultze, J.L., Bautor, J., and Parker, J.E. (2006). Salicylic acid-independent ENHANCED DISEASE SUSCEPTIBILITY1 signaling in *Arabidopsis* immunity and cell death is regulated by the monooxygenase *FMO1* and the Nudix hydrolase *NUDT7*. *Plant Cell* *18*, 1038-1051.

- Belkhadir, Y., Nimchuk, Z., Hubert, D.A., Mackey, D., and Dangl, J.L. (2004a). *Arabidopsis* RIN4 negatively regulates disease resistance mediated by RPS2 and RPM1 downstream or independent of the NDR1 signal modulator and is not required for the virulence functions of bacterial type III effectors AvrRpt2 or AvrRpm1. *Plant Cell* 16, 2822-2835.
- Belkhadir, Y., Subramaniam, R., and Dangl, J.L. (2004b). Plant disease resistance protein signaling: NBS-LRR proteins and their partners. *Curr Opin Plant Biol* 7, 391-399.
- Bendahmane, A., Farnham, G., Moffett, P., and Baulcombe, D.C. (2002). Constitutive gain-of-function mutants in a nucleotide binding site-leucine rich repeat protein encoded at the *Rx* locus of potato. *Plant J* 32, 195-204.
- Bergelson, J., Kreitman, M., Stahl, E.A., and Tian, D. (2001). Evolutionary dynamics of plant *R*-genes. *Science* 292, 2281-2285.
- Bernoux, M., Burdett, H., Williams, S.J., Zhang, X., Chen, C., Newell, K., Lawrence, G.J., Kobe, B., Ellis, J.G., Anderson, P.A., *et al.* (2016). Comparative Analysis of the Flax Immune Receptors L6 and L7 Suggests an Equilibrium-Based Switch Activation Model. *Plant Cell* 28, 146-159.
- Bernoux, M., Ve, T., Williams, S., Warren, C., Hatters, D., Valkov, E., Zhang, X., Ellis, J.G., Kobe, B., and Dodds, P.N. (2011). Structural and functional analysis of a plant resistance protein TIR domain reveals interfaces for self-association, signaling, and autoregulation. *Cell Host Microbe* 9, 200-211.
- Bhattacharjee, S., Halane, M.K., Kim, S.H., and Gassmann, W. (2011). Pathogen effectors target *Arabidopsis* EDS1 and alter its interactions with immune regulators. *Science* 334, 1405-1408.
- Bieri, S., Mauch, S., Shen, Q.H., Peart, J., Devoto, A., Casais, C., Ceron, F., Schulze, S., Steinbiss, H.H., Shirasu, K., *et al.* (2004). RAR1 positively controls steady state levels of barley MLA resistance proteins and enables sufficient MLA6 accumulation for effective resistance. *Plant Cell* 16, 3480-3495.
- Bigeard, J., Colcombet, J., and Hirt, H. (2015). Signaling mechanisms in pattern-triggered immunity (PTI). *Mol Plant* 8, 521-539.
- Boller, T., and Felix, G. (2009). A renaissance of elicitors: perception of microbe-associated molecular patterns and danger signals by pattern-recognition receptors. *Annu Rev Plant Biol* 60, 379-406.
- Bombliès, K., Lempe, J., Epple, P., Warthmann, N., Lanz, C., Dangl, J.L., and Weigel, D. (2007). Autoimmune response as a mechanism for a Dobzhansky-Muller-type incompatibility syndrome in plants. *PLoS Biol* 5, e236.
- Bombliès, K., and Weigel, D. (2007). Hybrid necrosis: autoimmunity as a potential gene-flow barrier in plant species. *Nat Rev Genet* 8, 382-393.
- Bonardi, V., Tang, S., Stallmann, A., Roberts, M., Cherkis, K., and Dangl, J.L. (2011). Expanded functions for a family of plant intracellular immune receptors beyond specific recognition of pathogen effectors. *Proc Natl Acad Sci U S A* 108, 16463-16468.
- Botella, M.A., Parker, J.E., Frost, L.N., Bittner-Eddy, P.D., Beynon, J.L., Daniels, M.J., Holub, E.B., and Jones, J.D. (1998). Three genes of the *Arabidopsis* *RPP1* complex resistance locus recognize distinct *Peronospora parasitica* avirulence determinants. *Plant Cell* 10, 1847-1860.

- Böter, M., Amigues, B., Peart, J., Breuer, C., Kadota, Y., Casais, C., Moore, G., Kleanthous, C., Ochsenbein, F., Shirasu, K., *et al.* (2007). Structural and functional analysis of SGT1 reveals that its interaction with HSP90 is required for the accumulation of Rx, an R protein involved in plant immunity. *Plant Cell* *19*, 3791-3804.
- Bourras, S., McNally, K.E., Ben-David, R., Parlange, F., Roffler, S., Praz, C.R., Oberhaensli, S., Menardo, F., Stirnweis, D., Frenkel, Z., *et al.* (2015). Multiple Avirulence Loci and Allele-Specific Effector Recognition Control the Pm3 Race-Specific Resistance of Wheat to Powdery Mildew. *Plant Cell* *27*, 2991-3012.
- Box, M.S., Coustham, V., Dean, C., and Mylne, J.S. (2011). Protocol: A simple phenol-based method for 96-well extraction of high quality RNA from *Arabidopsis*. *Plant Methods* *7*, 7.
- Boyes, D.C., Nam, J., and Dangl, J.L. (1998). The *Arabidopsis thaliana* RPM1 disease resistance gene product is a peripheral plasma membrane protein that is degraded coincident with the hypersensitive response. *Proc Natl Acad Sci U S A* *95*, 15849-15854.
- Brandl, M.T., and Lindow, S.E. (1998). Contribution of indole-3-acetic acid production to the epiphytic fitness of *erwinia herbicola*. *Appl Environ Microbiol* *64*, 3256-3263.
- Brodersen, P., Petersen, M., Pike, H.M., Olszak, B., Skov, S., Odum, N., Jorgensen, L.B., Brown, R.E., and Mundy, J. (2002). Knockout of *Arabidopsis* ACCELERATED-CELL-DEATH11 encoding a sphingosine transfer protein causes activation of programmed cell death and defense. *Genes Dev* *16*, 490-502.
- Bruggeman, Q., Raynaud, C., Benhamed, M., and Delarue, M. (2015). To die or not to die? Lessons from lesion mimic mutants. *Front Plant Sci* *6*, 24.
- Büttner, D., and He, S.Y. (2009). Type III protein secretion in plant pathogenic bacteria. *Plant Physiol* *150*, 1656-1664.
- Caddick, M.X., Greenland, A.J., Jepson, I., Krause, K.P., Qu, N., Riddell, K.V., Salter, M.G., Schuch, W., Sonnewald, U., and Tomsett, A.B. (1998). An ethanol inducible gene switch for plants used to manipulate carbon metabolism. *Nat Biotechnol* *16*, 177-180.
- Cai, X.Z., Xu, Q.F., Wang, C.C., and Zheng, Z. (2006). Development of a virus-induced gene-silencing system for functional analysis of the RPS2-dependent resistance signalling pathways in *Arabidopsis*. *Plant Mol Biol* *62*, 223-232.
- Cao, H., Bowling, S.A., Gordon, A.S., and Dong, X. (1994). Characterization of an *Arabidopsis* mutant that is nonresponsive to inducers of systemic acquired resistance. *Plant Cell* *6*, 1583-1592.
- Césari, S., Bernoux, M., Moncuquet, P., Kroj, T., and Dodds, P.N. (2014a). A novel conserved mechanism for plant NLR protein pairs: the "integrated decoy" hypothesis. *Front Plant Sci* *5*, 606.
- Césari, S., Kanzaki, H., Fujiwara, T., Bernoux, M., Chalvon, V., Kawano, Y., Shimamoto, K., Dodds, P., Terauchi, R., and Kroj, T. (2014b). The NB-LRR proteins RGA4 and RGA5 interact functionally and physically to confer disease resistance. *EMBO J* *33*, 1941-1959.
- Césari, S., Thilliez, G., Ribot, C., Chalvon, V., Michel, C., Jauneau, A., Rivas, S., Alaux, L., Kanzaki, H., Okuyama, Y., *et al.* (2013). The rice resistance protein pair RGA4/RGA5 recognizes the *Magnaporthe oryzae* effectors AVR-Pia and AVR1-CO39 by direct binding. *Plant Cell* *25*, 1463-1481.

- Chae, E., Bomblies, K., Kim, S.T., Karelina, D., Zaidem, M., Ossowski, S., Martin-Pizarro, C., Laitinen, R.A., Rowan, B.A., Tenenboim, H., *et al.* (2014). Species-wide genetic incompatibility analysis identifies immune genes as hot spots of deleterious epistasis. *Cell* **159**, 1341-1351.
- Chandra-Shekara, A.C., Navarre, D., Kachroo, A., Kang, H.G., Klessig, D., and Kachroo, P. (2004). Signaling requirements and role of salicylic acid in HRT- and rrt-mediated resistance to turnip crinkle virus in *Arabidopsis*. *Plant J* **40**, 647-659.
- Chen, Z., Agnew, J.L., Cohen, J.D., He, P., Shan, L., Sheen, J., and Kunkel, B.N. (2007). *Pseudomonas syringae* type III effector AvrRpt2 alters *Arabidopsis thaliana* auxin physiology. *Proc Natl Acad Sci U S A* **104**, 20131-20136.
- Cheng, Y.T., Germain, H., Wiermer, M., Bi, D., Xu, F., Garcia, A.V., Wirthmueller, L., Despres, C., Parker, J.E., Zhang, Y., *et al.* (2009). Nuclear pore complex component MOS7/Nup88 is required for innate immunity and nuclear accumulation of defense regulators in *Arabidopsis*. *Plant Cell* **21**, 2503-2516.
- Chinchilla, D., Bauer, Z., Regenass, M., Boller, T., and Felix, G. (2006). The *Arabidopsis* receptor kinase FLS2 binds flg22 and determines the specificity of flagellin perception. *Plant Cell* **18**, 465-476.
- Chinchilla, D., Zipfel, C., Robatzek, S., Kemmerling, B., Nurnberger, T., Jones, J.D., Felix, G., and Boller, T. (2007). A flagellin-induced complex of the receptor FLS2 and BAK1 initiates plant defence. *Nature* **448**, 497-500.
- Clarke, J.D., Aarts, N., Feys, B.J., Dong, X., and Parker, J.E. (2001). Constitutive disease resistance requires *EDS1* in the *Arabidopsis* mutants *cpr1* and *cpr6* and is partially *EDS1*-dependent in *cpr5*. *Plant J* **26**, 409-420.
- Clough, S.J., and Bent, A.F. (1998). Floral dip: a simplified method for *Agrobacterium*-mediated transformation of *Arabidopsis thaliana*. *Plant J* **16**, 735-743.
- Collier, S.M., Hamel, L.P., and Moffett, P. (2011). Cell death mediated by the N-terminal domains of a unique and highly conserved class of NB-LRR protein. *Mol Plant Microbe Interact* **24**, 918-931.
- Collins, M.O., Yu, L., Campuzano, I., Grant, S.G., and Choudhary, J.S. (2008). Phosphoproteomic analysis of the mouse brain cytosol reveals a predominance of protein phosphorylation in regions of intrinsic sequence disorder. *Mol Cell Proteomics* **7**, 1331-1348.
- Cui, H., Tsuda, K., and Parker, J.E. (2015). Effector-triggered immunity: from pathogen perception to robust defense. *Annu Rev Plant Biol* **66**, 487-511.
- Dangl, J.L., and Jones, J.D. (2001). Plant pathogens and integrated defence responses to infection. *Nature* **411**, 826-833.
- Day, B., Dahlbeck, D., and Staskawicz, B.J. (2006). NDR1 interaction with RIN4 mediates the differential activation of multiple disease resistance pathways in *Arabidopsis*. *Plant Cell* **18**, 2782-2791.
- Delaney, T.P., Friedrich, L., and Ryals, J.A. (1995). *Arabidopsis* signal transduction mutant defective in chemically and biologically induced disease resistance. *Proc Natl Acad Sci U S A* **92**, 6602-6606.

- Dellagi, A., Brisset, M.N., Paulin, J.P., and Expert, D. (1998). Dual role of desferrioxamine in *Erwinia amylovora* pathogenicity. *Mol Plant Microbe Interact* *11*, 734-742.
- Denancé, N., Sanchez-Vallet, A., Goffner, D., and Molina, A. (2013). Disease resistance or growth: the role of plant hormones in balancing immune responses and fitness costs. *Front Plant Sci* *4*, 155.
- DeYoung, B.J., and Innes, R.W. (2006). Plant NBS-LRR proteins in pathogen sensing and host defense. *Nat Immunol* *7*, 1243-1249.
- Ding, X., Cao, Y., Huang, L., Zhao, J., Xu, C., Li, X., and Wang, S. (2008). Activation of the indole-3-acetic acid-amido synthetase GH3-8 suppresses expansin expression and promotes salicylate- and jasmonate-independent basal immunity in rice. *Plant Cell* *20*, 228-240.
- Dong, J., Chen, C., and Chen, Z. (2003). Expression profiles of the *Arabidopsis* *WRKY* gene superfamily during plant defense response. *Plant Mol Biol* *51*, 21-37.
- Dornmair, K., Goebels, N., Weltzien, H.U., Wekerle, H., and Hohlfeld, R. (2003). T-cell-mediated autoimmunity: novel techniques to characterize autoreactive T-cell receptors. *Am J Pathol* *163*, 1215-1226.
- Eitas, T.K., Nimchuk, Z.L., and Dangl, J.L. (2008). *Arabidopsis* TAO1 is a TIR-NB-LRR protein that contributes to disease resistance induced by the *Pseudomonas syringae* effector AvrB. *Proc Natl Acad Sci U S A* *105*, 6475-6480.
- Feys, B.J., Moisan, L.J., Newman, M.A., and Parker, J.E. (2001). Direct interaction between the *Arabidopsis* disease resistance signaling proteins, EDS1 and PAD4. *EMBO J* *20*, 5400-5411.
- Flor, H. (1942). Inheritance of pathogenicity in *Melampsora lini*. *Phytopathology* *32*, 653-699.
- Frost, D., Way, H., Howles, P., Luck, J., Manners, J., Hardham, A., Finnegan, J., and Ellis, J. (2004). Tobacco transgenic for the flax rust resistance gene *L* expresses allele-specific activation of defense responses. *Mol Plant Microbe Interact* *17*, 224-232.
- Fu, Z.Q., and Dong, X. (2013). Systemic acquired resistance: turning local infection into global defense. *Annu Rev Plant Biol* *64*, 839-863.
- Gao, Z., Chung, E.H., Eitas, T.K., and Dangl, J.L. (2011). Plant intracellular innate immune receptor Resistance to *Pseudomonas syringae* pv. *maculicola* 1 (*RPM1*) is activated at, and functions on, the plasma membrane. *Proc Natl Acad Sci U S A* *108*, 7619-7624.
- García, A.V., Blanvillain-Baufume, S., Huibers, R.P., Wiermer, M., Li, G., Gobbato, E., Rietz, S., and Parker, J.E. (2010). Balanced nuclear and cytoplasmic activities of EDS1 are required for a complete plant innate immune response. *PLoS Pathog* *6*, e1000970.
- Gaudin, V., and Jouanin, L. (1995). Expression of *Agrobacterium rhizogenes* auxin biosynthesis genes in transgenic tobacco plants. *Plant Mol Biol* *28*, 123-136.
- Germain, H., Qu, N., Cheng, Y.T., Lee, E., Huang, Y., Dong, O.X., Gannon, P., Huang, S., Ding, P., Li, Y., *et al.* (2010). MOS11: a new component in the mRNA export pathway. *PLoS Genet* *6*, e1001250.
- Glickmann, E., Gardan, L., Jacquet, S., Hussain, S., Elasri, M., Petit, A., and Dessaux, Y. (1998). Auxin production is a common feature of most pathovars of *Pseudomonas syringae*. *Mol Plant Microbe Interact* *11*, 156-162.

Görlach, J., Volrath, S., Knauf-Beiter, G., Hengy, G., Beckhove, U., Kogel, K.H., Oostendorp, M., Staub, T., Ward, E., Kessmann, H., *et al.* (1996). Benzothiadiazole, a novel class of inducers of systemic acquired resistance, activates gene expression and disease resistance in wheat. *Plant Cell* *8*, 629-643.

Guo, Y.L., Fitz, J., Schneeberger, K., Ossowski, S., Cao, J., and Weigel, D. (2011). Genome-wide comparison of nucleotide-binding site-leucine-rich repeat-encoding genes in *Arabidopsis*. *Plant Physiol* *157*, 757-769.

Gutierrez, J.R., Balmuth, A.L., Ntoukakis, V., Mucyn, T.S., Gimenez-Ibanez, S., Jones, A.M., and Rathjen, J.P. (2010). Prf immune complexes of tomato are oligomeric and contain multiple Pto-like kinases that diversify effector recognition. *Plant J* *61*, 507-518.

Hao, W., Collier, S.M., Moffett, P., and Chai, J. (2013). Structural basis for the interaction between the potato virus X resistance protein (Rx) and its cofactor Ran GTPase-activating protein 2 (RanGAP2). *J Biol Chem* *288*, 35868-35876.

Harris, C.J., Sloatweg, E.J., Goverse, A., and Baulcombe, D.C. (2013). Stepwise artificial evolution of a plant disease resistance gene. *Proc Natl Acad Sci U S A* *110*, 21189-21194.

Heidrich, K., Wirthmueller, L., Tasset, C., Pouzet, C., Deslandes, L., and Parker, J.E. (2011). *Arabidopsis* EDS1 connects pathogen effector recognition to cell compartment-specific immune responses. *Science* *334*, 1401-1404.

Heil, M., Hilpert, A., Kaiser, W., and Linsenmair, K.E. (2000). Reduced growth and seed set following chemical induction of pathogen defence: does systemic acquired resistance (SAR) incur allocation costs? *J Ecology* *88*, 645-654.

Hellens, R.P., Allan, A.C., Friel, E.N., Bolitho, K., Grafton, K., Templeton, M.D., Karunairetnam, S., Gleave, A.P., and Laing, W.A. (2005). Transient expression vectors for functional genomics, quantification of promoter activity and RNA silencing in plants. *Plant Methods* *1*, 13.

Hoisington, D.A., Neuffer, M.G., and Walbot, V. (1982). Disease lesion mimics in maize. I. Effect of genetic background, temperature, developmental age, and wounding on necrotic spot formation with Les1. *Dev Biol* *93*, 381-388.

Holt, B.F., 3rd, Belkhadir, Y., and Dangl, J.L. (2005). Antagonistic control of disease resistance protein stability in the plant immune system. *Science* *309*, 929-932.

Howles, P., Lawrence, G., Finnegan, J., McFadden, H., Ayliffe, M., Dodds, P., and Ellis, J. (2005). Autoactive alleles of the flax *L6* rust resistance gene induce non-race-specific rust resistance associated with the hypersensitive response. *Mol Plant Microbe Interact* *18*, 570-582.

Hu, G., deHart, A.K., Li, Y., Ustach, C., Handley, V., Navarre, R., Hwang, C.F., Aegerter, B.J., Williamson, V.M., and Baker, B. (2005). *EDS1* in tomato is required for resistance mediated by TIR-class *R* genes and the receptor-like *R* gene *Ve*. *Plant J* *42*, 376-391.

Hu, Y., Ding, L., Spencer, D.M., and Nunez, G. (1998). WD-40 repeat region regulates Apaf-1 self-association and procaspase-9 activation. *J Biol Chem* *273*, 33489-33494.

Hu, Y., Dong, Q., and Yu, D. (2012). *Arabidopsis* WRKY46 coordinates with WRKY70 and WRKY53 in basal resistance against pathogen *Pseudomonas syringae*. *Plant Sci* *185-186*, 288-297.

- Hu, Z., Yan, C., Liu, P., Huang, Z., Ma, R., Zhang, C., Wang, R., Zhang, Y., Martinon, F., Miao, D., *et al.* (2013). Crystal structure of NLR4 reveals its autoinhibition mechanism. *Science* *341*, 172-175.
- Hu, Z., Zhou, Q., Zhang, C., Fan, S., Cheng, W., Zhao, Y., Shao, F., Wang, H.W., Sui, S.F., and Chai, J. (2015). Structural and biochemical basis for induced self-propagation of NLR4. *Science* *350*, 399-404.
- Huang, X., Li, J., Bao, F., Zhang, X., and Yang, S. (2010). A gain-of-function mutation in the *Arabidopsis* disease resistance gene *RPP4* confers sensitivity to low temperature. *Plant Physiol* *154*, 796-809.
- Hubert, D.A., Tornero, P., Belkadir, Y., Krishna, P., Takahashi, A., Shirasu, K., and Dangl, J.L. (2003). Cytosolic HSP90 associates with and modulates the *Arabidopsis* RPM1 disease resistance protein. *EMBO J* *22*, 5679-5689.
- Huot, B., Yao, J., Montgomery, B.L., and He, S.Y. (2014). Growth-defense tradeoffs in plants: a balancing act to optimize fitness. *Mol Plant* *7*, 1267-1287.
- Iakoucheva, L.M., Brown, C.J., Lawson, J.D., Obradovic, Z., and Dunker, A.K. (2002). Intrinsic disorder in cell-signaling and cancer-associated proteins. *J Mol Biol* *323*, 573-584.
- Jacob, F., Vernaldi, S., and Maekawa, T. (2013). Evolution and conservation of plant NLR functions. *Front Immunol* *4*, 297.
- Jambunathan, N., Siani, J.M., and McNellis, T.W. (2001). A humidity-sensitive *Arabidopsis* copine mutant exhibits precocious cell death and increased disease resistance. *Plant Cell* *13*, 2225-2240.
- Jones, J.D., and Dangl, J.L. (2006). The plant immune system. *Nature* *444*, 323-329.
- Jupe, F., Pritchard, L., Etherington, G.J., Mackenzie, K., Cock, P.J., Wright, F., Sharma, S.K., Bolser, D., Bryan, G.J., Jones, J.D., *et al.* (2012). Identification and localisation of the NB-LRR gene family within the potato genome. *BMC Genomics* *13*, 75.
- Kadota, Y., and Shirasu, K. (2012). The HSP90 complex of plants. *Biochim Biophys Acta* *1823*, 689-697.
- Kadota, Y., Shirasu, K., and Guerois, R. (2010). NLR sensors meet at the SGT1-HSP90 crossroad. *Trends Biochem Sci* *35*, 199-207.
- Kadota, Y., Shirasu, K., and Zipfel, C. (2015). Regulation of the NADPH Oxidase RBOHD During Plant Immunity. *Plant Cell Physiol* *56*, 1472-1480.
- Kadota, Y., Sklenar, J., Derbyshire, P., Stransfeld, L., Asai, S., Ntoukakis, V., Jones, J.D., Shirasu, K., Menke, F., Jones, A., *et al.* (2014). Direct regulation of the NADPH oxidase RBOHD by the PRR-associated kinase BIK1 during plant immunity. *Mol Cell* *54*, 43-55.
- Kalde, M., Barth, M., Somssich, I.E., and Lippok, B. (2003). Members of the *Arabidopsis* WRKY group III transcription factors are part of different plant defense signaling pathways. *Mol Plant Microbe Interact* *16*, 295-305.
- Karasov, T.L., Kniskern, J.M., Gao, L., DeYoung, B.J., Ding, J., Dubiella, U., Lastra, R.O., Nallu, S., Roux, F., Innes, R.W., *et al.* (2014). The long-term maintenance of a resistance polymorphism through diffuse interactions. *Nature* *512*, 436-440.

- Kelley, L.A., Mezulis, S., Yates, C.M., Wass, M.N., and Sternberg, M.J. (2015). The Phyre2 web portal for protein modeling, prediction and analysis. *Nat Protoc* *10*, 845-858.
- Kieffer, M., Neve, J., and Kepinski, S. (2010). Defining auxin response contexts in plant development. *Curr Opin Plant Biol* *13*, 12-20.
- Kim, H.S., Desveaux, D., Singer, A.U., Patel, P., Sondek, J., Dangl, J.L. (2005). The *Pseudomonas syringae* effector AvrRpt2 cleaves its C-terminally acylated target, RIN4, from *Arabidopsis* membranes to block RPM1 activation. *PNAS* *102*, 6496-6501.
- Kim, H.S., Qi, D., Ashfield, T., Helm, M., Innes, R.W. (2016). Using decoys to expand the recognition specificity of a plant disease resistance protein. *Science* *351*, 684-687.
- Kim, M.G., da Cunha, L., McFall A.J., Belkhadir, Y., DebRoy, S., Dangl, J.L., Mackey, D., (2005). Two *Pseudomonas syringae* type III effectors inhibit RIN4-regulated basal defense in *Arabidopsis*. *Cell* *121*, 749-759.
- Kinkema, M., Fan, W., and Dong, X. (2000). Nuclear localization of NPR1 is required for activation of PR gene expression. *Plant Cell* *12*, 2339-2350.
- Knoth, C., Ringler, J., Dangl, J.L., and Eulgem, T. (2007). *Arabidopsis* WRKY70 is required for full RPP4-mediated disease resistance and basal defense against *Hyaloperonospora parasitica*. *Mol Plant Microbe Interact* *20*, 120-128.
- Krasileva, K.V., Dahlbeck, D., and Staskawicz, B.J. (2010). Activation of an *Arabidopsis* resistance protein is specified by the in planta association of its leucine-rich repeat domain with the cognate oomycete effector. *Plant Cell* *22*, 2444-2458.
- Krasileva, K.V., Zheng, C., Leonelli, L., Goritschnig, S., Dahlbeck, D., and Staskawicz, B.J. (2011). Global analysis of *Arabidopsis*/downy mildew interactions reveals prevalence of incomplete resistance and rapid evolution of pathogen recognition. *PLoS One* *6*, e28765.
- Le Roux, C., Huet, G., Jauneau, A., Camborde, L., Tremousaygue, D., Kraut, A., Zhou, B., Levallant, M., Adachi, H., Yoshioka, H., *et al.* (2015). A receptor pair with an integrated decoy converts pathogen disabling of transcription factors to immunity. *Cell* *161*, 1074-1088.
- Li, J., Brader, G., Kariola, T., and Palva, E.T. (2006). WRKY70 modulates the selection of signaling pathways in plant defense. *Plant J* *46*, 477-491.
- Li, L., Li, M., Yu, L., Zhou, Z., Liang, X., Liu, Z., Cai, G., Gao, L., Zhang, X., Wang, Y., *et al.* (2014). The FLS2-associated kinase BIK1 directly phosphorylates the NADPH oxidase RbohD to control plant immunity. *Cell Host Microbe* *15*, 329-338.
- Li, X., Clarke, J.D., Zhang, Y., and Dong, X. (2001). Activation of an EDS1-mediated *R*-gene pathway in the *snc1* mutant leads to constitutive, NPR1-independent pathogen resistance. *Mol Plant Microbe Interact* *14*, 1131-1139.
- Lin, W., Li, B., Lu, D., Chen, S., Zhu, N., He, P., and Shan, L. (2014). Tyrosine phosphorylation of protein kinase complex BAK1/BIK1 mediates *Arabidopsis* innate immunity. *Proc Natl Acad Sci U S A* *111*, 3632-3637.
- Liu, Y., Schiff, M., Marathe, R., and Dinesh-Kumar, S.P. (2002). Tobacco Rar1, EDS1 and NPR1/NIM1 like genes are required for N-mediated resistance to tobacco mosaic virus. *Plant J* *30*, 415-429.
- Liu, Z., and Xiao, T.S. (2015). Assembling the wheel of death. *Science* *350*, 376-377.

- Lorrain, S., Vailliau, F., Balague, C., and Roby, D. (2003). Lesion mimic mutants: keys for deciphering cell death and defense pathways in plants? *Trends Plant Sci* *8*, 263-271.
- Loutre, C., Wicker, T., Travella, S., Galli, P., Scofield, S., Fahima, T., Feuillet, C., and Keller, B. (2009). Two different CC-NBS-LRR genes are required for *Lr10*-mediated leaf rust resistance in tetraploid and hexaploid wheat. *Plant J* *60*, 1043-1054.
- Lu, D., Wu, S., Gao, X., Zhang, Y., Shan, L., and He, P. (2010). A receptor-like cytoplasmic kinase, BIK1, associates with a flagellin receptor complex to initiate plant innate immunity. *Proc Natl Acad Sci U S A* *107*, 496-501.
- Luck, J.E., Lawrence, G.J., Dodds, P.N., Shepherd, K.W., and Ellis, J.G. (2000). Regions outside of the leucine-rich repeats of flax rust resistance proteins play a role in specificity determination. *Plant Cell* *12*, 1367-1377.
- Lukasik, E., and Takken, F.L. (2009). STANDING strong, resistance proteins instigators of plant defence. *Curr Opin Plant Biol* *12*, 427-436.
- Maekawa, T., Cheng, W., Spiridon, L.N., Toller, A., Lukasik, E., Saijo, Y., Liu, P., Shen, Q.H., Micluta, M.A., Somssich, I.E., *et al.* (2011). Coiled-coil domain-dependent homodimerization of intracellular barley immune receptors defines a minimal functional module for triggering cell death. *Cell Host Microbe* *9*, 187-199.
- Maqbool, A., Saitoh, H., Franceschetti, M., Stevenson, C.E., Uemura, A., Kanzaki, H., Kamoun, S., Terauchi, R., and Banfield, M.J. (2015). Structural basis of pathogen recognition by an integrated HMA domain in a plant NLR immune receptor. *Elife* *4*.
- Marshak-Rothstein, A. (2006). Toll-like receptors in systemic autoimmune disease. *Nat Rev Immunol* *6*, 823-835.
- Mercado-Blanco, J., van der Drift, K.M., Olsson, P.E., Thomas-Oates, J.E., van Loon, L.C., and Bakker, P.A. (2001). Analysis of the pmsCEAB gene cluster involved in biosynthesis of salicylic acid and the siderophore pseudomonine in the biocontrol strain *Pseudomonas fluorescens* WCS374. *J Bacteriol* *183*, 1909-1920.
- Mestre, P., and Baulcombe, D.C. (2006). Elicitor-mediated oligomerization of the tobacco N disease resistance protein. *Plant Cell* *18*, 491-501.
- Meyers, B.C., Kozik, A., Griego, A., Kuang, H., and Michelmore, R.W. (2003). Genome-wide analysis of NBS-LRR-encoding genes in *Arabidopsis*. *Plant Cell* *15*, 809-834.
- Miya, A., Albert, P., Shinya, T., Desaki, Y., Ichimura, K., Shirasu, K., Narusaka, Y., Kawakami, N., Kaku, H., and Shibuya, N. (2007). CERK1, a LysM receptor kinase, is essential for chitin elicitor signaling in *Arabidopsis*. *Proc Natl Acad Sci U S A* *104*, 19613-19618.
- Moeder, W., and Yoshioka, K. (2008). Lesion mimic mutants: A classical, yet still fundamental approach to study programmed cell death. *Plant Signal Behav* *3*, 764-767.
- Moffett, P., Farnham, G., Peart, J., and Baulcombe, D.C. (2002). Interaction between domains of a plant NBS-LRR protein in disease resistance-related cell death. *EMBO J* *21*, 4511-4519.
- Muralidharan, S., Box, M.S., Sedivy, E.L., Wigge, P.A., Weigel, D., and Rowan, B.A. (2014). Different mechanisms for *Arabidopsis thaliana* hybrid necrosis cases inferred from temperature responses. *Plant Biol (Stuttg)* *16*, 1033-1041.

- Muskett, P., and Parker, J. (2003). Role of SGT1 in the regulation of plant R gene signalling. *Microbes Infect* 5, 969-976.
- Muskett, P.R., Kahn, K., Austin, M.J., Moisan, L.J., Sadanandom, A., Shirasu, K., Jones, J.D., and Parker, J.E. (2002). *Arabidopsis RAR1* exerts rate-limiting control of R gene-mediated defenses against multiple pathogens. *Plant Cell* 14, 979-992.
- Nakagawa, T., Kurose, T., Hino, T., Tanaka, K., Kawamukai, M., Niwa, Y., Toyooka, K., Matsuoka, K., Jinbo, T., and Kimura, T. (2007). Development of series of gateway binary vectors, pGWBs, for realizing efficient construction of fusion genes for plant transformation. *J Biosci Bioeng* 104, 34-41.
- Narusaka, M., Shirasu, K., Noutoshi, Y., Kubo, Y., Shiraishi, T., Iwabuchi, M., and Narusaka, Y. (2009). *RRS1* and *RPS4* provide a dual Resistance-gene system against fungal and bacterial pathogens. *Plant J* 60, 218-226.
- Navarro, L., Dunoyer, P., Jay, F., Arnold, B., Dharmasiri, N., Estelle, M., Voinnet, O., and Jones, J.D. (2006). A plant miRNA contributes to antibacterial resistance by repressing auxin signaling. *Science* 312, 436-439.
- Noutoshi, Y., Ito, T., Seki, M., Nakashita, H., Yoshida, S., Marco, Y., Shirasu, K., and Shinozaki, K. (2005). A single amino acid insertion in the WRKY domain of the *Arabidopsis* TIR-NBS-LRR-WRKY-type disease resistance protein SLH1 (sensitive to low humidity 1) causes activation of defense responses and hypersensitive cell death. *Plant J* 43, 873-888.
- Nürnberg, T., Brunner, F., Kemmerling, B., and Piater, L. (2004). Innate immunity in plants and animals: striking similarities and obvious differences. *Immunol Rev* 198, 249-266.
- Orr, H.A. (1996). Dobzhansky, Bateson, and the genetics of speciation. *Genetics* 144, 1331-1335.
- Palma, K., Thorgrimsen, S., Malinovsky, F.G., Fiil, B.K., Nielsen, H.B., Brodersen, P., Hofius, D., Petersen, M., and Mundy, J. (2010). Autoimmunity in *Arabidopsis acd11* is mediated by epigenetic regulation of an immune receptor. *PLoS Pathog* 6, e1001137.
- Palma, K., Zhang, Y., and Li, X. (2005). An importin alpha homolog, MOS6, plays an important role in plant innate immunity. *Curr Biol* 15, 1129-1135.
- Panstruga, R., Parker, J.E., and Schulze-Lefert, P. (2009). SnapShot: Plant immune response pathways. *Cell* 136, 978 e971-973.
- Park, S.W., Kaimoyo, E., Kumar, D., Mosher, S., and Klessig, D.F. (2007). Methyl salicylate is a critical mobile signal for plant systemic acquired resistance. *Science* 318, 113-116.
- Parker, J.E., Holub, E.B., Frost, L.N., Falk, A., Gunn, N.D., and Daniels, M.J. (1996). Characterization of *eds1*, a mutation in *Arabidopsis* suppressing resistance to *Peronospora parasitica* specified by several different *RPP* genes. *Plant Cell* 8, 2033-2046.
- Pearl, L.H., and Prodromou, C. (2006). Structure and mechanism of the Hsp90 molecular chaperone machinery. *Annu Rev Biochem* 75, 271-294.
- Peart, J.R., Cook, G., Feys, B.J., Parker, J.E., and Baulcombe, D.C. (2002). An EDS1 orthologue is required for N-mediated resistance against tobacco mosaic virus. *Plant J* 29, 569-579.

- Petersen, N.H., McKinney, L.V., Pike, H., Hofius, D., Zakaria, A., Brodersen, P., Petersen, M., Brown, R.E., and Mundy, J. (2008). Human GLTP and mutant forms of ACD11 suppress cell death in the *Arabidopsis acd11* mutant. *FEBS J* 275, 4378-4388.
- Pieterse, C.M., Leon-Reyes, A., Van der Ent, S., and Van Wees, S.C. (2009). Networking by small-molecule hormones in plant immunity. *Nat Chem Biol* 5, 308-316.
- Qi, D., and Innes, R.W. (2013). Recent advances in plant NLR structure, function, localization, and signaling. *Front Immunol* 4, 348.
- Qi, S., Pang, Y., Hu, Q., Liu, Q., Li, H., Zhou, Y., He, T., Liang, Q., Liu, Y., Yuan, X., *et al.* (2010). Crystal structure of the *Caenorhabditis elegans* apoptosome reveals an octameric assembly of CED-4. *Cell* 141, 446-457.
- Rairdan, G.J., Collier, S.M., Sacco, M.A., Baldwin, T.T., Boettrich, T., and Moffett, P. (2008). The coiled-coil and nucleotide binding domains of the Potato Rx disease resistance protein function in pathogen recognition and signaling. *Plant Cell* 20, 739-751.
- Rairdan, G.J., and Moffett, P. (2006). Distinct domains in the ARC region of the potato resistance protein Rx mediate LRR binding and inhibition of activation. *Plant Cell* 18, 2082-2093.
- Ravensdale, M., Bernoux, M., Ve, T., Kobe, B., Thrall, P.H., Ellis, J.G., and Dodds, P.N. (2012). Intramolecular interaction influences binding of the Flax L5 and L6 resistance proteins to their AvrL567 ligands. *PLoS Pathog* 8, e1003004.
- Reubold, T.F., Wohlgemuth, S., and Eschenburg, S. (2011). Crystal structure of full-length Apaf-1: how the death signal is relayed in the mitochondrial pathway of apoptosis. *Structure* 19, 1074-1083.
- Riedl, S.J., Li, W., Chao, Y., Schwarzenbacher, R., and Shi, Y. (2005). Structure of the apoptotic protease-activating factor 1 bound to ADP. *Nature* 434, 926-933.
- Robert-Seilaniantz, A., MacLean, D., Jikumaru, Y., Hill, L., Yamaguchi, S., Kamiya, Y., and Jones, J.D. (2011). The microRNA miR393 re-directs secondary metabolite biosynthesis away from camalexin and towards glucosinolates. *Plant J* 67, 218-231.
- Roberts, M., Tang, S., Stallmann, A., Dangl, J.L., and Bonardi, V. (2013). Genetic requirements for signaling from an autoactive plant NB-LRR intracellular innate immune receptor. *PLoS Genet* 9, e1003465.
- Roux, M., Schwessinger, B., Albrecht, C., Chinchilla, D., Jones, A., Holton, N., Malinovsky, F.G., Tor, M., de Vries, S., and Zipfel, C. (2011). The *Arabidopsis* leucine-rich repeat receptor-like kinases BAK1/SERK3 and BKK1/SERK4 are required for innate immunity to hemibiotrophic and biotrophic pathogens. *Plant Cell* 23, 2440-2455.
- Sambrook, J., Fritsch, E.F., and Maniatis, T. (1989). *Molecular Cloning*. Cold Spring Harbor Laboratory, Cold Spring Harbor.
- Sandhu, K.S. (2009). Intrinsic disorder explains diverse nuclear roles of chromatin remodeling proteins. *J Mol Recognit* 22, 1-8.
- Sarris, P.F., Duxbury, Z., Huh, S.U., Ma, Y., Segonzac, C., Sklenar, J., Derbyshire, P., Cevik, V., Rallapalli, G., Saucet, S.B., *et al.* (2015). A Plant Immune Receptor Detects Pathogen Effectors that Target WRKY Transcription Factors. *Cell* 161, 1089-1100.

- Schulze, B., Mentzel, T., Jehle, A.K., Mueller, K., Beeler, S., Boller, T., Felix, G., and Chinchilla, D. (2010). Rapid heteromerization and phosphorylation of ligand-activated plant transmembrane receptors and their associated kinase BAK1. *J Biol Chem* *285*, 9444-9451.
- Serino, L., Reimmann, C., Baur, H., Beyeler, M., Visca, P., and Haas, D. (1995). Structural genes for salicylate biosynthesis from chorismate in *Pseudomonas aeruginosa*. *Mol Gen Genet* *249*, 217-228.
- Shirano, Y., Kachroo, P., Shah, J., and Klessig, D.F. (2002). A gain-of-function mutation in an *Arabidopsis* Toll Interleukin1 receptor-nucleotide binding site-leucine-rich repeat type *R* gene triggers defense responses and results in enhanced disease resistance. *Plant Cell* *14*, 3149-3162.
- Shirasu, K. (2009). The HSP90-SGT1 chaperone complex for NLR immune sensors. *Annu Rev Plant Biol* *60*, 139-164.
- Shiu, S.H., and Bleecker, A.B. (2001). Plant receptor-like kinase gene family: diversity, function, and signaling. *Sci STKE* *2001*, re22.
- Sinapidou, E., Williams, K., Nott, L., Bahkt, S., Tor, M., Crute, I., Bittner-Eddy, P., and Beynon, J. (2004). Two TIR:NB:LRR genes are required to specify resistance to *Peronospora parasitica* isolate Cala2 in *Arabidopsis*. *Plant J* *38*, 898-909.
- Slootweg, E.J., Spiridon, L.N., Roosien, J., Butterbach, P., Pomp, R., Westerhof, L., Wilbers, R., Bakker, E., Bakker, J., Petrescu, A.J., *et al.* (2013). Structural determinants at the interface of the ARC2 and leucine-rich repeat domains control the activation of the plant immune receptors Rx1 and Gpa2. *Plant Physiol* *162*, 1510-1528.
- Sohn, K.H., Hughes, R.K., Piquerez, S.J., Jones, J.D., and Banfield, M.J. (2012). Distinct regions of the *Pseudomonas syringae* coiled-coil effector AvrRps4 are required for activation of immunity. *Proc Natl Acad Sci U S A* *109*, 16371-16376.
- Spoel, S.H., Mou, Z., Tada, Y., Spivey, N.W., Genschik, P., and Dong, X. (2009). Proteasome-mediated turnover of the transcription coactivator NPR1 plays dual roles in regulating plant immunity. *Cell* *137*, 860-872.
- Steinbrenner, A.D., Goritschnig, S., and Staskawicz, B.J. (2015). Recognition and activation domains contribute to allele-specific responses of an *Arabidopsis* NLR receptor to an oomycete effector protein. *PLoS Pathog* *11*, e1004665.
- Straus, M.R., Rietz, S., Ver Loren van Themaat, E., Bartsch, M., and Parker, J.E. (2010). Salicylic acid antagonism of EDS1-driven cell death is important for immune and oxidative stress responses in *Arabidopsis*. *Plant J* *62*, 628-640.
- Stuttman, J., Peine, N., Garcia, A.V., Wagner, C., Choudhury, S.R., Wang, Y., James, G.V., Griebel, T., Alcazar, R., Tsuda, K., *et al.* (2016). *Arabidopsis thaliana* DM2h (*R8*) within the Landsberg *RPP1-like Resistance* Locus underlies three different cases of *EDS1*-conditioned autoimmunity. *PLoS Genet* *12*, e1005990.
- Sukarta, O.C., Slootweg, E.J., and Goverse, A. (2016). Structure-Informed Insights for NLR Functioning in Plant Immunity. *Semin Cell Dev Biol*.
- Sun, J.C., Ugolini, S., and Vivier, E. (2014). Immunological memory within the innate immune system. *EMBO J* *33*, 1295-1303.

- Sun, Y., Li, L., Macho, A.P., Han, Z., Hu, Z., Zipfel, C., Zhou, J.M., and Chai, J. (2013). Structural basis for flg22-induced activation of the *Arabidopsis* FLS2-BAK1 immune complex. *Science* *342*, 624-628.
- Suzuki, S., He, Y., and Oyaizu, H. (2003). Indole-3-Acetic acid production in *Pseudomonas fluorescens* HP72 and its association with suppression of creeping bentgrass brown patch. *Curr Microbiol* *47*, 138-143.
- Swarup, R., and Peret, B. (2012). AUX/LAX family of auxin influx carriers-an overview. *Front Plant Sci* *3*, 225.
- Swiderski, M.R., Birker, D., and Jones, J.D. (2009). The TIR domain of TIR-NB-LRR resistance proteins is a signaling domain involved in cell death induction. *Mol Plant Microbe Interact* *22*, 157-165.
- Szabo, L.J., and Bushnell, W.R. (2001). Hidden robbers: the role of fungal haustoria in parasitism of plants. *Proc Natl Acad Sci U S A* *98*, 7654-7655.
- Takahashi, A., Casais, C., Ichimura, K., and Shirasu, K. (2003). HSP90 interacts with RAR1 and SGT1 and is essential for RPS2-mediated disease resistance in *Arabidopsis*. *Proc Natl Acad Sci U S A* *100*, 11777-11782.
- Takahashi, A., Kawasaki, T., Henmi, K., Shi, I.K., Kodama, O., Satoh, H., and Shimamoto, K. (1999). Lesion mimic mutants of rice with alterations in early signaling events of defense. *Plant J* *17*, 535-545.
- Takken, F.L., Albrecht, M., and Tameling, W.I. (2006). Resistance proteins: molecular switches of plant defence. *Curr Opin Plant Biol* *9*, 383-390.
- Takken, F.L., and Govere, A. (2012). How to build a pathogen detector: structural basis of NB-LRR function. *Curr Opin Plant Biol* *15*, 375-384.
- Tameling, W.I., Elzinga, S.D., Darmin, P.S., Vossen, J.H., Takken, F.L., Haring, M.A., and Cornelissen, B.J. (2002). The tomato *R* gene products I-2 and MI-1 are functional ATP binding proteins with ATPase activity. *Plant Cell* *14*, 2929-2939.
- Tameling, W.I., Vossen, J.H., Albrecht, M., Lengauer, T., Berden, J.A., Haring, M.A., Cornelissen, B.J., and Takken, F.L. (2006). Mutations in the NB-ARC domain of I-2 that impair ATP hydrolysis cause autoactivation. *Plant Physiol* *140*, 1233-1245.
- Tang, X., Frederick, R.D., Zhou, J., Halterman, D.A., Jia, Y., and Martin, G.B. (1996). Initiation of plant disease resistance by physical interaction of AvrPto and Pto kinase. *Science* *274*, 2060-2063.
- Tian, D., Traw, M.B., Chen, J.Q., Kreitman, M., and Bergelson, J. (2003). Fitness costs of *R*-gene-mediated resistance in *Arabidopsis thaliana*. *Nature* *423*, 74-77.
- Ting, J.P., Lovering, R.C., Alnemri, E.S., Bertin, J., Boss, J.M., Davis, B.K., Flavell, R.A., Girardin, S.E., Godzik, A., Harton, J.A., *et al.* (2008). The NLR gene family: a standard nomenclature. *Immunity* *28*, 285-287.
- Todesco, M., Balasubramanian, S., Hu, T.T., Traw, M.B., Horton, M., Epple, P., Kuhns, C., Sureshkumar, S., Schwartz, C., Lanz, C., *et al.* (2010). Natural allelic variation underlying a major fitness trade-off in *Arabidopsis thaliana*. *Nature* *465*, 632-636.

- Tör, M., Gordon, P., Cuzick, A., Eulgem, T., Sinapidou, E., Mert-Turk, F., Can, C., Dangl, J.L., and Holub, E.B. (2002). *Arabidopsis* SGT1b is required for defense signaling conferred by several downy mildew resistance genes. *Plant Cell* *14*, 993-1003.
- Tornero, P., Merritt, P., Sadanandom, A., Shirasu, K., Innes, R.W., and Dangl, J.L. (2002). RAR1 and NDR1 contribute quantitatively to disease resistance in *Arabidopsis*, and their relative contributions are dependent on the R gene assayed. *Plant Cell* *14*, 1005-1015.
- Torres, M.A., Dangl, J.L., and Jones, J.D. (2002). *Arabidopsis* gp91phox homologues *AtrbohD* and *AtrbohF* are required for accumulation of reactive oxygen intermediates in the plant defense response. *Proc Natl Acad Sci U S A* *99*, 517-522.
- Torres, M.A., Jones, J.D., and Dangl, J.L. (2005). Pathogen-induced, NADPH oxidase-derived reactive oxygen intermediates suppress spread of cell death in *Arabidopsis thaliana*. *Nat Genet* *37*, 1130-1134.
- Tsuda, K., and Katagiri, F. (2010). Comparing signaling mechanisms engaged in pattern-triggered and effector-triggered immunity. *Curr Opin Plant Biol* *13*, 459-465.
- Tsuda, K., Sato, M., Stoddard, T., Glazebrook, J., and Katagiri, F. (2009). Network properties of robust immunity in plants. *PLoS Genet* *5*, e1000772.
- Ueda, H., Yamaguchi, Y., and Sano, H. (2006). Direct interaction between the tobacco mosaic virus helicase domain and the ATP-bound resistance protein, N factor during the hypersensitive response in tobacco plants. *Plant Mol Biol* *61*, 31-45.
- van der Biezen, E.A., and Jones, J.D. (1998). The NB-ARC domain: a novel signalling motif shared by plant resistance gene products and regulators of cell death in animals. *Curr Biol* *8*, R226-227.
- van Loon, L.C., Rep, M., and Pieterse, C.M. (2006). Significance of inducible defense-related proteins in infected plants. *Annu Rev Phytopathol* *44*, 135-162.
- van Ooijen, G., Mayr, G., Kasiem, M.M.A., Albrecht, M., Cornelissen, B.J.C., Takken, F.L.W. (2008). Structure-function analysis of the NB-ARC domain of plant disease resistance proteins. *J Exp Botany* *59*, 1383-1397.
- van Verk, M.C., Bol, J.F., and Linthorst, H.J. (2011). WRKY transcription factors involved in activation of SA biosynthesis genes. *BMC Plant Biol* *11*, 89.
- Venugopal, S.C., Jeong, R.D., Mandal, M.K., Zhu, S., Chandra-Shekara, A.C., Xia, Y., Hersh, M., Stromberg, A.J., Navarre, D., Kachroo, A., *et al.* (2009). Enhanced disease susceptibility 1 and salicylic acid act redundantly to regulate resistance gene-mediated signaling. *PLoS Genet* *5*, e1000545.
- Vlot, A.C., Klessig, D.F., and Park, S.W. (2008). Systemic acquired resistance: the elusive signal(s). *Curr Opin Plant Biol* *11*, 436-442.
- von Moltke, J., Ayres, J.S., Kofoed, E.M., Chavarria-Smith, J., and Vance, R.E. (2013). Recognition of bacteria by inflammasomes. *Annu Rev Immunol* *31*, 73-106.
- Wang, D., Amornsiripanitch, N., and Dong, X. (2006). A genomic approach to identify regulatory nodes in the transcriptional network of systemic acquired resistance in plants. *PLoS Pathog* *2*, e123.

- Wang, D., Pajerowska-Mukhtar, K., Culler, A.H., and Dong, X. (2007). Salicylic acid inhibits pathogen growth in plants through repression of the auxin signaling pathway. *Curr Biol* *17*, 1784-1790.
- Wang, G.F., Ji, J., El-Kasmi, F., Dangl, J.L., Johal, G., and Balint-Kurti, P.J. (2015). Molecular and functional analyses of a maize autoactive NB-LRR protein identify precise structural requirements for activity. *PLoS Pathog* *11*, e1004674.
- Wang, J., Zhang, L., Li, J., Lawton-Rauh, A., and Tian, D. (2011). Unusual signatures of highly adaptable *R*-loci in closely-related *Arabidopsis* species. *Gene* *482*, 24-33.
- Warren, R.F., Merritt, P.M., Holub, E., and Innes, R.W. (1999). Identification of three putative signal transduction genes involved in *R* gene-specified disease resistance in *Arabidopsis*. *Genetics* *152*, 401-412.
- Wiermer, M., Palma, K., Zhang, Y., and Li, X. (2007). Should I stay or should I go? Nucleocytoplasmic trafficking in plant innate immunity. *Cell Microbiol* *9*, 1880-1890.
- Wildermuth, M.C., Dewdney, J., Wu, G., and Ausubel, F.M. (2001). Isochorismate synthase is required to synthesize salicylic acid for plant defence. *Nature* *414*, 562-565.
- Williams, S.J., Sohn, K.H., Wan, L., Bernoux, M., Sarris, P.F., Segonzac, C., Ve, T., Ma, Y., Saucet, S.B., Ericsson, D.J., *et al.* (2014). Structural basis for assembly and function of a heterodimeric plant immune receptor. *Science* *344*, 299-303.
- Williams, S.J., Sornaraj, P., deCourcy-Ireland, E., Menz, R.I., Kobe, B., Ellis, J.G., Dodds, P.N., and Anderson, P.A. (2011). An autoactive mutant of the M flax rust resistance protein has a preference for binding ATP, whereas wild-type M protein binds ADP. *Mol Plant Microbe Interact* *24*, 897-906.
- Wirthmueller, L., Zhang, Y., Jones, J.D., and Parker, J.E. (2007). Nuclear accumulation of the *Arabidopsis* immune receptor RPS4 is necessary for triggering EDS1-dependent defense. *Curr Biol* *17*, 2023-2029.
- Wolter, M., Hollricher, K., Salamini, F., and Schulze-Lefert, P. (1993). The *mlo* resistance alleles to powdery mildew infection in barley trigger a developmentally controlled defence mimic phenotype. *Mol Gen Genet* *239*, 122-128.
- Woodward, A.W., and Bartel, B. (2005). Auxin: regulation, action, and interaction. *Ann Bot* *95*, 707-735.
- Wu, Y., Zhang, D., Chu, J.Y., Boyle, P., Wang, Y., Brindle, I.D., De Luca, V., and Despres, C. (2012). The *Arabidopsis* NPR1 protein is a receptor for the plant defense hormone salicylic acid. *Cell Rep* *1*, 639-647.
- Xiao, S., Brown, S., Patrick, E., Brearley, C., and Turner, J.G. (2003). Enhanced transcription of the *Arabidopsis* disease resistance genes *RPW8.1* and *RPW8.2* via a salicylic acid-dependent amplification circuit is required for hypersensitive cell death. *Plant Cell* *15*, 33-45.
- Yanaba, K., Bouaziz, J.D., Matsushita, T., Magro, C.M., St Clair, E.W., and Tedder, T.F. (2008). B-lymphocyte contributions to human autoimmune disease. *Immunol Rev* *223*, 284-299.
- Yang, S., and Hua, J. (2004). A haplotype-specific Resistance gene regulated by *BONZAI1* mediates temperature-dependent growth control in *Arabidopsis*. *Plant Cell* *16*, 1060-1071.

- Yang, S., Zhang, Q., Guo, J., Charkowski, A.O., Glick, B.R., Ibekwe, A.M., Cooksey, D.A., and Yang, C.H. (2007). Global effect of indole-3-acetic acid biosynthesis on multiple virulence factors of *Erwinia chrysanthemi* 3937. *Appl Environ Microbiol* *73*, 1079-1088.
- Yant, L., Mathieu, J., Dinh, T.T., Ott, F., Lanz, C., Wollmann, H., Chen, X., and Schmid, M. (2010). Orchestration of the floral transition and floral development in *Arabidopsis* by the bifunctional transcription factor APETALA2. *Plant Cell* *22*, 2156-2170.
- Yu, S., Galvão, V.C., Zhang, Y.C., Horrer, D., Zhang, T.Q., Hao, Y.H., Feng, Y.Q., Wang, S., Schmid, M., and Wang, J.W. (2012). Gibberellin regulates the *Arabidopsis* floral transition through miR156-targeted SQUAMOSA promoter binding-like transcription factors. *Plant Cell* *24*, 3320-3332.
- Yu, X., Wang, L., Acehan, D., Wang, X., and Akey, C.W. (2006). Three-dimensional structure of a double apoptosome formed by the *Drosophila* Apaf-1 related killer. *J Mol Biol* *355*, 577-589.
- Yuan, S., and Akey, C.W. (2013). Apoptosome structure, assembly, and procaspase activation. *Structure* *21*, 501-515.
- Yuan, S., Topf, M., Reubold, T.F., Eschenburg, S., and Akey, C.W. (2013). Changes in Apaf-1 conformation that drive apoptosome assembly. *Biochemistry* *52*, 2319-2327.
- Yue, J.X., Meyers, B.C., Chen, J.Q., Tian, D., and Yang, S. (2012). Tracing the origin and evolutionary history of plant nucleotide-binding site-leucine-rich repeat (NBS-LRR) genes. *New Phytol* *193*, 1049-1063.
- Zhang, L., Chen, S., Ruan, J., Wu, J., Tong, A.B., Yin, Q., Li, Y., David, L., Lu, A., Wang, W.L., *et al.* (2015). Cryo-EM structure of the activated NAIP2-NLRC4 inflammasome reveals nucleated polymerization. *Science* *350*, 404-409.
- Zhang, M., Kadota, Y., Prodromou, C., Shirasu, K., and Pearl, L.H. (2010). Structural basis for assembly of Hsp90-Sgt1-CHORD protein complexes: implications for chaperoning of NLR innate immunity receptors. *Mol Cell* *39*, 269-281.
- Zhang, Y., Goritschnig, S., Dong, X., and Li, X. (2003). A gain-of-function mutation in a plant disease resistance gene leads to constitutive activation of downstream signal transduction pathways in *suppressor of npr1-1, constitutive 1*. *Plant Cell* *15*, 2636-2646.
- Zhang, Y., and Li, X. (2005). A putative nucleoporin 96 Is required for both basal defense and constitutive resistance responses mediated by *suppressor of npr1-1, constitutive 1*. *Plant Cell* *17*, 1306-1316.
- Zhang, Z., Wu, Y., Gao, M., Zhang, J., Kong, Q., Liu, Y., Ba, H., Zhou, J., and Zhang, Y. (2012). Disruption of PAMP-induced MAP kinase cascade by a *Pseudomonas syringae* effector activates plant immunity mediated by the NB-LRR protein SUMM2. *Cell Host Microbe* *11*, 253-263.
- Zhao, T., Rui, L., Li, J., Nishimura, M.T., Vogel, J.P., Liu, N., Liu, S., Zhao, Y., Dangl, J.L., Tang D. (2015). A truncated NLR protein, TIR-NBS2, is required for activated defense responses in the *exo70B1* mutant. *PLoS Genet* *11*, e1004945.
- Zhao, Z., Andersen, S.U., Ljung, K., Dolezal, K., Miotk, A., Schultheiss, S.J., and Lohmann, J.U. (2010). Hormonal control of the shoot stem-cell niche. *Nature* *465*, 1089-1092.

Zhong, Y., Kinio, A., and Saleh, M. (2013). Functions of NOD-Like Receptors in Human Diseases. *Front Immunol* 4, 333.

Zhou, F., Menke, F.L., Yoshioka, K., Moder, W., Shirano, Y., and Klessig, D.F. (2004a). High humidity suppresses *ssi4*-mediated cell death and disease resistance upstream of MAP kinase activation, H₂O₂ production and defense gene expression. *Plant J* 39, 920-932.

Zhou, T., Wang, Y., Chen, J.Q., Araki, H., Jing, Z., Jiang, K., Shen, J., and Tian, D. (2004b). Genome-wide identification of NBS genes in *japonica* rice reveals significant expansion of divergent non-TIR NBS-LRR genes. *Mol Genet Genomics* 271, 402-415.

Zipfel, C., Kunze, G., Chinchilla, D., Caniard, A., Jones, J.D., Boller, T., and Felix, G. (2006). Perception of the bacterial PAMP EF-Tu by the receptor EFR restricts *Agrobacterium*-mediated transformation. *Cell* 125, 749-760.

Zipfel, C., Robatzek, S., Navarro, L., Oakeley, E.J., Jones, J.D., Felix, G., and Boller, T. (2004). Bacterial disease resistance in *Arabidopsis* through flagellin perception. *Nature* 428, 764-767.

PUBLICATIONS

Eunyoung Chae, E., Diep T. N. Tran, Detlef Weigel (2016). Cooperation and conflict in the plant immune system. PLoS Pathogens 12(3): e1005452. doi:10.1371/journal.ppat.1005452.

LEBENS LAUF

DIEP THI NGOC TRAN

Department of Molecular Biology

Max Planck Institute for Developmental Biology

Spemannstrasse 35-37

D-72076, Tübingen

GERMANY

Email: diep.tran@tuebingen.mpg.de

dieptranvn@gmail.com

Personal information

Date of Birth August 13, 1985

Place of Birth Hanoi, Vietnam

Nationality Vietnamese

Education

2011 - present PhD student at Max Planck Institute for Developmental Biology, and Eberhard Karls Universität Tübingen, Tübingen, Germany. Supervisors: Prof. Dr. Detlef Weigel and Prof. Dr. Hans-Georg Rammensee

2009 M.S. in Genetics, Hanoi University of Science, Hanoi, Vietnam. Supervisor: Prof. Dr. Hai Van Nong

2007 B.S. in Biology, Hanoi University of Science, Hanoi, Vietnam. Supervisors: Prof. Dr. Hai Van Nong and Dr. Ha Thi-Viet Bui

Professional Experience

2007-2011 Assistant Researcher, Applied DNA Technology Laboratory, Institute of Biotechnology, Hanoi, Vietnam

Awards and Fellowships

2012 Poster Prize, PhD Symposium 2012, Max Planck Institute for Developmental Biology, Tübingen, Germany

2011 PhD fellowship, International PhD Program in the Biological Sciences, Max Planck Institute for Developmental Biology, Tübingen, Germany

- 2003 Undergraduate Fellowship, Honour Programme for Talented Students, Hanoi University of Science, Hanoi, Vietnam
- 2003 Award of the Minister of Education and Training of Vietnam for the Second Prize in the National Olympic Competition in Biology

Research Interest

- Molecular biology and evolution
- Plant innate immunity
- Biochemical mechanism of NLR activation in autoimmune hybrids
- Functional evolution of NLR genes

Presentation

- June 2014 “Molecular Mechanism of Autoimmunity Triggered by a Pair of NB-LRRs”. 8th SPPS PhD Students Conference, Uppsala, Sweden (Oral Presentation)
- August 2015 “Autoimmunity Triggered by Activation of Paired NLRs”. 26th Congress of SPPS Plant Biology Scandinavia 2015, Stockholm, Sweden (Poster Presentation)